SYNTHESIS AND STRUCTURES OF GERMANIUM(II) CALIXARENES AND CLUSTERS

By

REBECCA ANNE GREEN

Bachelor of Science in Chemistry

Towson University

Towson, Maryland

2005

Submitted to the Faculty of the
Graduate College of the
Oklahoma State University
in partial fulfillment of
the requirements for
the Degree of
MASTER OF SCIENCE
July, 2009

SYNTHESIS AND STRUCTURES OF

GERMANIUM(II) CALIXARENES

AND CLUSTERS

Thesis Approved:

Dr. Charles Scott Weinert
Thesis Adviser

Dr. Allen Apblett

Dr. Richard Bunce

Dr. A. Gordon Emslie
Dean of the Graduate College

ACKNOWLEDGMENTS

This work would not have been possible without the dedicated tutelage of my adviser Dr. Charles Scott Weinert. During the time I spent in his research laboratory he consistently provided an environment in which I could continually learn and grow as a chemist. I am very grateful for all of his guidance and support. I am also very grateful to Dr. Allen Apblett, Dr. Richard Bunce, Dr. LeGrande Slaughter and again to Dr. Scott Weinert for all that they taught me in the classes that I took with them. The knowledge that they passed on is invaluable to me. I would like to thank Dr. Asfaha Iob for always helping me when I had a question about an instrument. I am grateful to Gianna Bell-Eunice for always helping me whenever I had a question or a NMR experiment to run. I am indebted to Tony and Mary Wetherby for their unwavering support and encouragement throughout my stay and I am thankful to consider them family. The years in lab, months in classes and hours spent studying were made more enjoyable with the company of Monika Amadoruge; she could always brighten my day with a good impression. To the newest lab mates, Erin Short and Christian Samanamu, I wish you all the best during your time in the Weinert group and don't forget that you joined the coolest group ever. I am eternally grateful for the love and support that my family has shown me during all of my academic endeavors, their encouragement and support through everything means more than I could ever express. Finally, I thank God to Whom I owe everything.

TABLE OF CONTENTS

LIST OF TABLES

Table Page

Chapter One

Chapter Two

Chapter Three

LIST OF FIGURES

Figure Page

Chapter One

Chapter Two

Chapter Three

LIST OF SCHEMES

Scheme Page

Chapter One

Chapter One: Introduction

Introduction

The growing interest in organogermanium compounds arises from their technical applications in semi-conductors, thermochromic and optics materials[1,2] as well as their activity in biological systems.[3] Over the past 60 years, germylene chemistry has come a long way. Initially, the field was pioneered by Professors M. Lesbre and J. Satgé at the University of Toulouse, France,[3] and since this time it has taken advantage of the developments in carbene chemistry, which was a part of mechanistic work in organic chemistry, since germylenes can be considered heavy congeners of carbenes. This led to the ability to synthesize many different germylene compounds by studying similar reactions to those that were investigated for the related carbenes. Germylene chemistry is also built upon the knowledge of stannylene chemistry, and the germanium compounds often exhibit similar reactivities. For example, $M[N(SiMe_3)_2]_2$ (M = Ge or Sn) reacts with $[Pt(cod)_2]$ to yield $[Pt\{M(N(SiMe_3)_2)_2\}_3$ (**Scheme 1**).

$$3\ M[N(SiMe_3)_2]_2 + [Pt(cod)_2] \rightarrow [Pt\{M(N(SiMe_3)_2)_2\}_3]$$

Scheme 1. Reaction of $[Pt(cod)_2]$ with $M[N(SiMe_3)_2]_2$.

Stannylenes are also considered to be heavy analogues of carbenes and can be thought of as a member of the Group 14 family R_2M where M = C, Si, Ge, Sn and Pb. The lower oxidation state of tin is firmly established and is often more stable than the tetravalent state, especially with chloride ligands. Stannylenes were most likely among the first organotin products synthesized approximately 140 years ago; however, since the analytical methods to characterize these products were lacking, the detection and identification of these short lived intermediates was not possible. What these original products most likely contained were cyclic or open-chained penta- or hexamers and polystannanes.[3] As the technology progressed to allow for better characterization of these products, the identity of these compounds was confirmed. This led to the postulation that stannylenes consist of a $5sp^3$ electronic configuration rather than the previously thought $5s^25p^2$ configuration.[3] The divalent stannylenes were short-lived intermediates and polymerized quickly and as the chemistry progressed it became apparent that divalent Group 14 compounds required electronic or steric stabilization, or both. So in 1956 dicyclopentadienyl tin, the first example of a kinetically stable monomer with a lone pair of electrons, was reported by E.O. Fischer.[3] As stannylene chemistry grew, germylene chemistry began to follow by means of performing analogous reaction to those of the stannylenes using germanium instead.

Research in germylene chemistry began shortly after 1948 when organogermanium chemistry became of interest. There were several uncertainties about germylene chemistry that were also investigated with carbenes and silylenes. These issues ranged from isolation of the compounds, characterization of their structures, and uncertainty as to whether the products generated came from reactive intermediates or if

they arose from germylenoid compounds. Shown below (**Schemes 2,3** and **4**)[3] are examples of reactions that generated R_2Ge compounds. One of the most common reactions to synthesize monomeric germylenes was from thermal or UV irradiation of 7,7-disubstituted -7-germabenzonorbornadienes formed from a tetraphenylgermole and dehydrobenzene.[3]

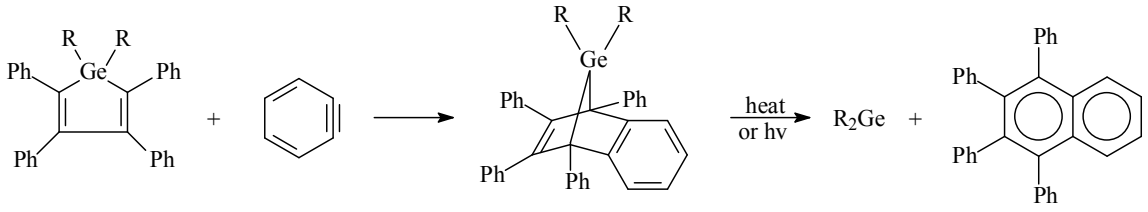

Scheme 2. Reaction of 7,7-disubstituted-7-germabenzonorbornadiene to yield R_2Ge.

$$n\ Ph_2GeH_2 + n\ Et_2Hg \xrightarrow[-2n\ EtH]{exoth.} (\text{-}Ph_2Ge\text{-}Hg\text{-})_n \xrightarrow[or\ hv]{heat} n\ Ph_2Ge + n\ Hg$$

Scheme 3. Irradiation of the germyl mercurial to yield the diphenylgermylene.

$$Ar_2Ge(SiMe_3)_2 \xrightarrow{hv} Ar_2Ge + Me_3Si{-}{-}SiMe_3$$

Scheme 4. Irradiation of the diaryl bissilylgermane to yield the diarylgermylene. Ar can be Ph, 4-MePh, 2,6-Me_2Ph, 2,6-Et_2Ph, mesityl or 2,4,6-Pr^i_3Ph.

The R substituent on germanium in this reaction is most often a methyl group, which enhances the thermal stability of the 7,7-disubstituted-7-germabenzonorbornadiene, although ethyl, butyl, phenyl and 4-methylphenyl can be used. Selected germylenes and their λ_{max} (nm) data are collected in **Table 1**. Another route for the preparation of germylenes, which was also one of the first methods employed, is the decomposition of germyl mercury compounds under thermal or photolytic conditions (**Scheme 3**). Additionally, it was determined that diaryl bissilylgermanium compounds generated germylenes upon UV irradiation (**Scheme 4**). The driving force of this reaction is the formation of the Si – Si bond which is more stable than the Ge – Si bond.[3] The aryl ligands in these species (Ph_2Ge:) are necessary for the absorption of UV energy by the molecule.

Several other germylenes have been prepared by various other methods. Diphenylgermylene was generated by the thermolysis of 7,7-diphenyl-7-germanorbornadiene, and the subsequent trapping reaction with adamantanethione yielded the germathiirane which was further reacted with ethanol to form a germylmercaptan (**Scheme 5**). The germathiirane is stabilized by the steric protection of bulky substituents present around the ring system, and therefore the reaction of bulkier mesityl substituted germylene with adamantanethione was also investigated (**Scheme 6**). Hexamesitylcyclotrigermane was heated to generate the dimesitylgermylene and tetramesityldigermene, which was reacted with 2,3-dimethylbuta-1,3-diene to yield germacyclopent-3-ene and 1,2-digermacyclohex-4-ene (respectively) (**Scheme 7**). It was noted that without the use of a germylene trapping reagent, the cyclotrigermane was regenerated and recovered in almost quantitative yield.

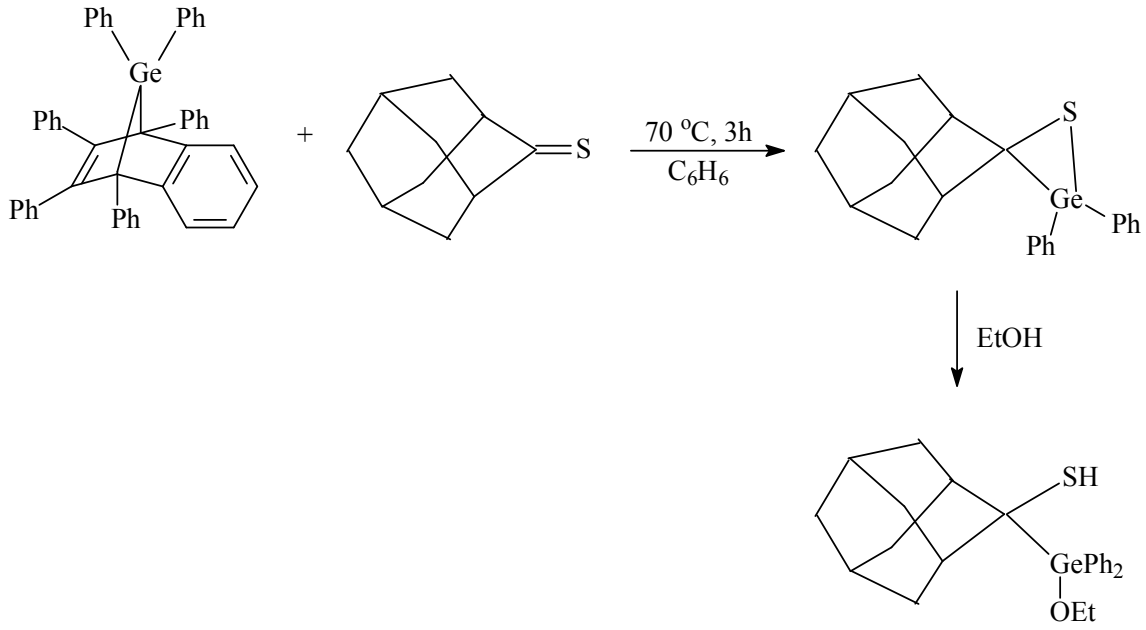

Scheme 5. Diphenylgermylene generated after thermolysis of 7,7-diphenyl-7-germabenzonorbornadiene and subsequent reaction with adamantanethione to yield the germathiirane and the reaction with ethanol to yield the germylmercaptan.[11]

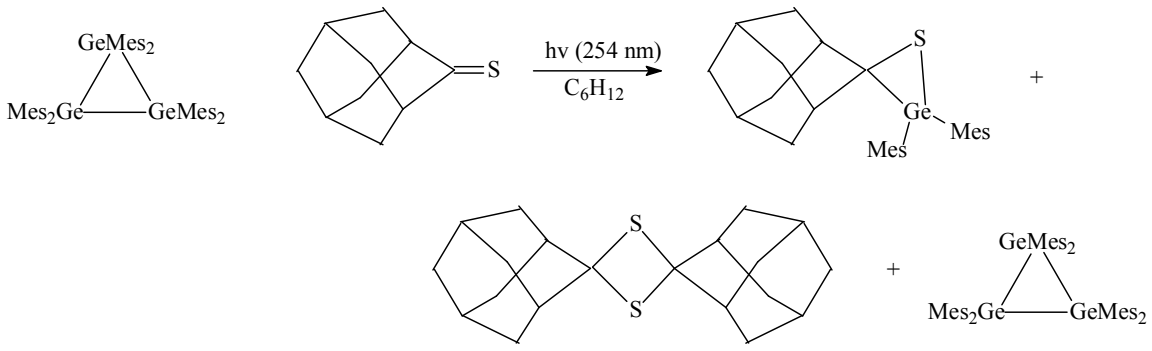

Scheme 6. Generation of dimesitylgermylene and subsequent reaction with adamantanethione to yield the germathiirane, adamantanethione dimer and unreacted hexamesitylcyclotrigermane.[11]

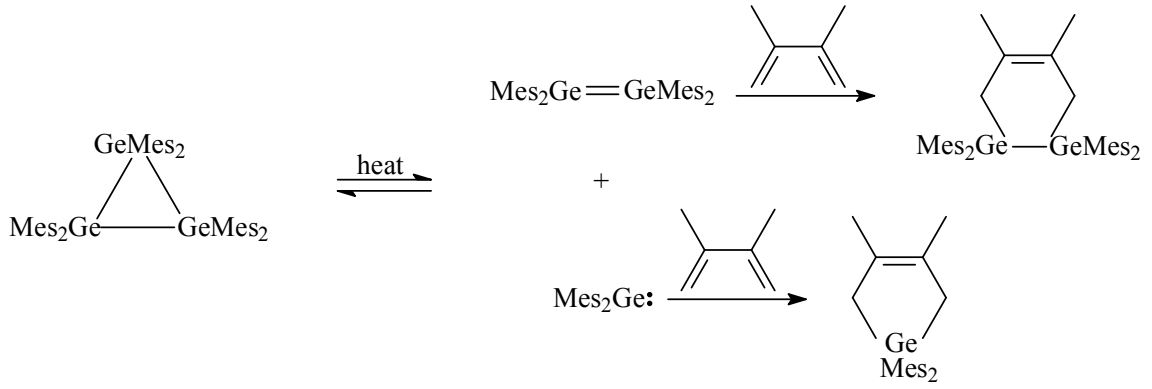

Scheme 7. Formation of tetramesityldigermene and dimesitylgermylene and their cycloaddition with 2,3-dimethylbuta-1,3-diene to yield 1,2-digermacyclohex-4-ene and germacyclopent-3-ene.[12]

These reactions set the precedent for thermal decomposition to yield germylenes and digermenes. The short-lived monomeric species, such as Me_2Ge and Ph_2Ge are highly reactive and tend to polymerize

quickly, and so to be studied they are isolated in a hydrocarbon matrix at 77 K.[3] In order to impede the rapid polymerization that most monomeric germylenes tend to undergo, bulky ligands can also be used to stabilize the germylene either kinetically and/or thermodynamically. The use of these bulky ligands, including R = $[CH(SiMe_3)_2]_2$ or $[N(Bu^t)]_2SiMe_2$, can lead to monomeric germylene species which are in equilibrium with their digermenes. The use of even bulkier ligands, such as R = 2,4,6-Bu^t_3-Ph has been shown to yield stable monomers at -10 °C. Additionally, there are a variety of other bulky ligands that can be used to stabilize the monomeric germylenes such as aryl, alkyl, amido, aryloxo and arylthiolato groups;[4] and, of these, the amido ligands have proved useful when they incorporate bulky trimethylsilyl substituents. Although most germylenes are dimeric, $Ge[N(SiMe_3)_2]_2$ is monomeric at room temperature.

Typically, $Ge[N(SiMe_3)_2]_2$ was prepared by the reduction of germanium tetrachloride with tributyltin hydride to generate trichlorogermanium hydride as an intermediate which then loses hydrogen chloride to give dichlorogermanium·1,4-dioxane which is subsequently reacted with two equivalents of lithium hexamethyldisilazane to yield the desired germylene along with two equivalents of lithium chloride and 1,4-dioxane as the by-products (**Scheme 8**).[5] The acidic proton in $HGeCl_3$, however, results in side reactions which often diminish the yield so in an effort to improve upon this method E. J. Roskamp and coworkers established a synthesis of $Ge[N(SiMe_3)_2]_2$ through a triphenylphosphoniumtrichlorogermanate intermediate in 1992. This method involves a multistep synthesis beginning with the reaction of triphenylphosphine with germanium tetrachloride and tributyltin hydride in diethyl ether at room temperature to yield the triphenylphosphoniumtrichlorogermanate and tributyltinchloride (**Scheme 9**).[6] This

triphenylphosphoniumtrichlorogermanate is then reacted with triethylamine to yield triethylammoniumtrichlorogermanate and triphenylphosphine (**Scheme 10**).[6] Lastly, triethylammoniumtrichlorogermanate is reacted with three equivalents of lithium hexamethyldisilazane to afford $Ge[N(SiMe_3)_2]_2$ in 70 – 77 % yield as well as triethylamine, lithium chloride and hexamethyldisilazane as by-products (**Scheme 11**).[6] The benefit of this synthesis is the fact that the by-products that are produced are volatile which leads to a more facile work-up.[6]

$$GeCl_4 + Bu_3SnH \xrightarrow[-\ Bu_3SnCl]{\text{Dioxane}} [HGeCl_3] \xrightarrow[-\ HCl]{} GeCl_2{\cdot}\text{dioxane}$$

$$GeCl_2{\cdot}\text{1,4-dioxane} + 2\ LiNR_2 \longrightarrow Ge(NR_2)_2 + 2\ LiCl + \text{1,4-dioxane}$$

Scheme 8. Previous preparation of $Ge[N(SiMe_3)_2]_2$. $NR_2 = N(SiMe_3)_2$.[5]

$$Ph_3P + GeCl_4 \xrightarrow[Et_2O,\ RT]{nBu_3SnH} Ph_3\overset{+}{P}H\ \overset{-}{G}eCl_3$$

Scheme 9. Reaction of triphenylphosphine with germaniumtetrachloride and tributyltinhydride.

$$Ph_3\overset{+}{P}H\ \overset{-}{G}eCl_3 + Et_3N \xrightarrow[RT]{CH_2Cl_2} Et_3\overset{+}{N}H\ \overset{-}{G}eCl_3 + Ph_3P$$

Scheme 10. Reaction of triphenylphosphoniumtrichlorogermanate with triethyl amine.

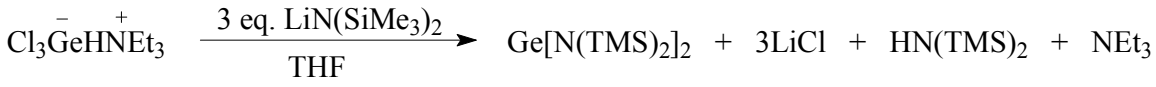

Scheme 11. Reaction of triethylammoniumtrichlorogermanate with three equivalents of lithium hexamethyldisilazane.

In $Ge[N(SiMe_3)_2]_2$ and other germylenes, a vacant p-orbital is able to accept electron density from a lewis basic species, rendering it a lewis acid while the lone pair of electrons housed in a sp^2 orbital is available for reaction as a lewis base.[7] The presence of both the lone pair of electrons and the vacant p-orbital allows for the formation of both di- and tetra-valent compounds. Bis[bis(trimethylsilyl)amido]germanium(II), ($Ge[N(SiMe_3)_2]_2$) and bis(bis-2,4,6-triisopropylphenyl)Ge(II) ($[Ge(Trip)_2]_2$) are two examples of germanium(II) containing compounds.[7] The divalent nature of these species arises from the careful selection of ligands. In the case of $Ge[N(SiMe_3)_2]_2$, the $-N(SiMe_3)_2$ groups are selected due to the fact that they are electron withdrawing, bulky, free of β-hydrogens, and soluble in hydrocarbons due to the presence of the methyl groups.[8] The electron withdrawing nature of the trimethylsilylamido groups causes germanium to become electron deficient which leads to the stabilization of the divalent species because the lone pair of electrons is less reactive. The bulky nature of the $-N(SiMe_3)_2$ groups kinetically stabilizes metals with low coordination numbers by inhibiting access to the metal center. The absence of any β-hydrogens and the presence of a β-silicon impedes metal-amide decomposition due to the energetically unfavorable β-elimination pathway. The solubility of these ligands that posses the trimethylsilylamido

groups in hydrocarbon solvents are enhanced due to the hydrophobic nature of the methyl groups.[8]

The ligand $[CH(SiMe_3)_2]_2$ provides substantial bulk which helps to protect the metal center against dimerization; there are no β-hydrogens present which removes the possibility of β-hydride elimination and the presence of a large number of methyl groups provides hydrocarbon solubility. The synthesis of $Ge[CH(SiMe_3)_2]_2$ first involves the formation of $Li[CH(SiMe_3)_2]$ from $(Me_3Si)_2CHCl$ with two equivalents of lithium metal also yielding lithium chloride. The bis(trimethylsilyl)methyllithium is then reacted with $Ge[N(SiMe_3)_2]_2$ to yield $Ge[CH(SiMe_3)_2]_2$ (**Scheme 12**). The Ge-Ge bond length in the digermene measures 2.347(2) Å, while the C – Ge – C bond angle measures 112.5(3) °. The crystal structure of $Ge[N(SiMe_3)_2]_2$ is shown in **Figure 1**. This germylene takes advantage of the use of bulky, electron withdrawing trimethylsilylamido groups pioneered by Bürger and Wannagat[8] to stabilize the monomeric state, and $Ge[N(SiMe_3)_2]_2$ is a stable, low-melting, thermochromic, yellow/orange colored monomer in the liquid phase at room temperature that becomes colorless at -196 °C.[7] The X-ray crystal structure shows a bent singlet state geometry rather than a linear triplet state (**Figure 2**).[9] The germanium – nitrogen bond distances measure 1.873(5) and 1.878(5) Å, while the N – Ge – N angle measures 107.1(2) °.[10] The germylene $Ge[N(SiMe_3)_2]_2$ is monomeric in the solid state while $\{Ge[CH(SiMe_3)_2]_2\}_2$ is dimeric, and the dimer forms through a double donor-acceptor bond (**Figure 3**).

$$(Me_3Si)_2CHCl + 2\,Li \longrightarrow Li[CH(SiMe_3)_2] + LiCl$$

$$2\,Li[CH(SiMe_3)_2] + Ge[N(SiMe_3)_2]_2 \longrightarrow Ge[CH(SiMe_3)_2]_2 + 2\,Li[N(SiMe_3)_2]$$

Scheme 12. Synthesis of $Ge[CH(SiMe_3)_2]_2$.[9]

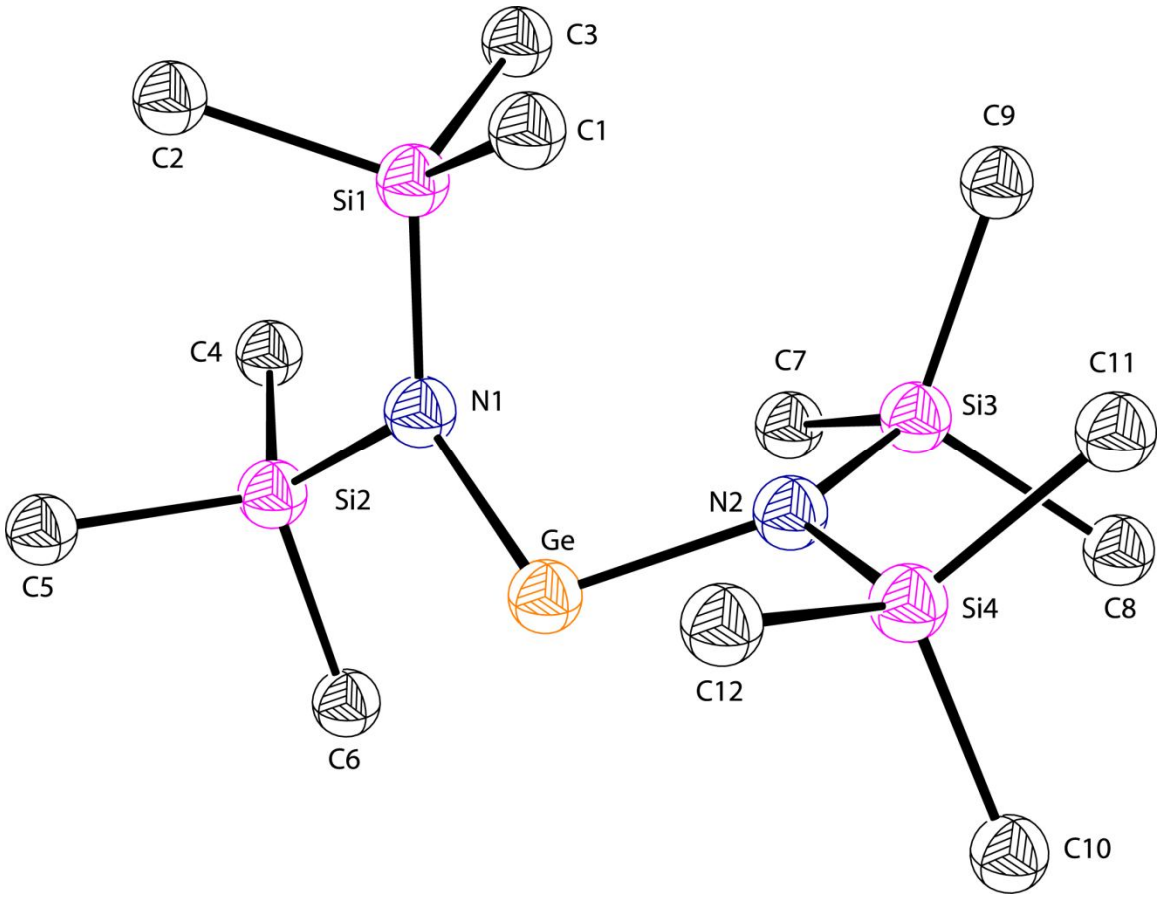

Figure 1. X-ray crystal structure of $Ge[N(SiMe_3)_2]_2$.

(*a*) (*b*)

Figure 2. Expected structures for monomeric $M(NR^1R^2)_2$. (*a*) singlet and (*b*) triplet ground state.

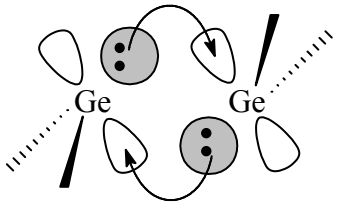

Figure 3. Schematic of the double donor-acceptor bond that yields $\{Ge[CH(SiMe_3)_2]_2\}_2$.

This can be attributed to the fact that when an electronegative ligand such as $-[N(SiMe_3)_2]_2$ is used, there is an increase in positive charge on Ge and this leads to a contraction and stabilization of the 4s lone-pair of electrons centered on Ge, and consequently leads to an increased singlet/triplet energy difference.

A variety of reactions is known and exemplify the versatility of these reagents (**Schemes 13 - 16**). These reactions involve both germylenes and the related stannylenes (MX_2), with transition metal compounds of the general formula, L_nM'-X', and the products can be categorized into one of seven types. These include MX_2 (*i*) acting as a terminal ligand, (*ii*) acting as a bridging ligand, (*iii*) inserting into a M' – X' bond which

generates a new ligand with the formula MX_2X', (*iv*) reacting as a *N*-centered nucleophile with respect to a transition metal-hydride containing compound to generate a new MX_2 species where X = $M'L_n$, (*v*) can act as a X^- transfer reagent, (*vi*) oxidatively adding to the M' center in a low oxidation state via a C – H bond insertion in $M(NR_2)_2$ with concomitant cyclometallation or (*vii*) acting as a reducing agent.

The use of $Ge[N(SiMe_3)_2]_2$ as a precursor for other germanium(II) materials has been explored, such as serving as a source of germanium(II) for the formation of calixarene complexes and in germanium aryloxides. This has been evidenced through the reaction of $Ge[N(SiMe_3)_2]$ with *p*-Bu^{t}calix[8]arene which yielded {*p*-Bu^{t}calix[8]arene}Ge_4 that contains two Ge_2O_2 rhombi as well as reaction with $HOC_6H_3Bu^t$-2-Me-6 which generates the germanium(II) aryloxide complex, $Ge(OC_6H_3Bu^t\text{-}2\text{-}Me\text{-}6)_2$ which is monomeric in the solid state. The cluster complexes $Ge_8(\mu_3\text{-}O)_6(OC_6H_3Bu^t\text{-}2\text{-}Me\text{-}4)_4$ and $[Ge_4O_3(OC_6H_3Bu^t\text{-}2\text{-}Me\text{-}4)_4 \cdot NH_3]_2$ can also be prepared from $Ge[N(SiMe_3)_2]_2$ and $HOC_6H_3Bu^t$-2-Me-4.

Table 1. λ_{max} (nm) data for selected germylenes.[3]

RR'Ge	UV_{max} (nm)	Source
R = R' = Me	420	**1**
R = R' = Bu	440	**1**
R = Ph; R' = Me	440	**1**
R = R' = Ph	466	**3**
R = R' = Tol	471	**3**
R = R' = Xy	543	**3**
R = R' = Ar	544	**3**
R = R' = Mes	550	**3**
R = R' = Ar'	558	**3**
R = Mes; R' = Bu^t	508	**3**

1 = 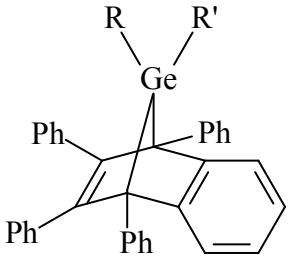

3 = R,R'Ge($SiMe_3$)$_2$

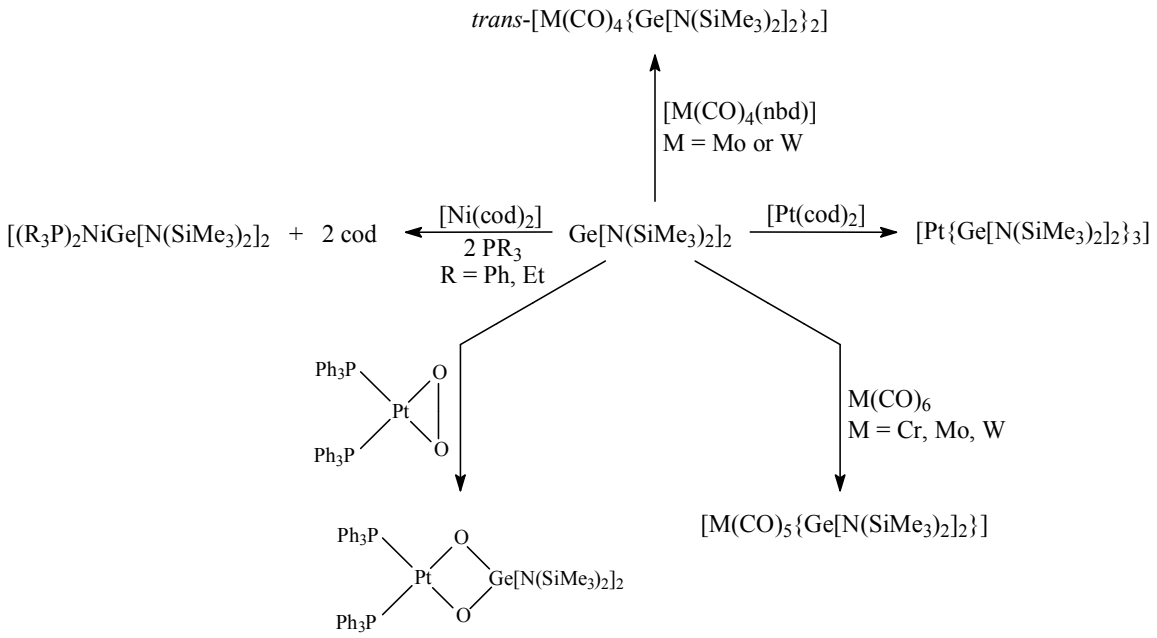

Scheme 13. Reactions of $Ge[N(SiMe_3)_2]_2$ with various reagents demonstrating the versatility of the amide.[4, 8,13]

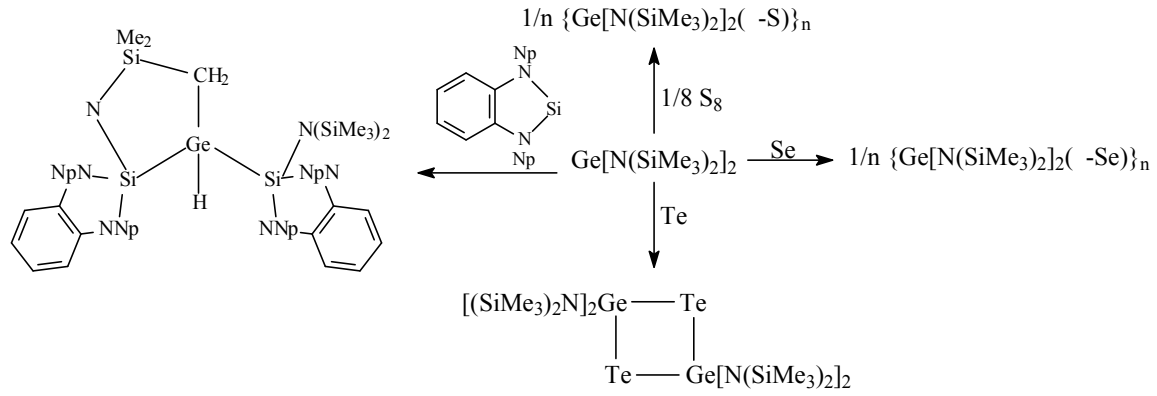

Scheme 14. Reactions of $Ge[N(SiMe_3)_2]_2$ with group 16 elements.[14,15]

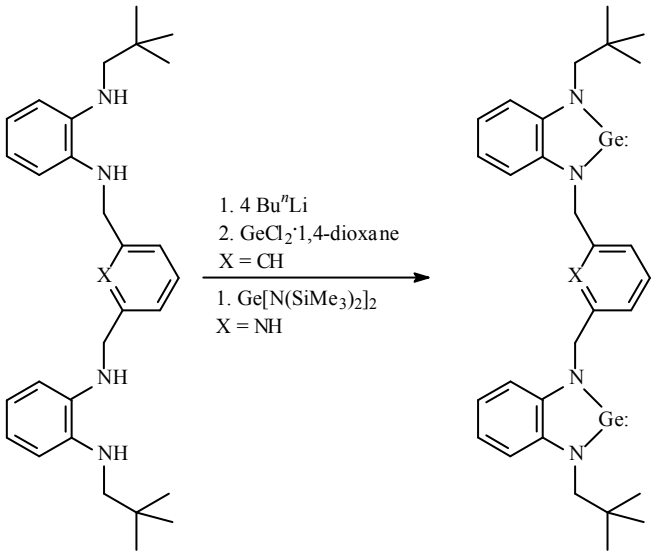

Scheme 15. Formation of bis(germylenes).[16]

$$Ge[CH(SiMe_3)_2]_2 \xrightarrow[2\ PR_3]{[Ni(cod)_2]} [(R_3P)_2NiGe[CH(SiMe_3)_2]_2 + 2\ cod$$

R = Ph or Et

Scheme 16. Reaction of $Ge[CH(SiMe_3)_2]_2$ with nickel dicyclooctadiene.[8]

References

(1) James, S. W.; Tatam, R. P. *Meas. Sci. Technol.* **2003**, *14*, R49.
(2) Allsop, T.; Zhang, L.; Bennion, I. *Optics Communications* **2001**, *191*, 181.
(3) Neumann, W. P. *Chem. Rev.* **1991**, *91*, 311-334.
(4) Lappert, M. F.; Rowe, R. S. *Coordination Chemistry Reviews* **1990**, *100*, 267.
(5) Chorley, R. W.; Hitchcock, P. B.; Lappert, M. F.; Leung, W. P.; Power, P. P.; Olmstead, M. M. *Inorg. Chim. Acta* **1992**, 203.
(6) Zhu, Q.; Ford, K. L.; Roskamp, E. J. *Heteroatom Chemistry* **1992**, *3*, 647.
(7) Cotton, J. D.; Davidson, P. J.; Lappert, M. F. *Dalton Trans.* **1976**, *21*, 2275.
(8) Litz, K. E.; Bender IV, J. E.; Kampf, J. W.; Banaszak Holl, M. M. *Angew. Chem. Int. Ed. Engl.* **1997**, *36*, 496.
(9) Davidson, P. J.; Harris, D. H.; Lappert, M. F. *Dalton Trans.* **1976**, *21*, 2268.
(10) Power, P. P. *Chem. Rev.* **1999**, *99*, 3463.
(11) Ando, W.; Tsumuraya, T. *Tetrahedron Lett.* **1986**, *27*, 3251.
(12) Ando, W.; Tsumuraya, T. *J. Chem. Soc., Chem. Commun.* **1989**, 770.
(13) Litz, K. E.; Banaszak Holl, M. M.; Kampf, J. W.; Carpenter, G. B. *Inorg. Chem.* **1998**, *37*, 6461.
(14) Hitchcock, P. B.; Jasim, H. A.; Lappert, M. F.; Leung, W.; Rai, A. K.; Taylor, R. E. *Polyhedron* **1991**, *10*, 1203.
(15) Gehrhus, B.; Jitchcock, P. B.; Lappert, M. F. *Angew. Chem. Int. Ed. Engl.* **1997**, *36*, 2514.
(16) Hahn, F. E.; Zabula, A. V.; Pape, T.; Hepp, A. *Eur. J. Inorg. Chem.* **2007**, 2405.

Chapter Two: Synthesis of the germanium(II) calixarene {*p*-Bu$^t_8$calix[8]arene}Ge$_4$ and its reaction with $Fe_2(CO)_9$: Generation of the germanium(II)/iron(0) complex {*p*-Bu$^t_8$calix[8]arene}Ge$_4$[Fe(CO)$_4$]$_2$

Introduction

Germanium(II) aryloxide compounds are uncommon,[1-9] and among these only a few macrocyclic germanium(II) calixarene complexes have been reported.[1-4] These complexes contain Ge_2O_2 rhombi, which were observed in two different germanium(II) calix[4]arene complexes[1,2] as well as in the germanium aryloxide compounds, $[(Pr^i_2\text{-}2,6\text{-}C_6H_3O)_2Ge]_2$ and $[(Me_3\text{-}2,4,6\text{-}C_6H_2O)_2Ge]_2$,[5] while the reaction of $Ge[N(SiMe_3)_2]_2$ with calix[6]arene furnished a complex containing a Ge_2NO rhombus, $(C_6H_3)_6(CH_2)_6O_3Ge_2(NH_2)\{OSi(H)(NH_2)_2\}_2OSiMe_3$.[4] Germanium(II) calixarene compounds have the potential to serve as macrocyclic platforms for the support of multiple transition metal complexes, since each germanium center present in these species bears a lone pair of electrons that are available for coordination to unsaturated transition metal centers. These mixed main group/transition metal systems might exhibit intermetallic communication, and could function as switchable optical, electronic and magnetic materials.

The reaction of $Ge[N(SiMe_3)_2]_2$ with *para*-unsubstituted calix[8]arene gives the germanium(II) calixarene complex {calix[8]}Ge$_4$ [1]. The calix[8]arene complex exhibits a bowl-shaped structure that contains two Ge_2O_2 rhombohedral fragments, and compound

1 reacts with $Fe_2(CO)_9$ to give the octairon compound which contains four $GeFe_2$ triangles, {calix[8]arene}$[GeFe_2(CO)_8]_4$ (**2**). This reaction proceeds via a redox reaction that involves the oxidation of all four germanium(II) centers to germanium(IV) with the concomitant reduction of $Fe_2(CO)_9$ to generate four $Fe_2(CO)_8^{2-}$ fragments.[1] The reactivity of the *para-tert*-butyl substituted calix[8]arene, {*p*-Bu^t_8calix[8]arene}Ge_4 (**3**), with $Fe_2(CO)_9$ differs from that of **1**. The *para-tert*-butyl substituted complex {*p*-Bu^t_8calix[8]arene}Ge_4 (**3**), was prepared by the protonolysis reaction of *p*-Bu^t_8calix[8]arene with four equivalents of $Ge[N(SiMe_3)_2]_2$. Complex **3** reacts with $Fe_2(CO)_9$ to yield the germanium(II) complex {*p*-Bu^t_8calix[8]arene}$Ge_4[Fe(CO)_4]_2$ (**4**). The X-ray crystal structures of **3** and **4** were determined and both contain Ge_2O_2 rhombi that are connected to their respective calixarene macrocyclic frameworks by both terminal and bridging phenolic oxygen atoms.

Results and Discussion

The germanium(II) calixarene {*p*-Bu^t_8calix[8]arene}Ge_4 (**3**) was obtained in 94% yield by the protonolysis reaction between four equiv. of $Ge[N(SiMe_3)_2]_2$ and *para-tert*-butylcalix[8]arene (**Scheme 1**). Crystals of **3** sufficient for X-ray analysis were obtained from a hot hexane solution. The molecular structure of **3** is shown as an ORTEP diagram in **Figure 1** and selected bond distances and angles are collected in **Table 1**. Compound **3** co-crystallizes with three molecules of hexane in the unit cell, and the two halves of the molecule are related by a C_2 axis resulting in two equivalent Ge_2O_2 rhombi. One of the hexane molecules also resides on the C_2 axis. This contrasts with the structure of the

para-unsubstituted species {calix[8]arene}Ge_4 **(1)**, in which the geometries of the two individual Ge_2O_2 rhombi are slightly different.

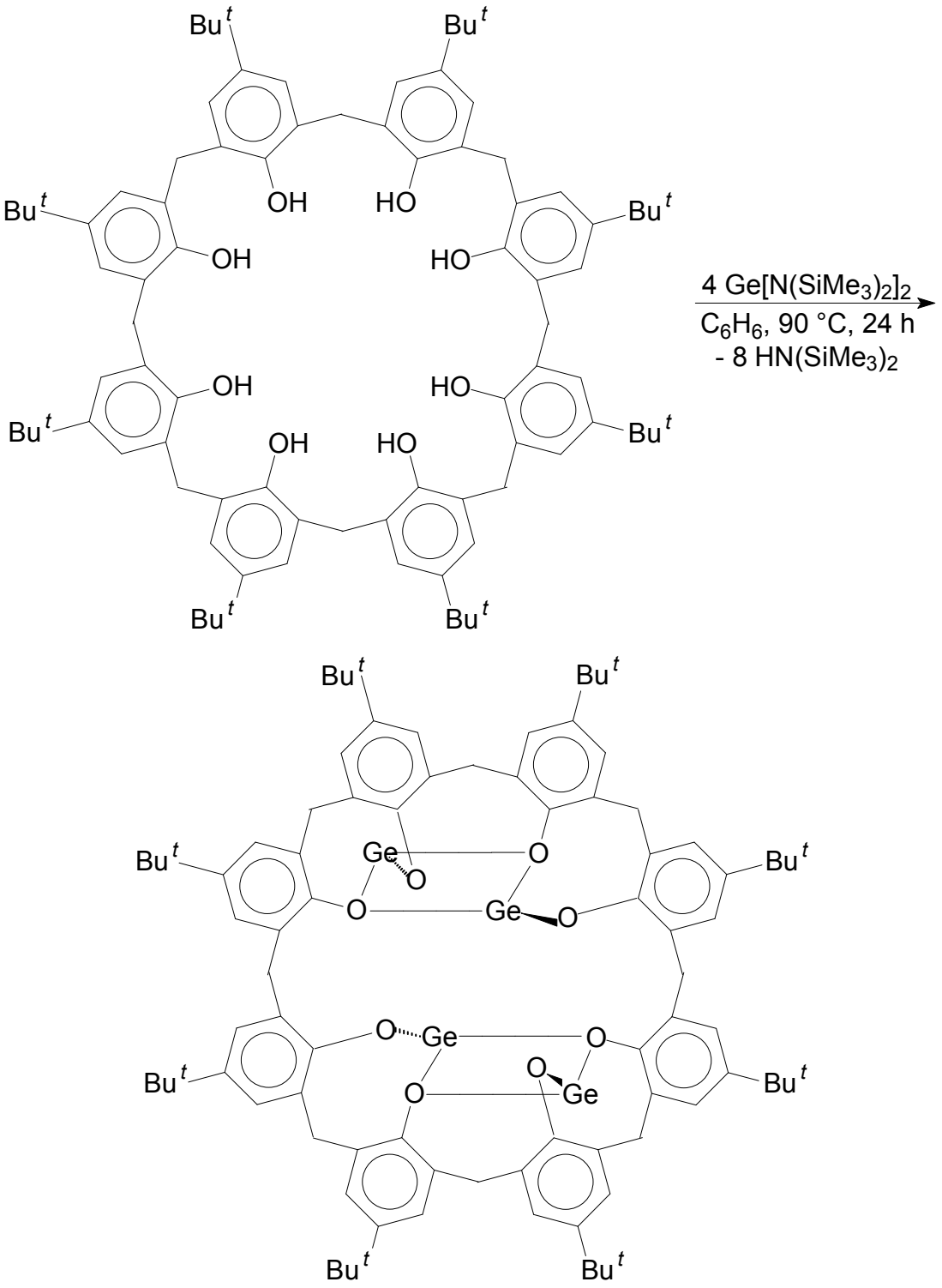

3, 94 %

Scheme 1. Reaction of *para-tert*-butylcalix[8]arene and $Ge[N(SiMe_3)_2]_2$

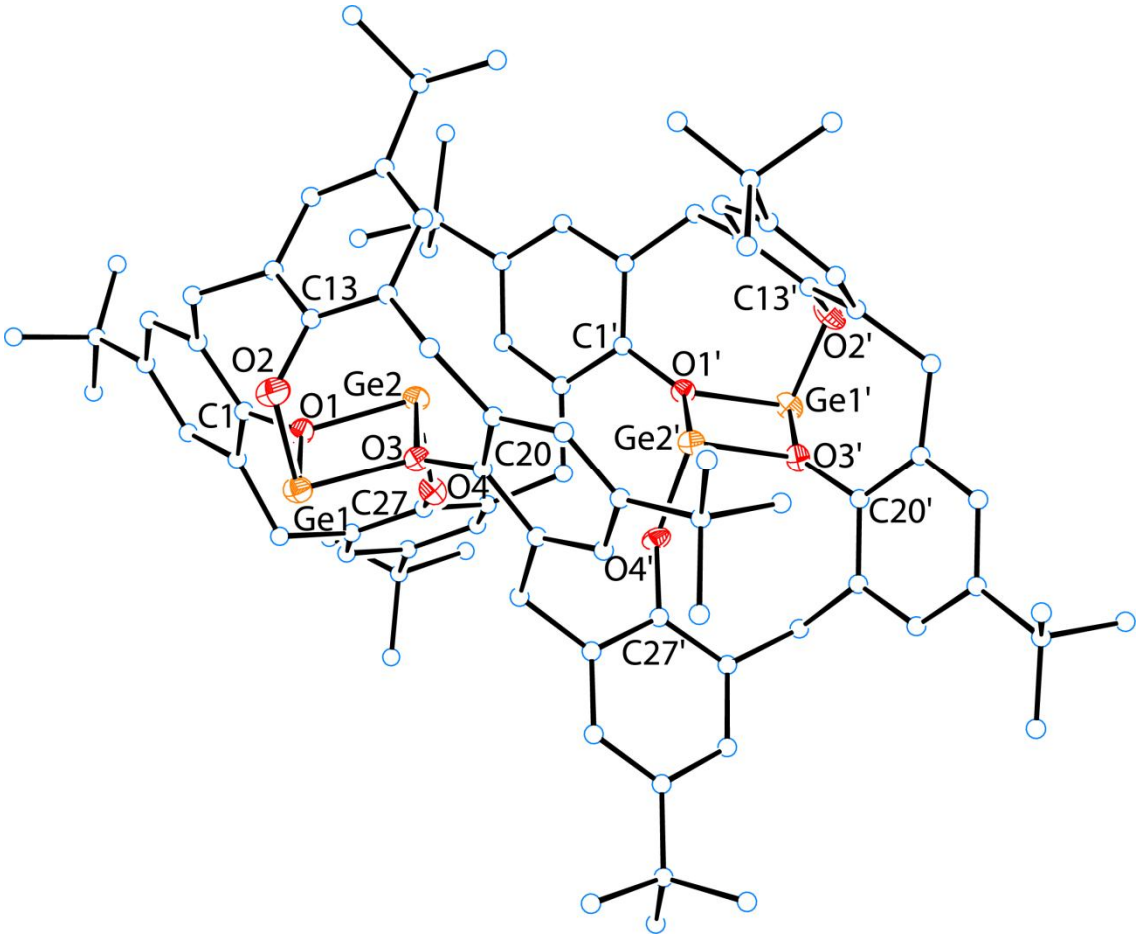

Figure 1. ORTEP diagram of **3**·3 C_6H_{14}. Germanium atoms are shown in orange, oxygen atoms in red and carbon atoms as white spheres. Hexane solvent molecules are not shown.

Table 1. Selected bond lengths (Å) and angles (°) for **3**·3 C_6H_{14}

Ge(1) – O(1)	2.008(3)	O(1) – Ge(1) – O(2)	93.5(1)
Ge(1) – O(2)	1.834(3)	O(1) – Ge(1) – O(3)	73.6(1)
Ge(1) – O(3)	1.980(3)	O(2) – Ge(1) – O(3)	90.6(1)
Ge(2) – O(1)	2.008(3)	O(1) – Ge(2) – O(3)	73.1(1)
Ge(2) – O(3)	2.000(3)	O(1) – Ge(2) – O(4)	91.8(1)
Ge(2) – O(4)	1.831(3)	O(3) – Ge(2) – O(4)	90.4(1)
O(1) – C(1)	1.394(5)	Ge(1) – O(1) – Ge(2)	106.0(1)
O(2) – C(13)	1.376(5)	Ge(1) – O(3) – Ge(2)	107.4(1)
O(3) – C(20)	1.391(5)	C(1) – O(1) – Ge(1)	124.7(2)
O(4) – C(27)	1.372(5)	C(1) – O(1) – Ge(2)	128.8(2)
		C(20) – O(3) – Ge(1)	134.1(2)
		C(20) – O(3) – Ge(2)	118.5(2)
		C(13) – O(2) – Ge(1)	120.0(2)
		C(27) – O(4) – Ge(2)	132.3(2)

The average Ge - O_{term} and Ge - O_{br} bond distances in **3** are 1.833(3) and 1.999(3) Å (respectively), and are nearly identical with those of compound **1** which has Ge – O_{term} distances averaging 1.833 Å and Ge – O_{br} distances averaging 2.000 Å (respectively). The average O_{br} – Ge - O_{br} bond angle of the Ge_2O_2 rhombi in **3** is 73.3(1) °, and the O_{br} – Ge - O_{term} bond angles have an average value of 91.6(1) °, which is close to the expected value of 90 °.

Although the average O_{br} – Ge - O_{br} bond angle in **3** (73.3(1) °) is similar to that of **1** (72.9(2) °), the average O_{br} – Ge - O_{term} bond angle in **3** (91.6(1) °) is significantly different than that of **1** (93.1(2) °). This structural dissimilarity is a result of the steric repulsions of the *tert*-butyl groups attached to the periphery of complex **3**, resulting in a more congested structure for **3** versus the *para*-unsubstituted compound **1**, which contains only aromatic protons in the *para*-positions (**Figures 2 and 3, respectively**). Maximization of the distance between the *tert*-butyl groups in **3** forces several of the *para*-carbon atoms of the eight aromatic rings in **3** closer together than in compound **1**. The distances between the *para*-carbon atoms at the top (C(10) – C(10')), and bottom (C(24) – C(24')) of the calix[8]arene bowl structure measure 6.26(2), and 8.42(2) Å (respectively) in **3**, while the corresponding distances in **1** are 6.88(2) Å, and 8.92(2) Å (**Figures 4 and 5, respectively**). The congested geometry in **3** is enforced by the presence of the *para*-*tert*-butyl groups thus results in a more acute O_{br} – Ge –O_{term} bond angle in this molecule.

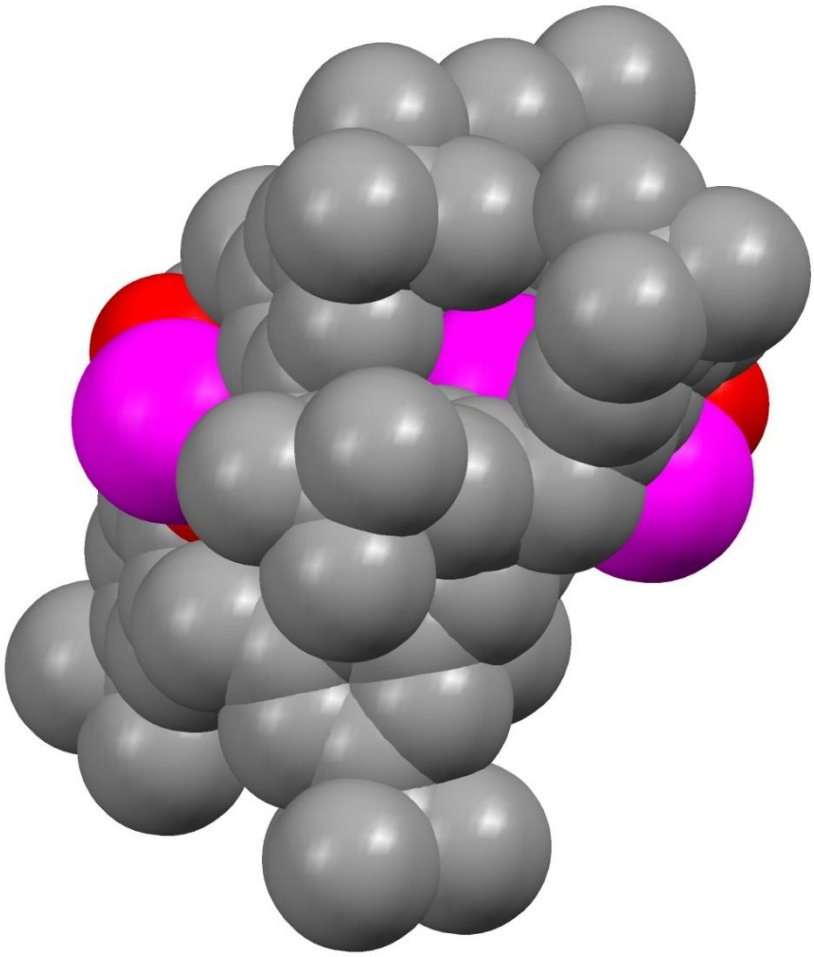

Figure 2. Space-filling diagram for compound **3**. Germanium atoms are shown in purple, oxygen atoms in red and carbon atoms in gray.

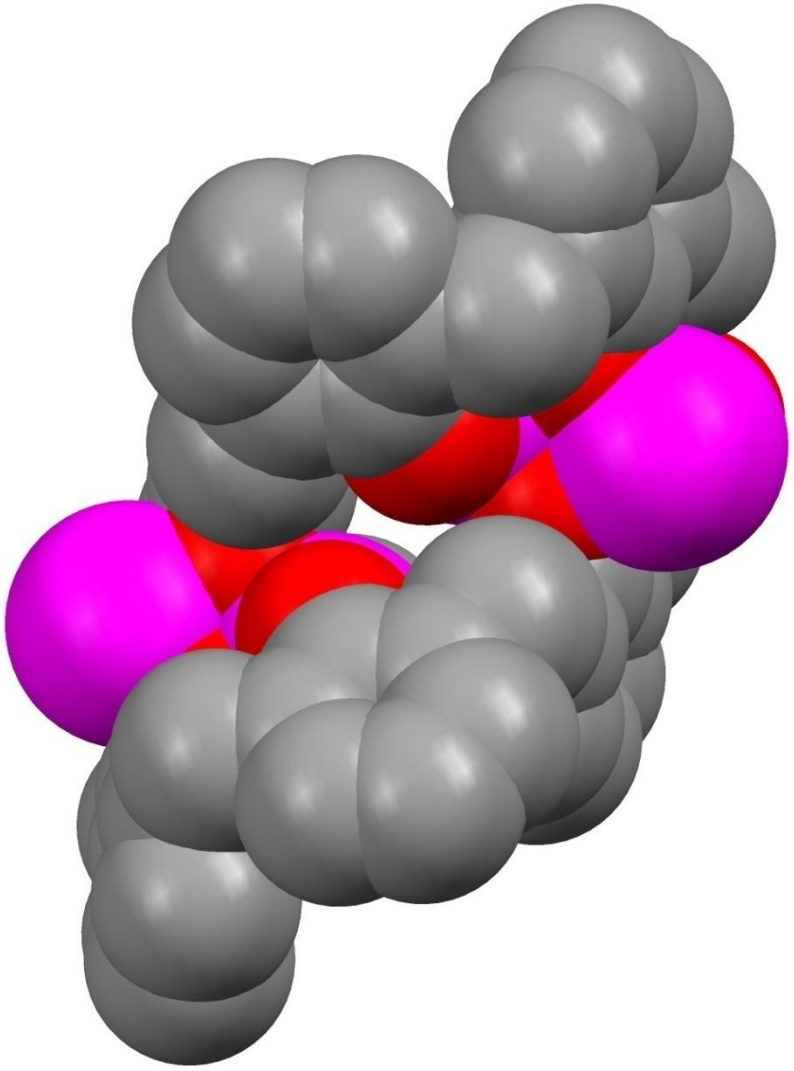

Figure 3. Space-filling diagram for compound **1**. Germanium atoms are shown in purple, oxygen atoms in red and carbon atoms in gray.

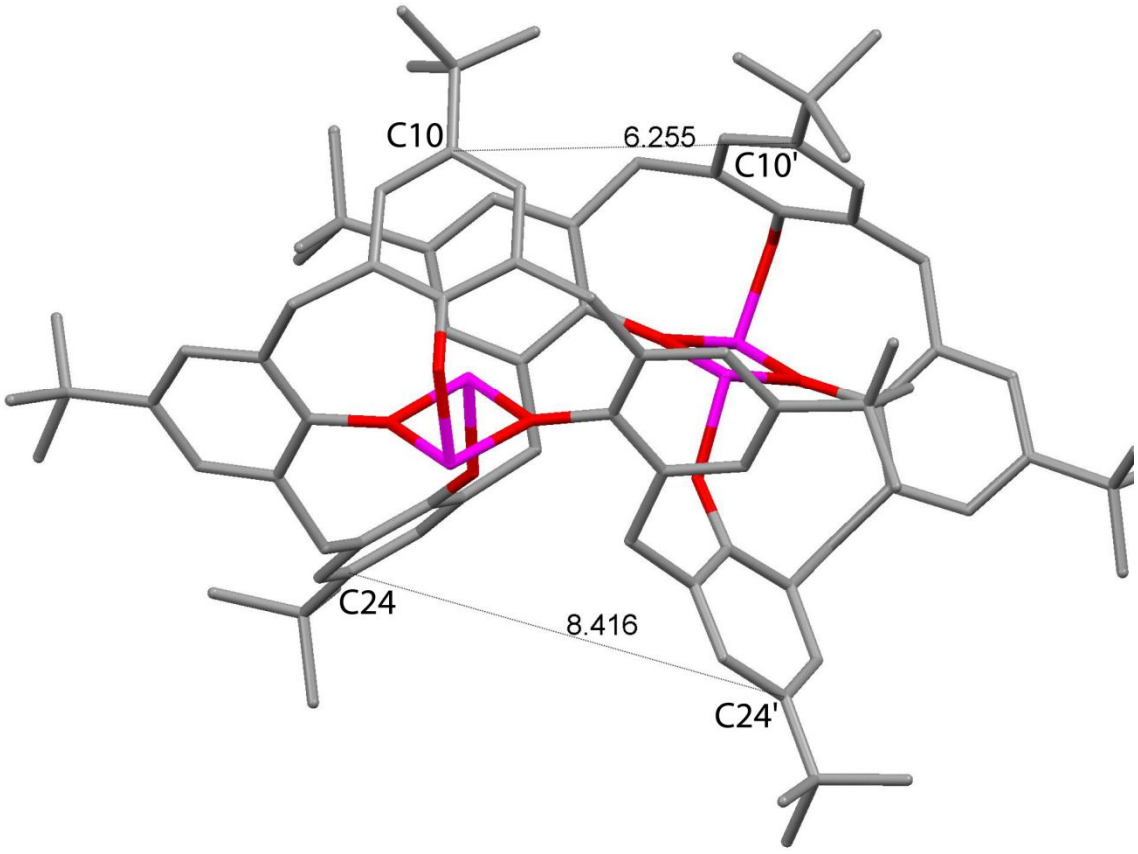

Figure 4. Wireframe drawing of compound **3**. Germanium atoms are shown in purple, oxygen atoms in red and carbon atoms in gray.

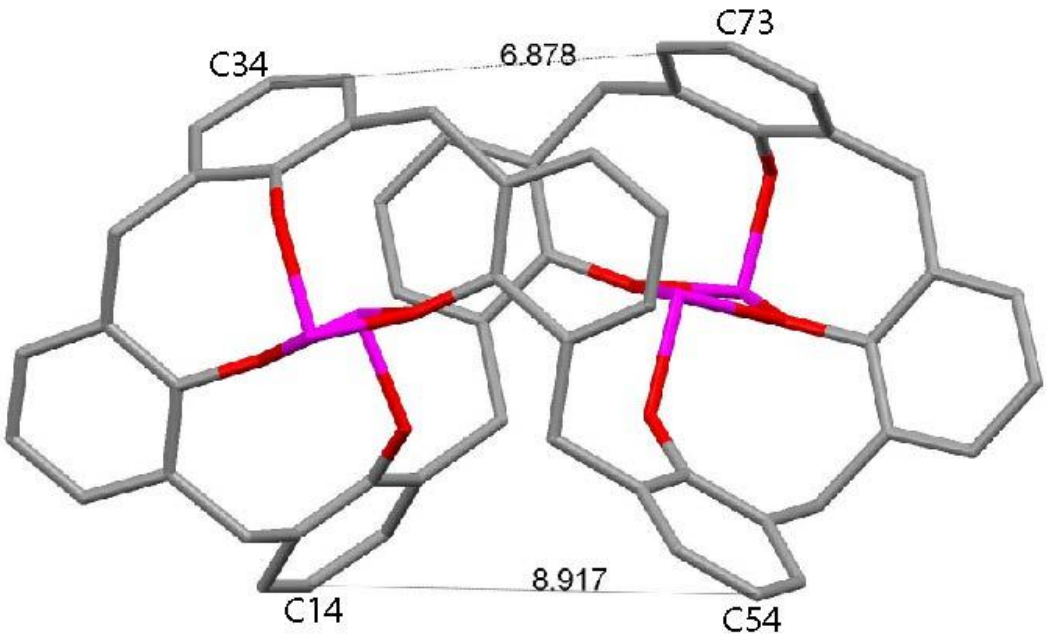

Figure 5. Wireframe drawing of compound **1**. Germanium atoms are shown in purple, oxygen atoms in red and carbon atoms in gray.

The ^{1}H NMR spectrum of **3** recorded in benzene-d_6 contains eight resonances for the methylene protons, which appear as doublets since the two protons of each of the individual -CH_2- groups are magnetically non-equivalent. The C_2-axis present in compound **3** results in the observation of eight, rather than sixteen, doublets. These are grouped into two sets of four resonances in the chemical shift range δ 5.90 – 4.61 ppm and a second grouping of four doublets ranging from δ 3.80 – 3.34 ppm. The four doublets corresponding to the eight protons which are directed inward toward the central cavity of **3** are shifted downfield due to their proximity to the eight aryloxide oxygen atoms, relative to those corresponding to the eight protons pointing away from the central cavity. This proximity results in anisotropic effects on the methylene protons from the aromatic rings, oxygen atoms and large germanium atoms. The more close contacts experienced by the methylene protons, the higher the degree of anisotropy they experience, and therefore the farther downfield they are shifted. In the solid state structure of **3**, H(14a) has one close contact with O(2) measuring 2.491 Å. There are two close contacts between H(21b) and O(3) and O(4) that measure 2.459 and 2.545 Å respectively while H(28b) has one close contact with O(4) measuring 2.221 Å. All of these distances are within the sum of the van der Waals radii of hydrogen and oxygen, which is 2.60 Å.

The protons attached to C(28) and C(28') are directed inward toward the Ge_2O_2 rhombi and result in the appearance of a doublet at δ 5.90 ppm (J = 17.6 Hz) in the ^{1}H NMR spectrum. There are two overlapping doublets that can be assigned to the four protons attached to C(14), C(14'), C(21) and C(21') that appear at δ 4.78 ppm (J = 12.8 Hz) which are directed inward toward the two Ge_2O_2 rhombi. There were no close

contacts present between the protons attached to C(7) and C(7') and the oxygen atoms and thus the doublet at δ 4.61 ppm is attributed to these protons. The remaining eight hydrogen atoms of the methylene groups that are directed outward from the two Ge_2O_2 rhombi give rise to four doublets in the range of δ 3.80 – 3.34 ppm. Figure **8** contains the ^{1}H NMR spectrum for these doublets. The doublet at δ 3.80 ppm is attributed to the protons of C(28) and C(28') with a close contact to O(1) of 2.945 Å, while the doublet observed at 3.34 ppm is attributed to the protons of C(7) and C(7') which have a single close contact measuring 3.203 Å. A similar pattern of eight resonances ranging from δ 5.83 – 3.24 ppm was observed in the ^{1}H NMR spectrum of **1**,[1] which is also C_2-symmetric in solution.

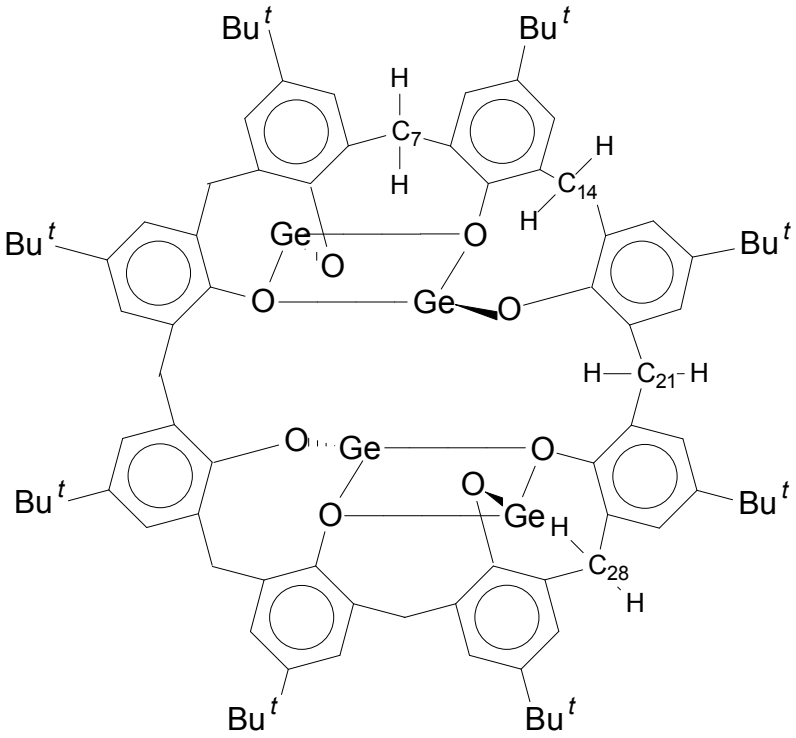

Figure 6. 2-D structure of **3** showing C_2-symmetry and carbon atom numbering scheme.

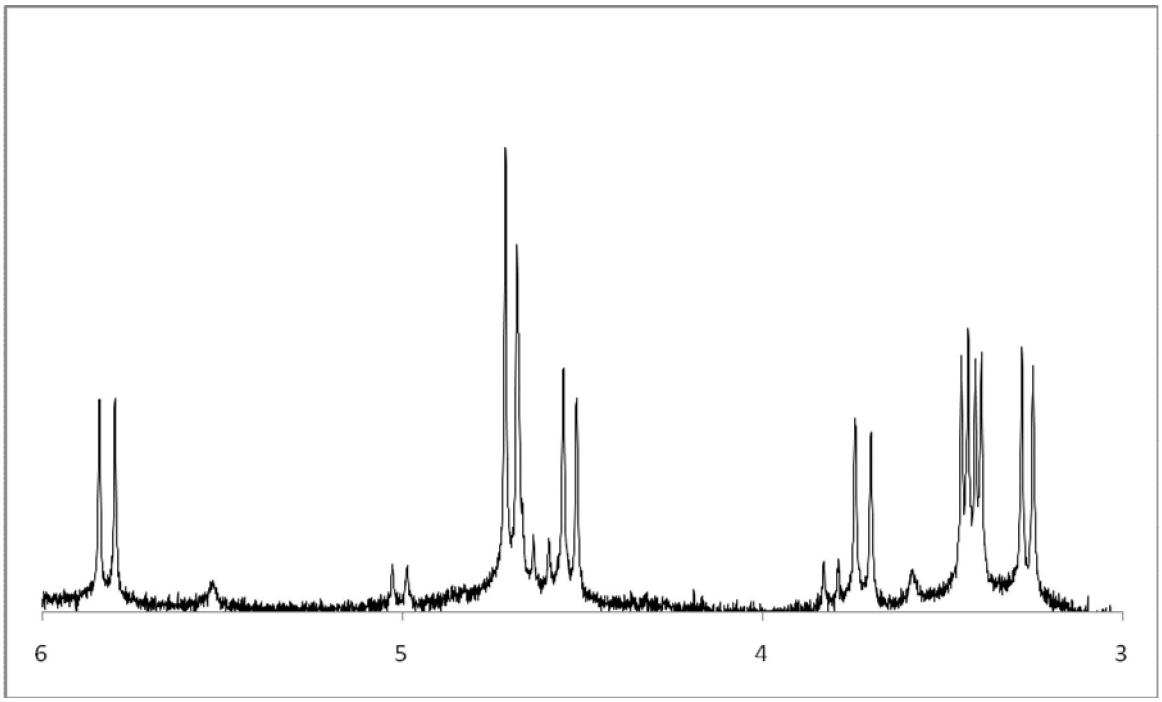

Figure 7. Methylene region from the ^{1}H NMR spectrum (C_6D_6, 25 °C) for compound **3**.

Four signals for the protons of the *tert*-butyl groups of **3** appear in the ^{1}H NMR spectrum at δ 1.41, 1.33, 1.32, and 0.87 ppm, indicating that each of the four pairs of symmetry-related *tert*-butyl groups are magnetically non-equivalent. The upfield resonance at δ 0.87 ppm arises from the protons of the *para*-*tert*-butyl groups bound to C(10) and C(10'), since these groups are directed inward toward the central cavity of compound **3,** and the protons experience anisotropic effects arising from the aromatic rings of the calix[8]arene system. The experienced magnetic anisotropy is due to the directional dependence of the *tert*-butyl groups relative to the aromatic rings that arises from the structural rigidity of the macrocycle, which is enforced by the presence of the two Ge_2O_2 rhombi. The protons from the *tert*-butyl groups experience three magnetic

fields, the applied field from the spectrometer, shielding from the valence electrons and the induced magnetic field due to the π-system of the aromatic rings. The π-system field can affect the chemical shift by either shielding or deshielding the hydrogen nuclei of the *tert*-butyl groups. The applied external field induces π-electron movement above and below the aromatic ring. This generates an opposing field at the center of the ring and a supporting field at the periphery of the ring. The protons in the supported regions, the region where the induced field is in the same direction as the external field, are deshielded because a weaker external field will bring about resonance for these nuclei. The protons in the opposing regions, where the induced field is opposite to the external field, are shielded because a stronger applied field is needed to bring about resonance for these nuclei. So, therefore the upfield signal at δ 0.87 ppm corresponds to the *tert*-butyl group which lies above the aromatic ring system.

The ^{13}C NMR spectrum of **3** also contains four signals for the methyl carbon atoms of the *para*-*tert*-butyl substituents at δ 32.3, 31.9, 31.5, and 31.0 ppm, while the carbon atoms of the four sets of symmetry-equivalent methylene groups appear at δ 34.4, 34.3, 34.2, and 34.0 ppm. The quaternary carbons of the *para*-*tert*-butyl groups appear as two overlapping resonances at δ 36.8, and 36.1 ppm. Since the structure of **3** is C_2-symmetric, twenty-four aromatic resonances are expected for the carbon atoms of the aromatic rings in the ^{13}C NMR spectrum of **3**, and these were observed in the chemical shift range of δ 152.4 – 124.8 ppm.

We have demonstrated that the reaction of **1** with $Fe_2(CO)_9$ yielded the ruby-red complex {calix[8]arene}$[GeFe_2(CO)_8]_4$ (**2**) that contains four $GeFe_2$ triangular moieties having two Ge – Fe single bonds and a Fe – Fe single bond (**Scheme 2a**).[1] The formation

of **2** resulted from a redox reaction involving oxidation of the four germanium(II) centers to germanium(IV) and concomitant reductive decarbonylation of $Fe_2(CO)_9$ to generate the four $[Fe_2(CO)_8]^{2-}$ fragments. The outcome of this reaction was different than that observed between the germanium(II) aryloxide $(Bu^t_2\text{-}2,6\text{-}Me\text{-}4\text{-}C_6H_2O)_2Ge$ and $Fe_2(CO)_9$, which yielded the iron complex **5** that contains a $Fe(CO)_4$ fragment and a dative Ge → Fe bond (**Scheme 2b**).[15]

The reaction of compound **3** with four equivalents of $Fe_2(CO)_9$ in benzene at 85 °C resulted in the formation of a yellow suspension that, after filtration and removal of the solvent *in vacuo*, yielded a yellow solid (**Scheme 3**). The outcome of the reaction of **3** with $Fe_2(CO)_9$ was clearly different than that of **1**, and recrystallization of the crude product from hot benzene furnished X-ray quality crystals which were shown to be the complex $\{p\text{-}Bu^t_8calix[8]arene\}Ge_4\{Fe(CO)_4\}_2$ (**4**). An ORTEP diagram and a wireframe drawing of **4** are shown in **Figures 8** and **9** (respectively) while selected bond distances and angles are collected in **Table 2**.

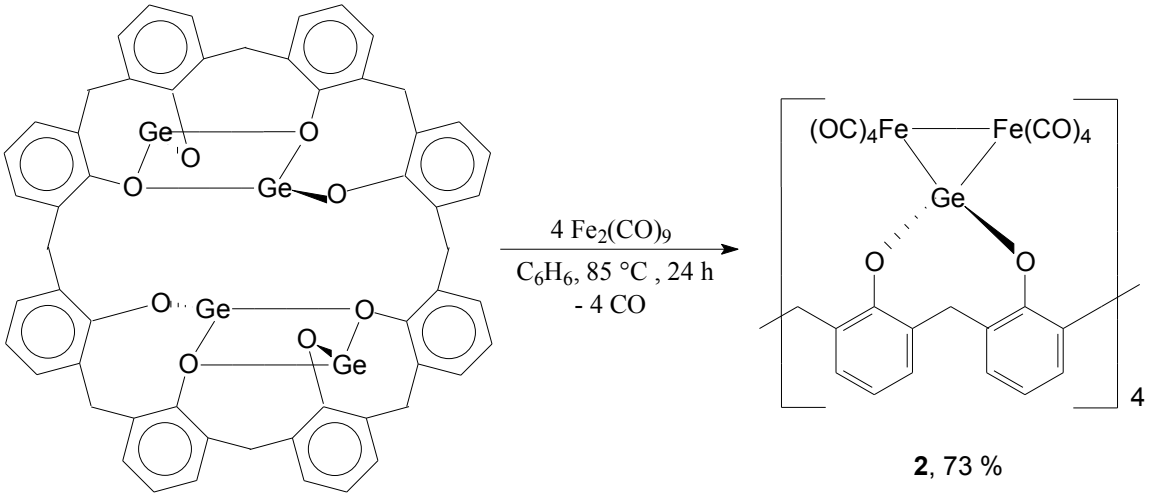

1

2, 73 %

Scheme 2a. Reaction of {calix[8]arene}Ge_4 with $Fe_2(CO)_9$.

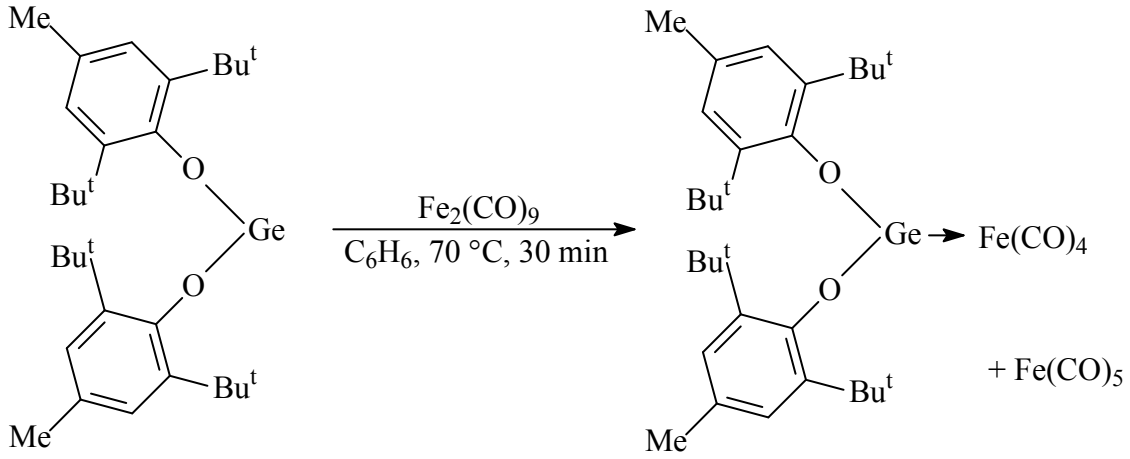

5, 18 %

Scheme 2b. Reaction of $Ge(OC_6H_2Bu^t_2$-2,6-Me-4 with $Fe_2(CO)_9$.

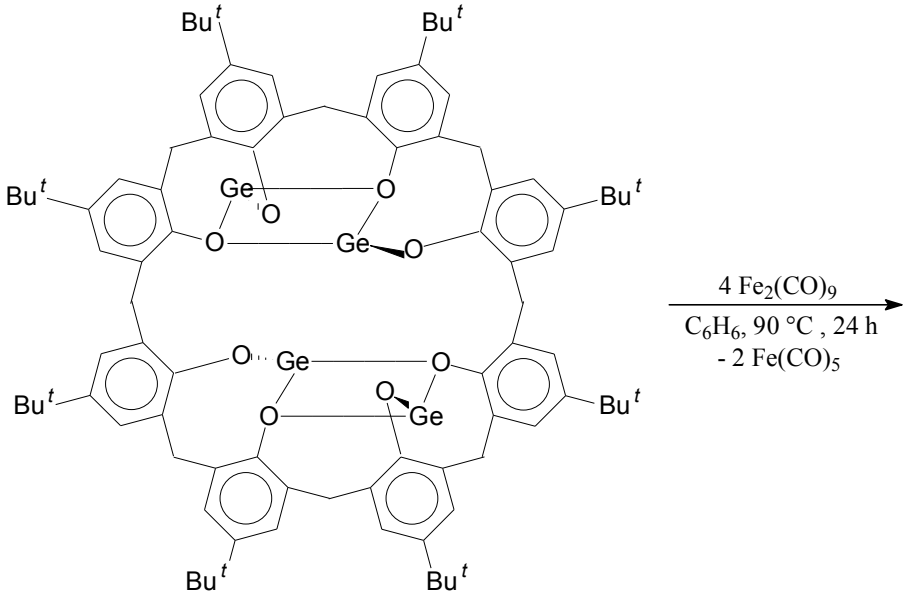

3

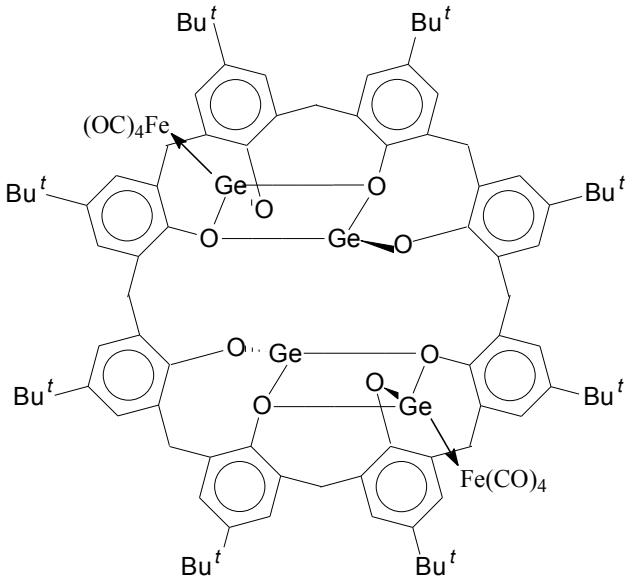

4, 77 %

Scheme 3. Reaction of {*p*-Bu$^t_8$calix[8]arene}Ge_4 with $Fe_2(CO)_9$.

The structure of **4** contains two $Fe(CO)_4$ groups bound to the two germanium atoms that are directed away from the central cavity of the molecule and point downward and outward from the top of the calix[8]arene bowl structure. The iron atoms in the two $Fe(CO)_4$ fragments in **4** are formally zero valent, and therefore all four germanium atoms remain in the 2+ oxidation state. As a result, the bridging oxygen interactions involving the donation of a lone pair of electrons from the aryloxide oxygen atoms into the vacant p-orbital on each of the germanium(II) atoms remain intact in **4**, while these interactions are disrupted in the structure of **3**. In contrast to **3** ({*p*-Bu^t_8calix[8]arene}Ge_4), the two Ge_2O_2 rhombi in **4** are puckered by 5.2 ° (Ge(1) – O(10) – Ge(2) – O(11)) and 3.5 ° (Ge(3) – O(14) – Ge(4) – O(15)). The Ge – Fe bonds in **4** involve the donation of the lone pair of electrons on each of the two divalent germanium atoms into a vacant orbital of the $Fe(CO)_4$ fragment via a σ-type interaction. Both of the iron atoms in **4** are present in a distorted trigonal bipyramidal environment, and the Fe – C bond distances in **4** average 1.791(7) Å which is identical to the average Fe – C bond length in $Ge[OC_6H_2Bu^t\text{-}2,6\text{-}Me\text{-}4]_2[Fe(CO)_4]$ (**5**) (1.791(1) Å).[15] The structures of **4** and **5** differ in that the $Ge(OAr)_2$ fragment of **5** occupies an equatorial position of the trigonal bipyramidal environment of the iron atom, while the germanium atoms of **4** are located in apical positions. It has been noted that for d^8 metal carbonyls with group 14 and 15 elements as ligands the heavier elements have preference for the equatorial site.[11] While the steric attributes of the ligands may play a role, the dominant factors are the σ-donor and the π-acceptor character of the ligands.

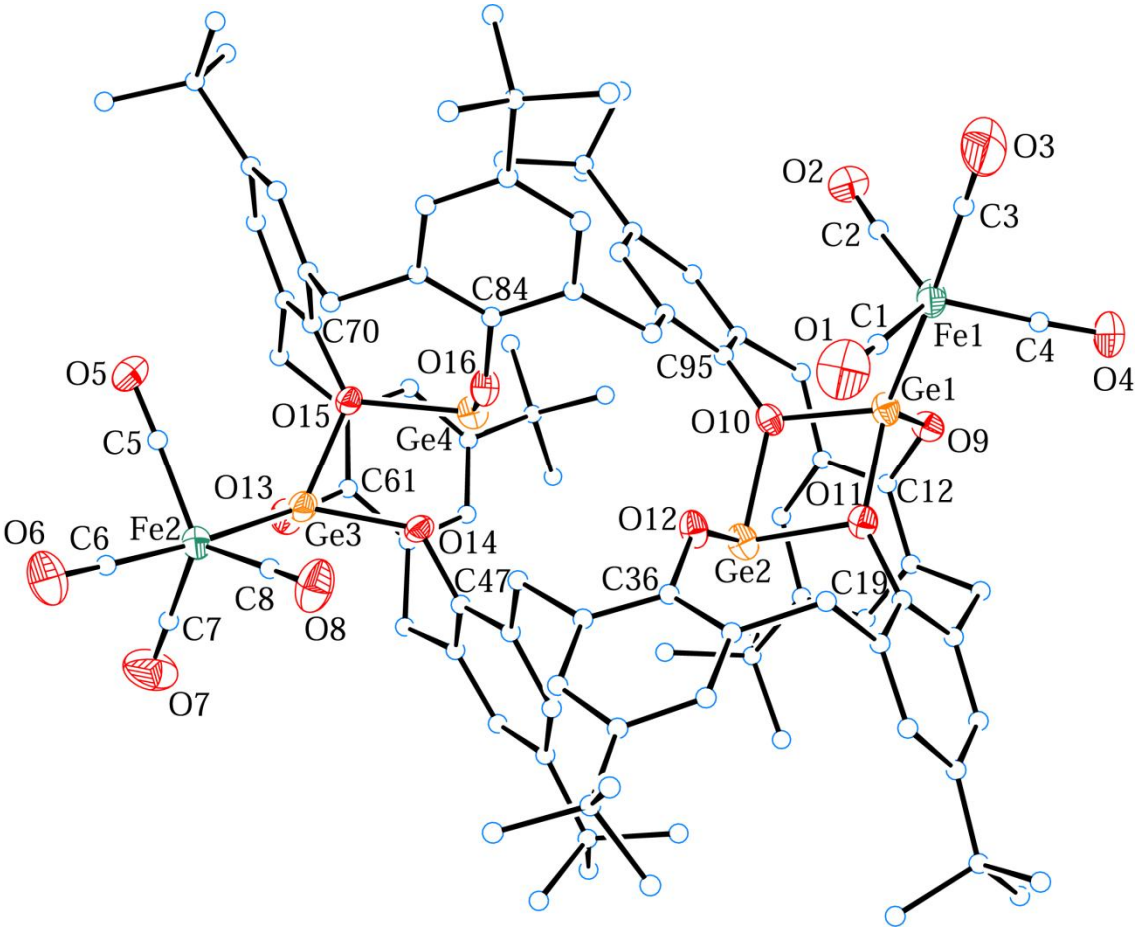

Figure 8. ORTEP diagram of compound **4**·6 C_6H_6. Germanium atoms are shown in orange, oxygen atoms in red, iron atoms in green and carbon atoms as white spheres.

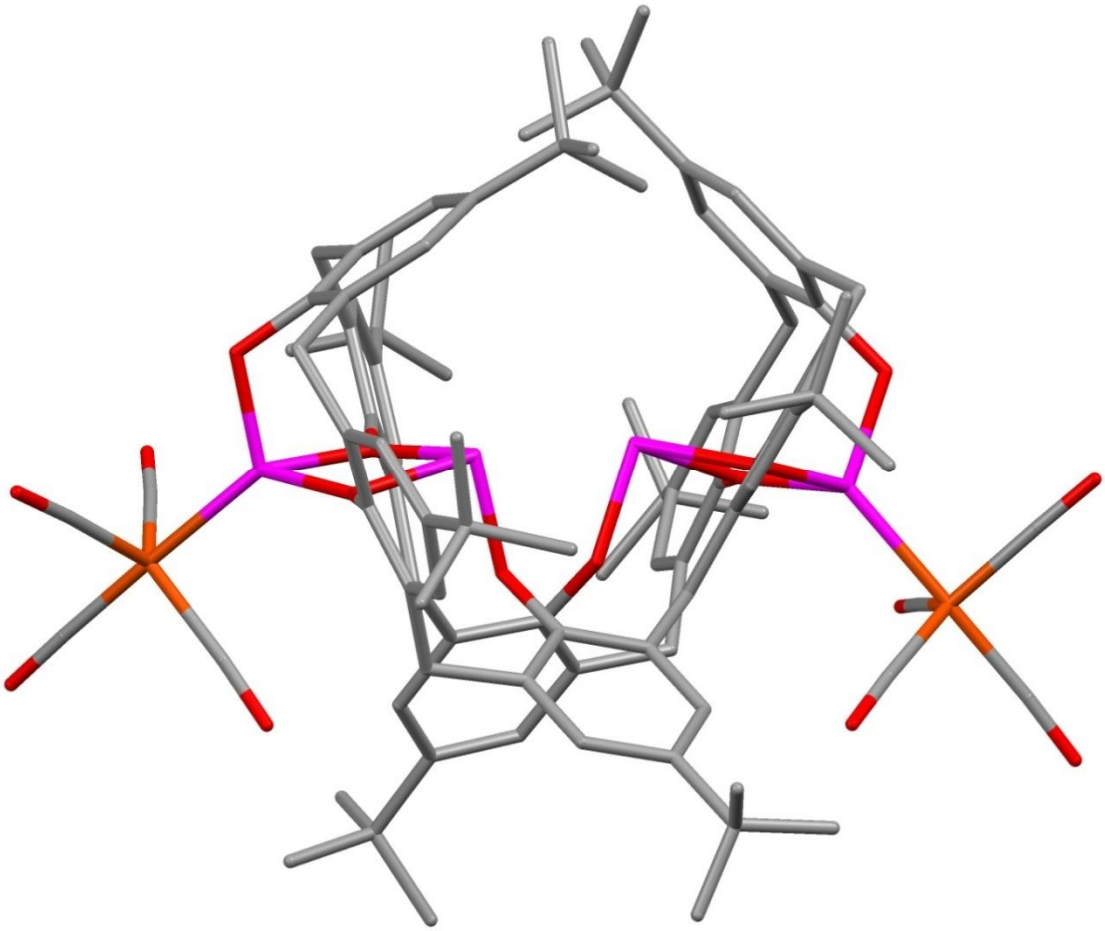

Figure 9. Wireframe drawing of compound **4**·6 C_6H_6. Germanium atoms are shown in purple, oxygen atoms in red, iron atoms in orange and carbon atoms in gray.

Table 2. Selected bond distances (Å) and angles (°) for **4**·6 C_6H_6

Ge(1) – Fe(1)	2.265(1)	O(9) – Ge(1) – O(10)	98.9(2)
Ge(2) – Fe(2)	2.264(1)	O(9) – Ge(1) – O(11)	98.3(2)
Ge(1) – O(9)	1.793(4)	O(10) – Ge(1) – O(11)	77.6(2)
Ge(1) – O(10)	1.902(3)	O(10) – Ge(2) – O(11)	71.1(1)
Ge(1) – O(11)	1.899(3)	O(10) – Ge(2) – O(12)	91.6(2)
Ge(2) – O(10)	2.031(3)	O(11) – Ge(2) – O(12)	91.7(2)
Ge(2) – O(11)	2.064(3)	Ge(1) – O(10) – Ge(2)	105.7(2)
Ge(2) – O(12)	1.815(4)	Ge(1) – O(11) – Ge(2)	104.5(2)
Ge(3) – O(13)	1.789(4)	O(9) – Ge(1) – Fe(1)	120.9(1)
Ge(3) – O(14)	1.906(3)	O(10) – Ge(1) – Fe(1)	119.6(1)
Ge(3) – O(15)	1.888(3)	O(11) – Ge(1) – Fe(1)	130.7(1)
Ge(4) – O(14)	2.115(3)	O(13) – Ge(3) – O(14)	100.4(2)
Ge(4) – O(15)	2.008(3)	O(13) – Ge(3) – O(15)	96.2(2)
Ge(4) – O(16)	1.813(3)	O(14) – Ge(3) – O(15)	77.8(1)
Fe(1) – C(1)	1.800(7)	O(14) – Ge(4) – O(15)	70.6(1)
Fe(1) – C(2)	1.805(7)	O(14) – Ge(4) – O(16)	95.1(1)
Fe(1) – C(3)	1.784(8)	O(15) – Ge(4) – O(16)	90.5(2)
Fe(1) – C(4)	1.789(7)	Ge(3) – O(14) – Ge(4)	103.2(2)
Fe(2) – C(5)	1.778(7)	Ge(3) – O(15) – Ge(4)	108.0(2)
Fe(2) – C(6)	1.784(8)	O(13) – Ge(3) – Fe(2)	118.8(1)
Fe(2) – C(7)	1.792(7)	O(14) – Ge(3) – Fe(2)	130.0(1)
Fe(2) – C(8)	1.798(7)	O(15) – Ge(3) – Fe(2)	123.2(1)
O(9) – C(12)	1.393(6)	C(61) – O(13) – Ge(3)	115.7(3)

O(10) – C(95)	1.426(6)	C(84) – O(16) – Ge(4)	138.9(3)
O(11) – C(19)	1.408(6)	C(12) – O(9) – Ge(1)	115.2(3)
O(12) – C(36)	1.381(6)	C(36) – O(12) – Ge(2)	126.8(4)
O(13) – C(61)	1.391(7)	C(19) – O(11) – Ge(1)	143.0(3)
O(14) – C(47)	1.409(6)	C(19) – O(11) – Ge(2)	109.7(3)
O(15) – C(70)	1.397(6)	C(95) – O(10) – Ge(1)	123.0(3)
O(16) – C(84)	1.370(6)	C(95) – O(10) – Ge(2)	129.8(3)
		C(47) – O(14) – Ge(3)	129.0(3)
		C(47) – O(14) – Ge(4)	125.7(3)
		C(70) – O(15) – Ge(3)	131.5(3)
		C(70) – O(15) – Ge(4)	120.2(3)

The equatorial site is preferred by poor σ-donors and good π-acceptors. In **5**, the two aryloxide oxygen atoms that are bound to germanium withdraw electron density from germanium thus rendering germanium a poor σ-donor to the vacant orbital of iron. The germylene, being electron deficient and having a vacant p orbital, is a good π-acceptor and the optimal arrangement for the germanium to accept electron density in the form of backbonding from iron is in the equatorial position. In **4**, the bridging aryloxide oxygen atoms donate a lone pair of electrons into a vacant p orbital of germanium. This interaction renders germanium a better σ-donor and a poorer π-acceptor. Since germanium is a poorer π-acceptor, there is less electron donation from iron to germanium and thus germanium is in the apical position. The two Ge – Fe bond lengths in **4** are nearly identical and measure 2.265(1) and 2.264(1) Å, which are only slightly longer than the Ge – Fe bond distance of 2.240(2) Å in **5**.

The relatively short Ge – Fe bond distances in both **4** and **5** indicate the presence of a Fe(*d*)→Ge(*p*) π-backbonding interaction. Although the π-type backbonding interaction occurring between the iron and germanium atoms would be expected to increase the electron density at germanium, the σ-type dative interaction involving the lone pairs of electrons at germanium presumably results in a net decrease in the electron density. This is manifested in the Ge(1) – O(9) and Ge(3) – O(13) bond distances of 1.793(4) and 1.789(4) Å (respectively) in **4** that are shorter than the germanium – oxygen bonds of free germanium(II) aryloxides, which typically range from 1.80 to 1.87 Å.[1-3,5-9,16] A similar effect was observed in compound **5**, where the two Ge – O distances are 1.776(6) and 1.778(6) Å.[15] The Ge – O_{term} bond distances for the remaining two germanium atoms in **4**, which are not bonded to $Fe(CO)_4$ fragments, are 1.815(4) and

1.813(3) Å for Ge(2) – O(12) and Ge(4) – O(16) (respectively), and these fall within the typical Ge – O distance range for germanium(II) aryloxides.

The ^{1}H NMR spectrum of **4** is similar in appearance to that of **3**. The numbering scheme for compound **4** is shown in **Figure 10**. Although the solid state structure of **4** lacks a C_2 axis, compound **4** is C_2 symmetric in solution since only eight resonances, rather than the expected 16, for the -CH_2- protons, were observed in its ^{1}H NMR spectrum. These features are again split into two groupings of doublets, with those in the chemical shift range δ 5.79 – 4.71 ppm corresponding to the methylene protons directed toward the central cavity of **4** and those in the range of δ 4.20 – 3.41 ppm directed away, for the same reasons (anisotropic effects) described above. Figure **11** contains a ^{1}H NMR spectrum for these doublets. In the solid state structure of **4**, H(45a) has two close contacts with O(12) and O(16) at distances of 2.494 and 2.342 Å, respectively. Hydrogen atom H(45a) has close contacts with oxygen atoms of both Ge_2O_2 rhombi. H(34a) has two close contacts with O(11) and O(12) that measure 2.450 and 2.525 Å respectively. There are two close contacts between H(78b) and O(15) and O(16) that measure 2.438 and 2.574 Å respectively. There is one close contact between H(89a) and O(12) measuring 2.246 Å and two contacts that are just beyond the sum of the van der Waals radii for oxygen and hydrogen that measure 2.627 and 2.642 Å to O(10) and O(16) respectively. This hydrogen atom has close contacts with oxygen atoms of both Ge_2O_2 rhombi and gives rise to the doublet seen at δ 4.71 ppm (J = 14.8 Hz). The protons attached to C(55), C(18), C(10) and C(62) are directed away from the two Ge_2O_2 rhombi and give rise to the set of four observed upfield doublets. The doublet seen at 3.41 ppm (J = 14.8 Hz) is assigned to the outwardly directed H(62b) that has long contacts with

O(13) and O(15) that measure 3.216 and 3.767 Å to O(13) and O(15), respectively. The proton attached to C(45) that is directed inward toward the central cavity of the macrocycle and has two close contacts to the aryloxide oxygen atoms gives rise to a doublet seen at δ 5.79 ppm (J = 18.0 Hz). The hydrogen atom bound to C(34) that points toward the two Ge_2O_2 rhombi gives rise to the doublet seen at δ 4.93 ppm (J = 12.8 Hz). The doublet observed at δ 4.85 ppm (J = 15.6 Hz) is attributed to the H(78b).

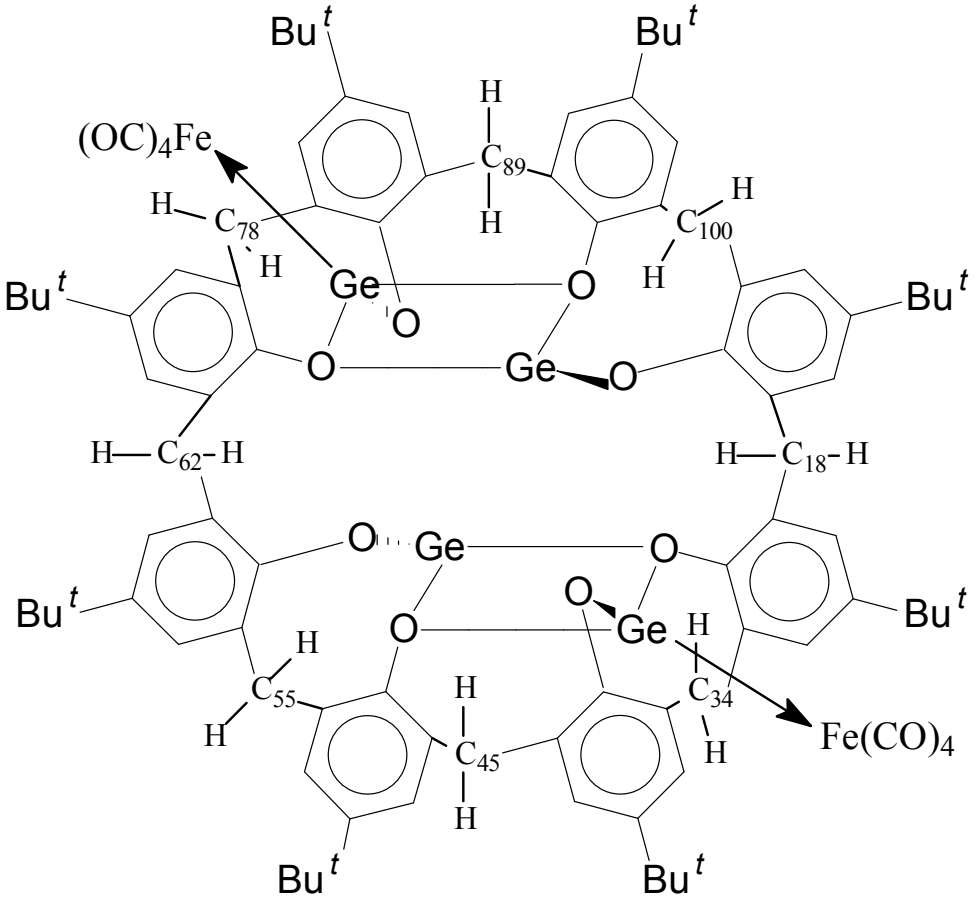

Figure 10. 2-D structure of **4** showing C_2 symmetry that is present in solution. The protons that are directed inward toward the central cavity are labeled "a" and the protons that are directed outward from the macrocycle are labeled "b" in the text.

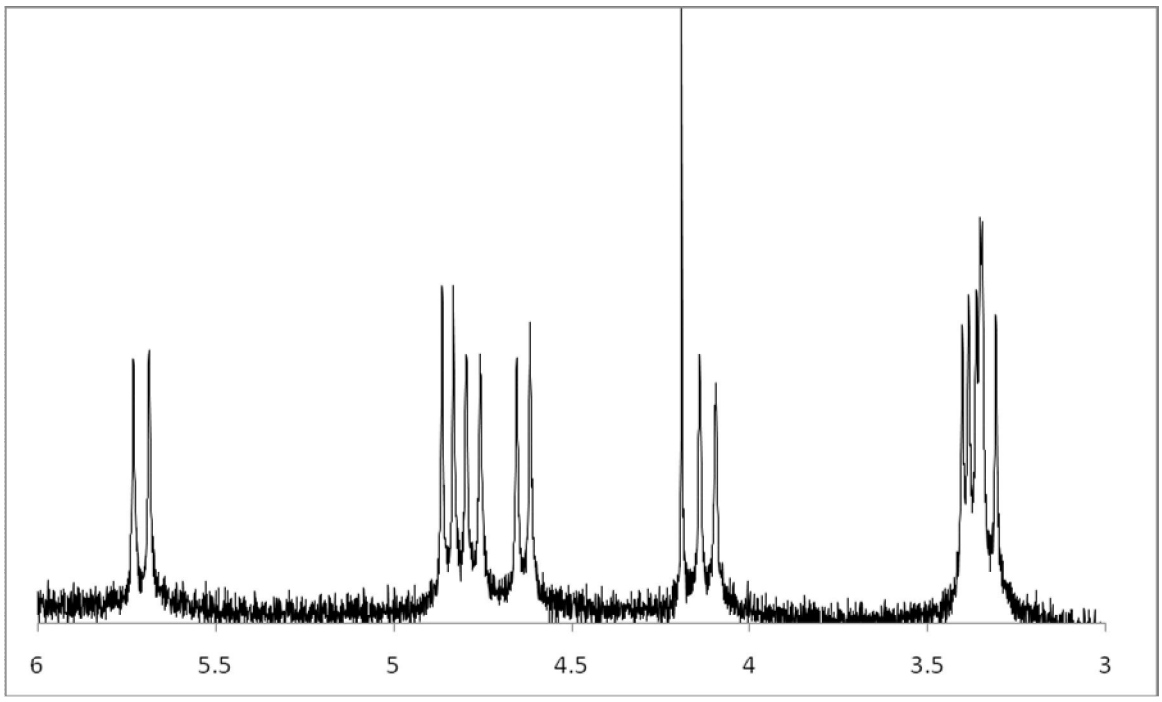

Figure 11. Methylene region from the ^{1}H NMR spectrum (C_6D_6, 25 °C) for compound **4**.

Four resonances were also observed for the protons of the *tert*-butyl groups of **4** at δ 1.32, 1.17, 1.23, and 0.78 ppm, again due to the magnetic non-equivalence of the four pairs of *tert*-butyl groups in **4**. The ^{1}H NMR resonances for the methylene protons directed inward toward the central cavity of **4** and those for the *tert*-butyl groups are shifted upfield relative to the corresponding resonances of **3** due to the overall reduction in electron density in **4** versus that of **3** resulting from the coordination of the two $Fe(CO)_4$ groups. The limited solubility of **4** in non-coordinating solvents precluded the acquisition of a meaningful ^{13}C NMR spectrum for this species.

Axial $Fe(CO)_4L$ complexes with idealized C_{3v} symmetry are expected to exhibit three CO stretching bands in their spectra, but the presence of the large

{Bu$^t_8$calix[8]arene}Ge_4 complex as the axial "ligand" lowers the overall symmetry of **4** such that four IR stretching bands are expected. The rigidity of the {Bu$^t_8$calix[8]arene}Ge_4 framework and the absence of an inversion center or a C_2 axis of rotation renders each of the $Fe(CO)_4$ fragments symmetrically non-equivalent, such that eight CO stretching bands are expected for **4**. A total of seven bands were observed in the IR spectrum (Nujol mull) of **4** at 2058, 1968, 1964, 1960, 1956, 1952, and 1948 cm^{-1}. The feature at 2058 cm^{-1} is considerably broadened relative to the other six bands, and corresponds to two overlapping bands that could not be resolved.

The difference in reactivity of compounds **1** and **3** with $Fe_2(CO)_9$ is also clearly different than the outcome of the three synthetic routes [17-19] employed for the preparation of the spirocyclic germanium(IV) complex $Ge[Fe_2(CO)_8]_2$ that contains two $Fe_2(CO)_8^{2-}$ fragments.

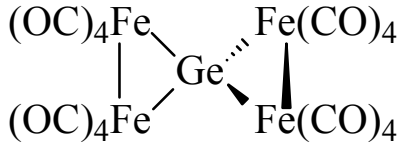

Figure 12. Spirocyclic germanium(IV) complex, $Ge[Fe_2(CO)_8]_2$.

In each case, a germanium(IV) precursor was used for the synthesis of $Ge[Fe_2(CO)_8]_2$, including treatment of either GeH_4 [17] or $Ge(CH{=}CH_2)_4$ with $Fe_2(CO)_9$.[18] The yield of $Ge[Fe_2(CO)_8]_2$ in each case was low, and the reactions involving $Fe_2(CO)_9$ also resulted in the formation of $Fe_3(CO)_{12}$ as a by-product. No other iron-containing by-products were detected in the reactions of **1** and **3** with $Fe_2(CO)_9$, and neither **2** nor **4** could be prepared from **1** or **3** using $Fe_3(CO)_{12}$ as the iron source.

The two germanium(II) calix[8]arene complexes **1** and **3** exhibit different reactivity with $Fe_2(CO)_9$ as a result of the different steric environments of the four germanium atoms in each molecule. The *para*-unsubstituted complex **1** undergoes a redox reaction with $Fe_2(CO)_9$ to generate a germanium(IV) macrocyclic species having four $GeFe_2$ triangles that contain $Fe_2(CO)_8^{2-}$ fragments. However, the reaction of the *para-tert*-butyl substituted complex **3** with $Fe_2(CO)_9$ results in the cleavage of the Fe – Fe bond to furnish the germanium(II) complex **4** that contains two neutral $Fe(CO)_4$ fragments. In contrast to **1** two of the four germanium atoms in compound **3** are not accessible to the incoming $Fe_2(CO)_9$ reagent due to steric effects, and as a result their reactivity toward $Fe_2(CO)_9$ more closely resembles that of the germanium(II) aryloxide $(Bu^t_2\text{-}2,6\text{-}Me\text{-}4\text{-}C_6H_2O)_2Ge$ rather than that of complex **1**.

Experimental Section

General Considerations

All manipulations were carried out using standard Schlenk, syringe, and glovebox techniques.[11] Solvents were dried and purified using a Glass Contour solvent purification system. The reagents *para-tert*-butylcalix[8]arene and $Fe_2(CO)_9$ were purchased from Aldrich and used as received, and $Ge[N(SiMe_3)_2]_2$ was prepared according to the literature procedure.[12-14] Infrared spectra were obtained using a Hewlett-Packard FT-IR spectrometer, while NMR spectra were recorded using a Varian Unity INOVA 400 spectrometer operating at 400 MHz and were referenced to residual protio solvent. Elemental analyses were conducted by Desert Analytics (Tuscon, AZ).

Preparation of {*p*-Bu$^t_8$calix[8]arene}Ge$_4$ (3)

To a solution of *p*-Bu$^t_8$calix[8]arene (2.500 g, 1.923 mmol) in benzene (20 mL) was added a solution of Ge[N(SiMe$_3$)$_2$]$_2$ (3.031 g, 7.705 mmol) in benzene (10 mL). The reaction mixture was sealed in a Schlenk tube and heated at 90 °C for 24 h. Volatiles were removed *in vacuo* and to yield 2.852 g (94%) of **1** as a colorless solid. ^{1}H NMR (C_6D_6, 25 °C) δ 7.49 (s, 1 H, *meta*- H), 7.46 (s, 1 H, *meta*- H), 7.27 (s, 1 H, *meta*- H), 7.19 (s, 1 H, *meta*- H), 7.17 (s, 1 H, *meta*- H), 7.14 (s, 1 H, *meta*- H), 7.06 (s, 1 H, *meta*- H), 6.82 (s, 1 H, *meta*- H), 5.90 (d, *J* = 17.6 Hz, 2H, -C*H*$_2$-), 4.78 (d, *J* = 12.8 Hz, 2H, -C*H*$_2$-), 4.78 (d, *J* = 12.8 Hz, 2H, -C*H*$_2$-), 4.61 (d, *J* = 14.8 Hz, 2H, -C*H*$_2$-), 3.80 (d, *J* = 17.6 Hz, 2H, -C*H*$_2$-), 3.51 (d, *J* = 14.8 Hz, 2H, -C*H*$_2$-), 3.49 (d, *J* = 12.8 Hz, 2H, -C*H*$_2$-), 3.34 (d, *J* = 12.8 Hz, 2H, -C*H*$_2$-), 1.41 (s, 18H, -C(C*H*$_3$)$_3$), 1.33 (s, 18H, -C(C*H*$_3$)$_3$), 1.32 (s, 18H, -C(C*H*$_3$)$_3$), 0.87 (s, 18H, -C(C*H*$_3$)$_3$) ppm. ^{13}C NMR (C_6D_6, 25 °C) δ 152.4, 151.5, 147.4, 146.1, 145.6, 144.7, 143.3, 137.8, 137.0, 134.5, 134.0, 133.3, 130.8, 129.6, 128.8, 128.2, 127.9, 127.4, 127.2, 126.5, 126.3, 126.1, 125.6, 124.8, 36.8, 36.1, 34.4, 34.3, 34.2, 34.0, 32.3, 31.9, 31.5, 31.0 ppm. Anal. Calcd. For $C_{88}H_{104}Ge_4O_8$: C, 66.89; H, 6.63. Found: C, 67.11; H, 6.55.

Preparation of {*p*-Bu$^t_8$calix[8]arene}Ge$_4${Fe(CO)$_4$}$_2$ (4)

To a solution of compound **1** (0.300 g, 0.190 mmol) in benzene (10 mL) was added a suspension of $Fe_2(CO)_9$ (0.283 g, 0.778 mmol) in benzene (20 mL). The reaction mixture was sealed in a Schlenk tube and heated at 90 °C for 24 h. The solution was filtered through Celite and the volatiles were removed from the filtrate *in vacuo* to yield a yellow solid which was recrystallized from hot benzene to yield **2** (0.282 g, 77 %) as yellow crystals. ^{1}H NMR (C_6D_6, 25 °C) δ 7.45 (s, 1 H, *meta*- H), 7.37 (s, 1 H, *meta*- H),

7.31 (s, 1 H, *meta*- H), 7.19 (s, 1 H, *meta*- H), 7.15 (s, 1 H, *meta*- H), 7.12 (s, 1 H, *meta*- H), 7.03 (s, 1 H, *meta*- H), 6.80 (s, 1 H, *meta*- H), 5.79 (d, J = 18.0 Hz, 2H, -CH_2-), 4.93 (d, J = 12.8 Hz, 2H, -CH_2-), 4.85 (d, J = 15.6 Hz, 2H, -CH_2-), 4.71 (d, J = 14.8 Hz, 2H, -CH_2-), 4.20 (d, J = 18.0 Hz, 2H, -CH_2-), 3.46 (d, J = 15.6 Hz, 2H, -CH_2-), 3.45 (d, J = 12.8 Hz, 2H, -CH_2-), 3.41 (d, J = 14.8 Hz, 2H, -CH_2-), 1.33 (s, 18H, -C(CH_3)$_3$), 1.25 (s, 18H, -C(CH_3)$_3$), 1.23 (s, 18H, -C(CH_3)$_3$), 0.78 (s, 18H, -C(CH_3)$_3$) ppm. IR (Nujol mull): 2058, 1968, 1964, 1960, 1956, 1952, and 1948 cm^{-1}. Anal. Calcd. For $C_{96}H_{104}Fe_2Ge_4O_{16}$: C, 60.18; H, 5.47. Found: C, 60.29; H, 5.54.

X-Ray Structure Determinations

Diffraction intensity data were collected with a Siemens P4/CCD diffractometer. Crystallographic data are collected in **Table 3**. Absorption corrections were applied for all data using SADABS. The structures were solved using direct methods, completed by Fourier syntheses, and refined by full-matrix least squares procedures of F^2. All non-hydrogen atoms were refined with anisotropic displacement coefficients, and hydrogen atoms were treated as idealized contributions. Contributions from the six benzene molecules of **2** were removed using SQUEEZE. All software and sources of scattering factors are contained in the SHEXTL (5.10) program package (G. Sheldrick, Bruker XRD, Madison, WI). Molecular structure diagrams were drawn using the ORTEP3 program (L. J. Farrugia, Glasgow).

Crystallographic Data

Table 3. Crystal data and structure refinement for compounds **3**·3 C_6H_{14} and **4**·6 C_6H_6.

Compound	**3**·3 C_6H_{14}	**4**·6 C_6H_6
Formula	$C_{106}H_{144}Ge_4O_8$	$C_{105}H_{112}Fe_2Ge_4O_{16}$
Formula weight (g/mol)	1836.57	2032.01
Temperature (K)	100(2)	100(2)
Wavelength (Å)	0.71073	0.71073
Crystal system	Monoclinic	Monoclinic
Space group	C_2/c	$P2/c$
Unit cell dimensions	a = 28.5205(18) Å	a = 25.976(2) Å
	b = 22.2776(14) Å	b = 13.9043(1) Å
	c = 19.6029(13) Å	c = 27.856(3) Å
	α = 90 °	α = 90 °
	β = 126.531(1) °	β = 100.9960(10) °
	γ = 90 °	γ = 90 °
Volume (Å^3)	10008.1(11)	9876.3(15)
Z	4	4
P_{calc} (g/cm^3)	1.219	1.367
Absorption coefficient (mm^{-1})	1.243	1.551
F(000)	3888	4200
Crystal Size (mm^3)	0.44 x 0.12 x 0.13	0.22 x 0.20 x 0.12
Theta range for data collection	1.39 ° to 25.38 °	0.80 ° to 25.38 °

Index ranges	-34<=h<=34, -26<=k<=26, -23<=l<=23	-31<=h<=31, -16<=k<=16, -32<=l<=33
Reflections collected	54644	92545
Independent reflections	9192 [R(int) = 0.0730]	17921 [R(int) = 0.0559]
Radiation	Mo Kα	Mo Kα
Completeness to theta = 25.00 °	100.0 %	99.0 %
Absorption correction	Multi-scan	Multi-scan
Max. and min. transmission	0.8858 and 0.6109	
Refinement method	Full-matrix least-squares on F^2	Full-matrix least-squares on F^2
Data / restraints / parameters	9192 / 0 / 532	17921 / 6 / 1044
Goodness-of-fit on F^2	1.106	1.151
Final R indices [I>2sigma(I)]	R1 = 0.0510, wR2 = 0.1260	R1 = 0.0672, wR2 = 0.1891
R indices (all data)	R1 = 0.0828 wR2 = 0.1447	R1 = 0.0929 wR2 = 0.2059
Largest diff. peak and hole	1.607 and -0.631 e $Å^{-3}$	2.831 and -1.645 e $Å^{-3}$

References

(1) Wetherby Jr. A. E.; Goeller, L. R.; DiPasquale, A. G.; Rheingold, A. L.; Weinert, C. S. *Inorg. Chem*. **2007**, *46*, 7579-7586.

(2) Mc Burnett, B. G.; Cowley, A. H. *Chem. Commun.* **1999**, 17.

(3) Hascall, T.; Rheingold, A. L.; Guzei, I.; Parkin, G. *Chem. Commun.* **1998**, 101.

(4) Wetherby Jr., A. E.; Rheingold, A. L.; Feasley, C. L.; Weinert, C. S. *Polyhedron* **2008**, *27*, 1841.

(5) Weinert, C. S.; Fenwick, A. E.; Fanwick, P. E.; Rothwell, I. P. *J. Chem. Soc.,Dalton Trans.* **2003**, 1795.

(6) Weinert, C. S.; Fanwick, P. E.; Rothwell, I. P *J. Chem. Soc., Dalton Trans.* **2002**, 2948.

(7) Çetinkaya, B.; Gemrükçü, I.; Lappert, M. F.; Atwood, J. L.; Rogers, R. D.; Zaworotko, M. J. *J. Am. Chem. Soc.* **1980**, *102*, 2088.

(8) Gerung, H.; Boyle, T. J.; Tribby, L. J.; Bunge, S. D.; Brinker, C. J.; Han, S. M. *J. Am. Chem. Soc.* **2006**, *128*, 5244.

(9) Gerung, H.; Bunge, S. D.; Boyle, T. J.; Brinker, C. J.; Han, S. M. *Chem. Commun.* **2005**, 1914.

(10) Shriver, D. F.; Drezdzon, M. A. *The Manipulation of Air Sensitive Compounds*; John Wiley and Sons, New York, 1986.

(11) Gynane, M. J. S.; Harris, D. H.; Lappert, M. F.; Power, P. P.; Rivière, P.; Rivière-Baudet, M. *J. Chem. Soc., Dalton Trans.* **1977**, 2004.

(12) Harris, D. H.; Lappert, M. F. *J. Chem. Soc., Chem. Commun.* **1974**, 895.

(13) Zhu, Q.; Ford, K. L.; Roskamp, E. J. *Heteroatom Chem.* **1992**, *3*, 647.

(14) Hitchcock, P. B.; Lappert, M. F.; Thomas, S. A.; Thorne, A. J.; Carty, A. J.; Taylor, N. J. *J. Organomet. Chem.* **1986**, *315*, 27.

(15) Anema, S. G.; Barris, G. C.; Mackay, K. M.; Nicholson, B. K. *J. Organomet. Chem.* **1988**, *350*, 207.

(16) Batsanov, A. S.; Rybin, L. V.; Rybinskaya, M. I.; Struchkov, Y. T.; Salimgareeve, I. M.; Bogatova, N. G. *J. Organomet. Chem.* **1983**, *249*, 319.

(17) Melzer, D.; Weiss, E. *J. Organomet. Chem.* **1983**, *255*, 335.

Chapter Three: Formation and structures of unprecedented germanium(II) aryloxo/oxo clusters

Introduction

The synthesis and structure of the first germanium(II) aryloxide was reported in 1980,[1] and a number of additional reports describing the synthesis and structures of germanium(II) aryloxides have recently appeared.[2-7] Recent interest in germanium(II) compounds has arisen due to their utility as molecular precursors for germanium-based nanomaterials, which are expected to overcome some of the shortcomings of current silicon-based materials due to the higher electron and hole mobility and smaller band gap in germanium.[8-10] The nature of the ligands attached to the germanium(II) center in the precursor has an influence on the morphology of the resulting nanomaterials. For example, the germanium(II) amide $Ge[N(SiMe_3)_2]_2$ has been used for the preparation of Ge nanocrystals,[11] but the aryloxide species $Ge(OC_6H_3Bu^t_2\text{-}2,6)_2$ generates Ge nanowires measuring 0.1 – 10 μm in length, where the length of the materials depends on the reaction temperature employed.[2] Complexes of this type are still relatively uncommon, and thus the establishment of a library of these materials is an important endeavor.

The germanium(II) aryloxides which have been prepared and structurally characterized typically adopt one of two possible structural motifs.[1-6,12-14] These species can be monomeric or dimeric, where the latter structures include two terminal and two bridging aryloxide ligands leading to a Ge_2O_2 rhombus in the center of the molecule. The

preference for one structure over the other appears to be related to the steric attributes of the aryloxide ligands, since the complexes $[Ge(OAr)_2]_2$ (Ar = $OC_6H_2Me_3$-2,4,6 or $OC_6H_3Pr^i_2$-2,6) are dimeric[4] while the complexes $Ge(OAr)_2$ (Ar = $OC_6H_3Ph_2$-2,6,[4] $OC_6H_3Bu^t_2$-2,6,[2] or $OC_6H_2Bu^t_2$-2,6-Me-4[1]) are monomeric. The composition and structure of the germanium(II) aryloxide precursors should have a significant effect on the morphology of the resulting germanium nanomaterials prepared from them, and variation of the aryloxide ligands is a possible method to "tune" the size and properties of the nanomaterials.

Structurally characterized germanium(II) aryloxides are often monomeric in the solid state, as shown by the X-ray crystal structures of $Ge(OC_6H_3Bu^t$-2,6)$_2$ (**1**),[2] $Ge(OC_6H_2Bu^t$-2,6-Me-4)$_2$ (**2**),[1] $Ge(OC_6H_3Ph$-2,6)$_2$ (**3**),[4] $Ge(OC_6HPh$-2,3,5,6)$_2$ (**4**),[4] (*R*)-[Ge{$O_2C_{20}H_{10}(SiMe_2Ph)_2$-3,3'}{$NH_3$}][3] and its (*S*)-analogue,[6] and (*R,R*)-[Ge{$OC_{20}H_{10}$-($OSiMe_3$)-2'-($SiMe_3$)$_2$-3,3'}$_2$].[3] However, these species can also adopt dimeric structures that have bridging aryloxide ligands, as found in the structures of $[Ge(OC_6H_2Me$-2,4,6)$_2]_2$ (**5**) and $[Ge(OC_6H_3Pr^i$-2,6)$_2]_2$ (**6**).[4] The central core of these two molecules consists of a Ge_2O_2 rhombus where the two oxygen atoms are those of the bridging aryloxide ligands. This structural motif has also been observed in four crystallographically characterized germanium(II) calix[4]- and calix[8]arene complexes[5,6] and the structure of the germanium(II) calix[6]arene complex having a similar Ge_2NO rhombus has also been recently reported.[13] In order to probe the steric threshold for formation of the dimeric structure, we treated the germanium(II) amide $Ge[N(SiMe_3)_2]_2$ (**7**) with two equivalents of $HOC_6H_3Bu^t$-2-Me-6, $HOC_6H_4Bu^t$-4 or $HOC_6H_3Bu^t$-2-Me-4 (**8**). The first reaction yielded the monomeric complex $Ge(OC_6H_3Bu^t$-2-Me-6)$_2$ (**9**); however, the latter two

reactions yielded two germanium(II) clusters containing terminal aryloxide ligands and oxo bridges which have unprecedented structures.

Results and Discussion

The structure of **9**, prepared from **7** and 2 equiv. of $HOC_6H_3Bu^t$-2-Me-6 is shown in **Scheme 1**. In order to ascertain whether **9** adopts a monomeric or dimeric structure in the solid state, the X-ray crystal structure of **9** was determined. Crystals of **9** were grown from a hot benzene solution, and an ORTEP diagram of **9** is illustrated in **Figure 1** while selected bond distances and angles are collected in **Table 1**. Compound **9** crystallizes with two independent molecules in the unit cell. The Ge – O bond distances in one molecule of **9** are slightly shorter than those of the other and measure 1.807(2), 1.813(2), 1.812(2) and 1.805(2) Å for Ge(1) – O(1), Ge(1) – O(2), Ge(1') – O(1) and Ge(1') – O(2') (respectively) while the average Ge – O distance is 1.809 Å which is similar to those in other monomeric germanium(II) aryloxides. The O – Ge – O bond angles in each of the molecules closely approach the ideal value of 90 °, and differ from one another by 1.30(9) °. The bond angles O(1) – Ge(1) – O(2) and O(1') – Ge(2') – O(2') measure 91.48(9) and 90.18(9) ° (respectively), with an average O – Ge – O bond angle of 90.83(9) °. There is no evidence for the presence of bridging aryloxide ligands, since the closest separation of individual molecules in the unit cell is 4.34 Å, and this distance is well outside the range for O_{br} – Ge – O_{br} interactions (1.95 to 2.05 Å).[4-6,13,14] The ^1H NMR spectrum of **9** at 25 °C exhibits two sharp singlets at δ 2.24 and δ 1.52 ppm for the methyl- and *tert*-butyl- substituents (respectively) that are both shifted downfield from those of the free phenol at δ 2.23 and δ 1.31 ppm. The sharp appearance of these features

in the spectrum of **9** suggests that this species is monomeric in solution, and the appearance of the spectrum also remained unchanged during a variable temperature (-80 °C to 90 °C) NMR experiment in toluene-d_8.

$$\underset{\mathbf{7}}{Ge[N(SiMe_3)_2]_2} + 2\ HOC_6H_3Bu^t\text{-}2\text{-}Me\text{-}6 \xrightarrow[12\ h,\ 25\ ^oC]{C_6H_6} \underset{-2\ HN(SiMe_3)_2}{} \underset{\mathbf{9}}{Ge(OC_6H_3Bu^t\text{-}2\text{-}Me\text{-}6)_2}$$

Scheme 1. Synthesis and crystal structure of $Ge(OC_6H_3Bu^t\text{-}2\text{-}Me\text{-}6)_2$ (**9**).

The inductive electron-donating properties of three methyl groups in the *ortho*- and *para*- positions of **5** versus those of the *ortho*-*tert*-butyl groups in **9** are approximately similar, and therefore the propensity for these species to adopt monomeric versus dimeric structures is expected to be governed by steric effects. The steric attributes of the 2-*tert*-butyl-6-methylphenolate substituents in **9** can be regarded as intermediate between those of the 2,6-di-*tert*-butylphenolate substituents of $Ge(OC_6H_3Bu^t\text{-}2,6)_2$ (**1**)[2] and the mesitylphenolate substituents of $[Ge(OC_6H_2Me_3\text{-}2,4,6)_2]_2$ (**5**).[4] In contrast, the 2,6-di-*iso*-propylphenolate-substituted species $[Ge(OC_6H_3Pr^i_2\text{-}2,6)_2]_2$ (**6**) has been found to adopt a dimeric structure which is maintained in solution, although bridge-terminal ligand exchange was demonstrated to occur by variable temperature ^{1}H NMR spectroscopy.[4] The monomeric nature of **9** can be attributed to the steric effects of the 2-*tert*-butyl group, despite the presence of the relatively sterically unencumbering 6-methyl group. Thus, the incorporation of a single *tert*-butyl group in the *ortho*-position and a second substituent in the second *ortho*-

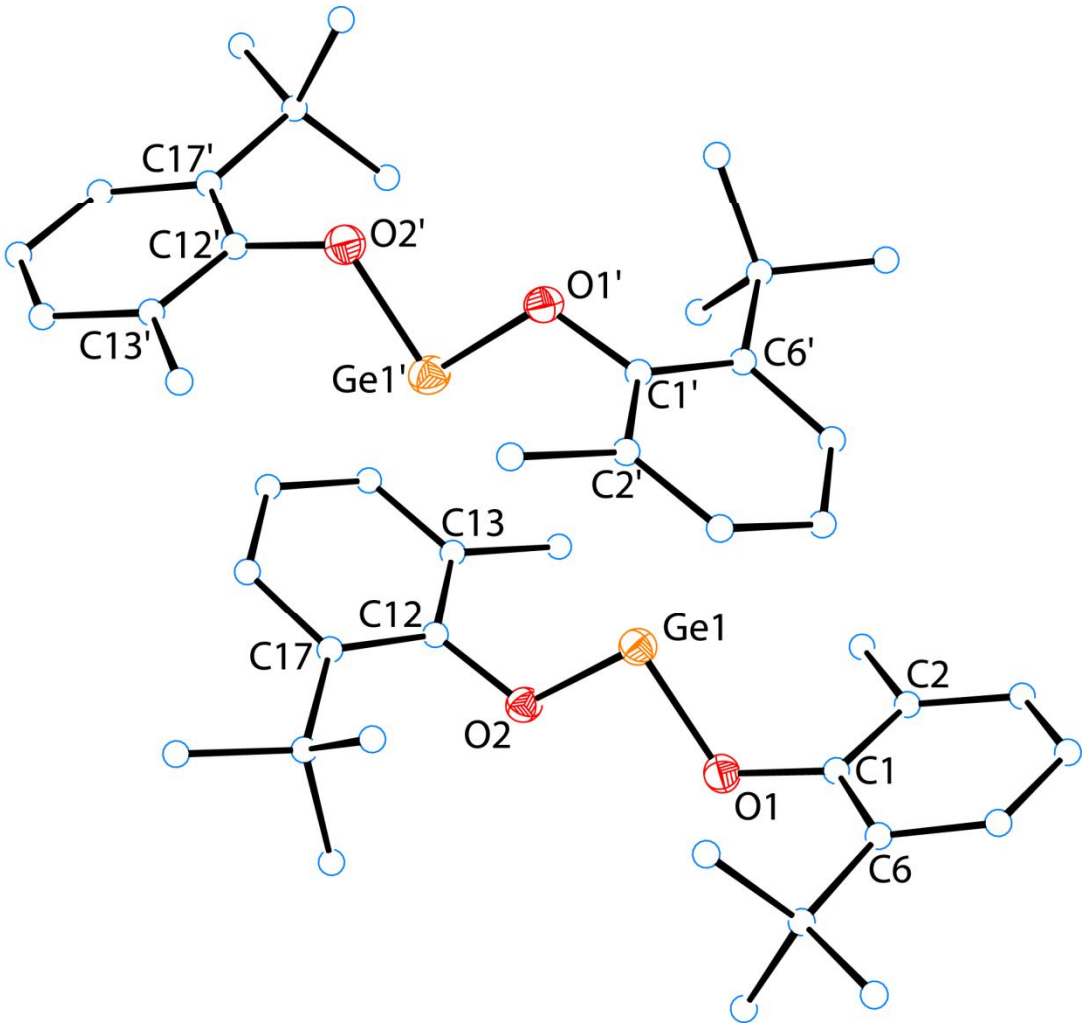

Figure 1. ORTEP diagram of compound **9**. Thermal ellipsoids are drawn at 50 % probability. Oxygen atoms are shown in red, germanium atoms in orange and carbon atoms as white spheres.

Table 1. Selected bond distances (Å) and angles (°) for 9.

Ge(1) – O(1)	1.807(2)	O(1) – Ge(1) – O(2)	91.48(9)
Ge(1) – O(2)	1.813(2)	C(1) – O(1) – Ge(1)	117.7(2)
O(1) – C(1)	1.391(3)	C(12) – O(2) – Ge(1)	116.9(2)
O(2) – C(12)	1.384(3)	O(1) – C(1) – C(2)	117.3(2)
Ge(1') – O(1')	1.812(2)	O(1) – C(1) – C(6)	120.6(2)
Ge(1') – O(2')	1.805(2)	C(2) – C(1) – C(6)	122.1(3)
O(1') – C(1')	1.385(3)	O(2') – Ge(1') – O(1')	90.18(9)
O(2') – C(12')	1.382(3)	C(1') – O(1') – Ge(1')	117.1(2)
$Ge(1) – O(1)_{avg}$	1.809(2)	C(12') – O(2') – Ge(1')	119.8(2)
$Ge(1) – O(2)_{avg}$	1.809(2)	O(1') – C(1') – C(2')	117.7(3)
$O(1) – C(1)_{avg}$	1.388(3)	O(1') – C(1') – C(6')	119.9(2)
$O(2) – C(12)_{avg}$	1.383(3)	C(2') – C(1') – C(6')	122.4(3)

position of the aryloxide ligand is sufficient to prevent dimerization of germanium(II) aryloxides.

The reaction of the related phenol, $HOC_6H_3Bu^t$-2-Me-4 (**8**), with the germanium(II) amide, $Ge[N(SiMe_3)_2]_2$ (**7**) was also investigated. In this reaction, a large cluster with a previously unobserved structure type, $Ge_8(\mu_3\text{-}O)_6(OC_6H_3Bu^t\text{-}2\text{-}Me\text{-}4)_4$ (**10**) was isolated. There are eight germanium(II) atoms that are connected together by six μ_3-oxo bridges. The four aryloxide groups are terminal and no bridging interactions are present. A second species was also obtained and its structure was determined to be $[Ge_4O_3(OC_6H_3Bu^t\text{-}2\text{-}Me\text{-}4)_4 \cdot NH_3]_2$ (**11**), which appears to be an intermediate in the formation of the larger $Ge_8(\mu_3\text{-}O)_6(OC_6H_3Bu^t\text{-}2\text{-}Me\text{-}4)_4$ cluster. Treatment of **7** with two equiv. of **8** furnished two different germanium aryloxide products (**Scheme 2**) that were selectively crystallized out of solution using benzene or hexane/toluene as the solvent, and both of these compounds have previously unknown structural motifs. The dimeric species $[Ge_4(\mu\text{-}O)_2(OC_6\text{-}H_3Bu^t\text{-}2\text{-}CH_3\text{-}4)_4 \cdot NH_3]_2$ (**11**) was obtained in 43 % yield upon crystallization from a hot benzene solution, and ORTEP diagrams of the dimer, asymmetric unit and cluster core diagram of **11** are shown in **Figures 2,3** and **4** (respectively), while selected bond distances and angles are collected in **Table 2**.

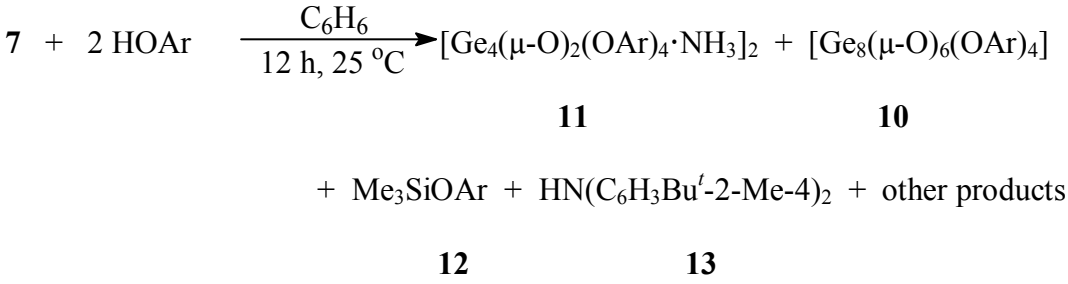

Scheme 2. Synthesis of $[Ge_4(\mu\text{-}O)_2(OC_6H_3\text{-}Bu^t\text{-}2\text{-}CH_3\text{-}4)_4\cdot NH_3]_2$ (**11**) and $[Ge_8(\mu_3\text{-}O)_6(OC_6H_3\text{-}Bu^t\text{-}2\text{-}CH_3\text{-}4)_4]$ (**10**). OAr = $OC_6H_3Bu^t$-2-Me-4.

All four germanium atoms in **11** are in the +2 oxidation state, and **11** contains two Ge_4O_2 rings that are related by a center of inversion which are held together by two Ge – Ge single bonds that measure 2.499(1) Å. The two Ge – Ge bonds within the individual Ge_4O_2 rings measure 2.482(1) and 2.491(1) Å, and all three of these distances are within the typical range for Ge – Ge single bonds.[19] The angle about Ge(4) is 82.97(8) °, which is significantly more acute than the ideal angle of 90 °, while the Ge(2) – Ge(4) – Ge(1') (88.03(8) °) and Ge(3) – Ge(4) – Ge(1') (85.26(9) °) angles are closer to the ideal bond angle. The Ge(4) atom is attached to three other germanium atoms, while Ge(2) and Ge(3) are connected to Ge(1) via two μ-O atoms. The Ge – μ-O distances in **11** are relatively uniform in length with an average value of 1.784(2) Å, and the Ge – O distances to the terminal aryloxide ligands lie within the typical range with an average value of 1.80(1) Å. The dimer forms through two coordinative interactions between Ge(1) and Ge(4') and Ge(1') and Ge(4). This suggests that dative bonding is occurring, although several examples of singly bonded oligogermanes exist with Ge – Ge bonds

measuring greater than 2.5 Å. Although the Ge(1) – Ge(4') and Ge(1') – Ge(4) distances are long, the singly bonded trigermanes $IBu^t{}_2Ge^1 – Ge^2Bu^t – Ge^3Bu^t{}_2I$, $BrBu^t{}_2Ge^1 – Ge^2Bu^t – Ge^3Bu^t{}_2Br$ and $MeBu^t{}_2Ge^1 – Ge^2Bu^t – Ge^3Bu^t{}_2Me$ have average Ge – Ge distances of 2.641, 2.609 and 2.620 Å (respectively), while the singly bonded digermanes $Bu^t{}_3Ge^1 – Ge^2Bu^t{}_3$ and $(C_6H_3Mes_2\text{-}2,6)Ge^1 – Ge^2Bu^t{}_3$ have Ge – Ge bond distances measuring 2.710(1) and 2.544(7) Å (respectively).[19] The Ge(3) atom is present in a distorted tetrahedral environment with bond angles ranging from 95.7(6) ° to 119.0(5) °. There are no oxygen atoms either bridging or terminally bound to Ge(4), but the Ge(4) is attached to Ge(2) and Ge(3) in a highly distorted bent geometry. The germanium atom Ge(2) is bound to three oxygen atoms (O(2), O(4) and O(5)) and Ge(4) and is in a distorted tetrahedral environment. The germanium – oxygen bond distances range from 1.779(2) Å to 1.819(2) Å, and the bond distances from germanium to the bridging oxygen atoms between Ge(1) – O(2) and Ge(1) – O(3) are nearly identical measuring, 1.790(2) Å and 1.792(2) Å (respectively). Germanium – oxygen bond lengths between Ge(3) – O(3) and Ge(3) – O(6) measure 1.777(2) Å and 1.793(2) Å (respectively). The two geminal germanium – oxygen bond distances, Ge(2) – O(4) and Ge(2) – O(5) measure 1.819(2) Å and 1.794(2) Å (respectively). Also bound to Ge(3) is a nitrogen atom with a bond distance of 1.998(2) Å, which is significantly shorter than that of other three coordinate germanium complexes with a neutral nitrogen donor ligand.[20-22] The nitrogen atom is due to a coordinated ammonia molecule. The source of the ammonia comes from the reaction of hexamethyldisilazane with $HOC_6H_3Bu^t$-2-Me-4 to yield the silylated phenol and ammonia as products (**Scheme 3**).

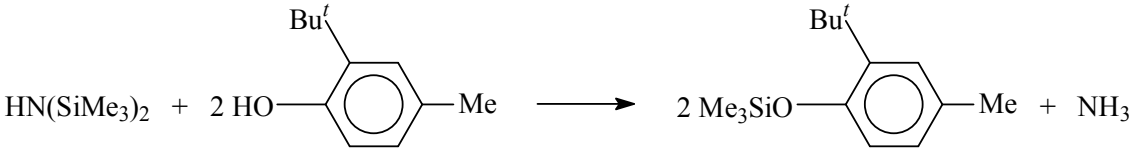

Scheme 3. Reaction of hexamethyldisilazane with $HOC_6H_3Bu^t$-2-Me-4 to yield the silylated phenol and ammonia.

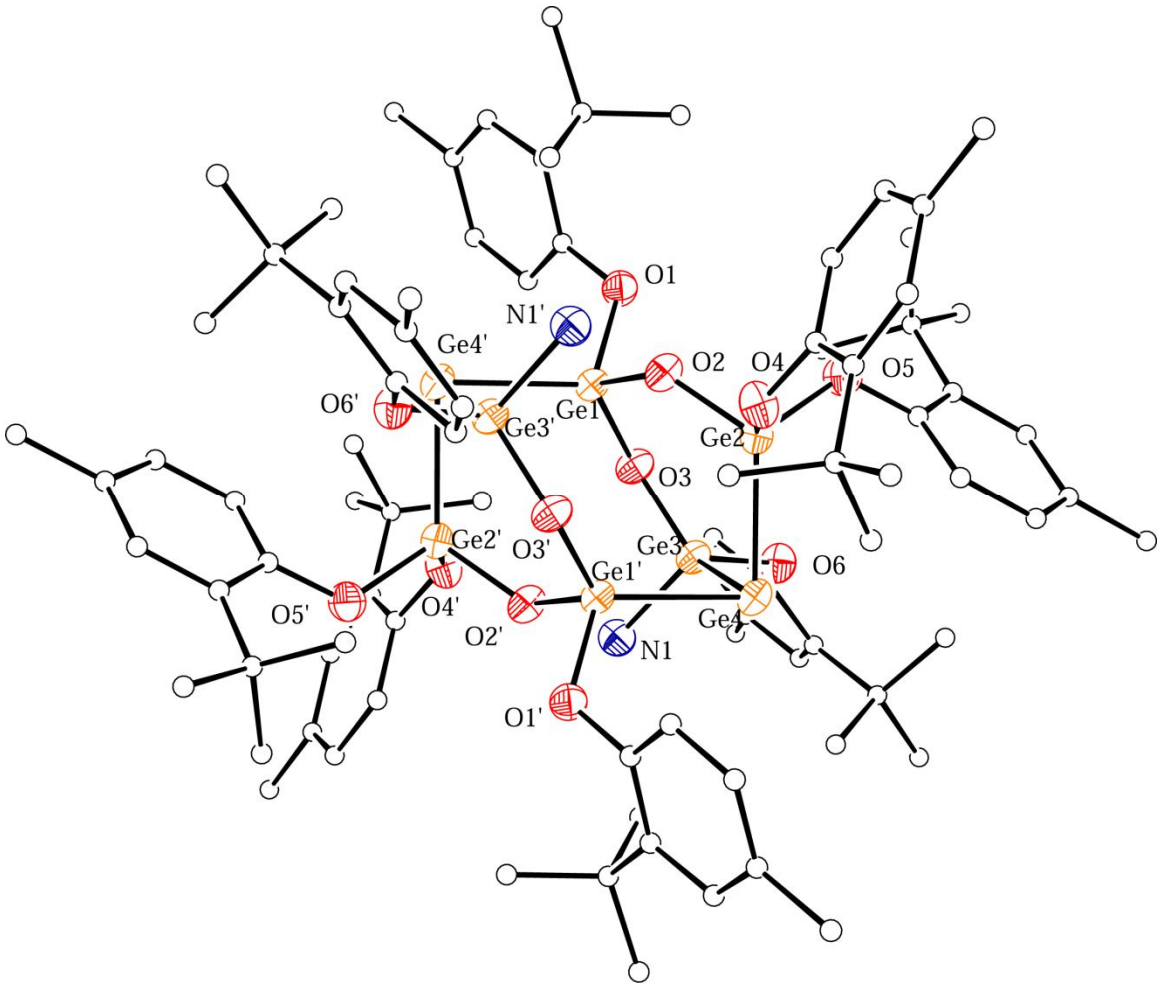

Figure 2. ORTEP diagram of **11**. Oxygen atoms are shown in red, germanium atoms in orange, nitrogen atoms in blue and carbon atoms are shown as white spheres.

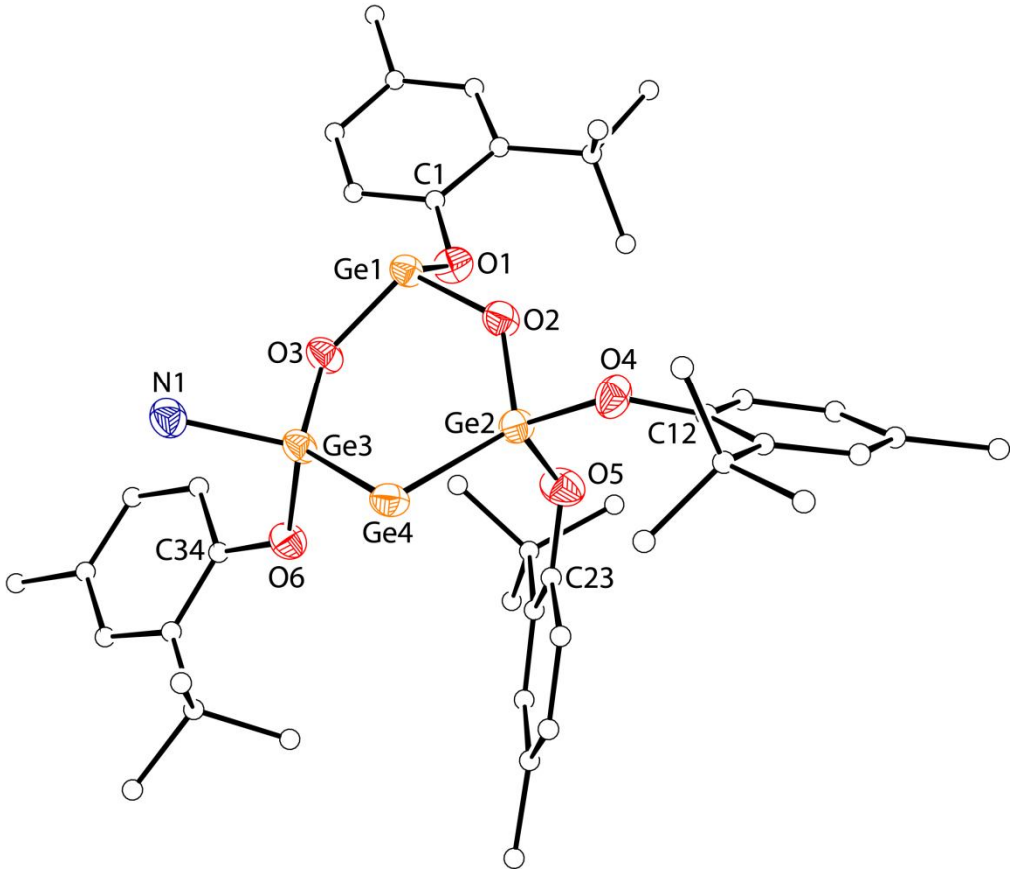

Figure 3. ORTEP diagram of the asymmetric unit of **11**. Oxygen atoms are shown in red, germanium atoms in orange, nitrogen atom in blue and carbon atoms as white spheres.

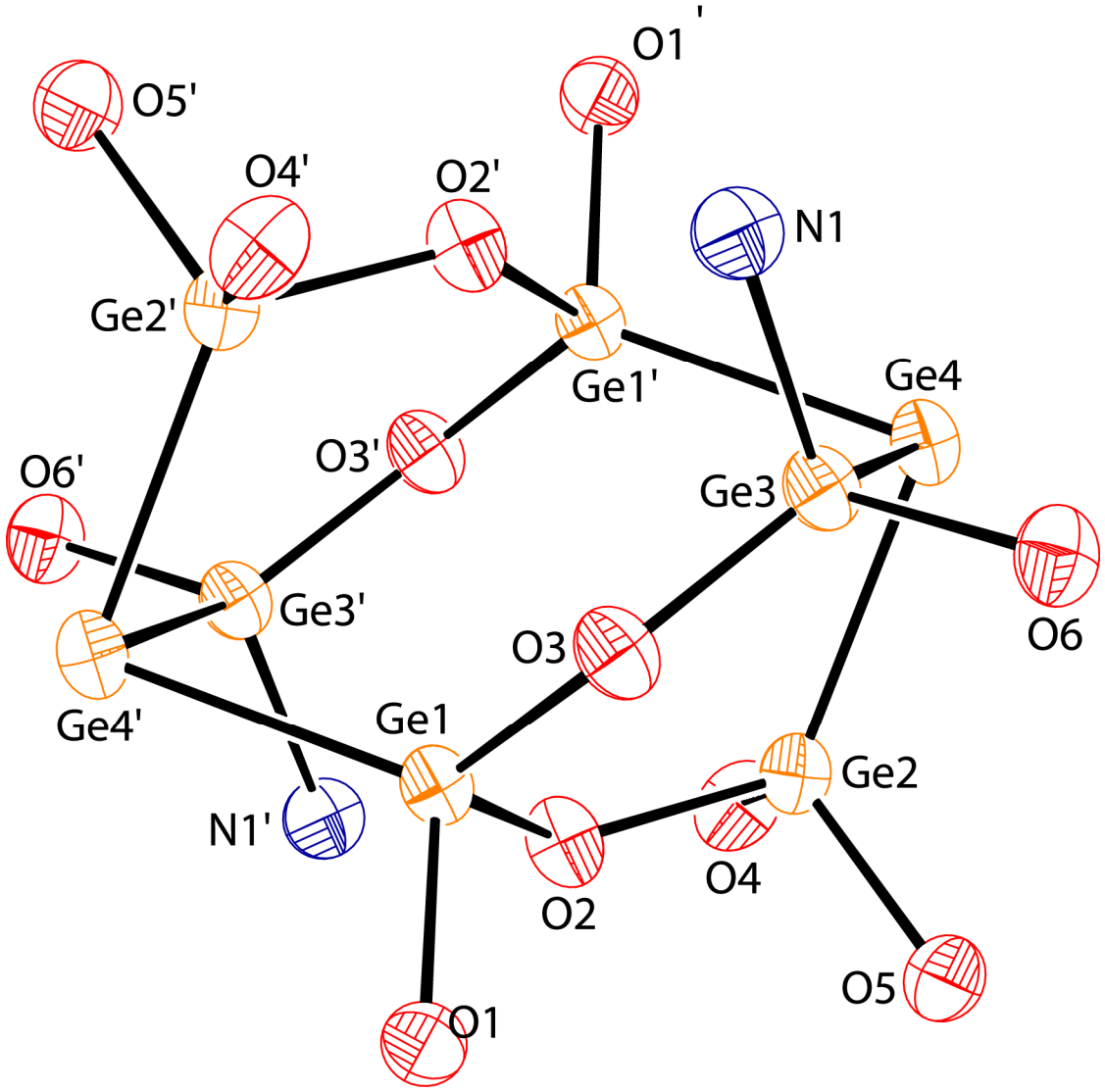

Figure 4. Cluster core diagram of **11**. Oxygen atoms are shown in red and germanium atoms in orange.

Table 2. Selected bond lengths (Å) and angles (°) for 11

Ge(1) – O(2)	1.790(2)	O(2) – Ge(1) – O(3)	107.39(9)
Ge(1) – O(3)	1.792(2)	O(2) – Ge(1) – O(1)	98.21(9)
Ge(1) – O(1)	1.799(2)	O(3) – Ge(1) – O(1)	103.84(9)
Ge(1) – Ge(4)	2.499(1)	O(2) – Ge(2) – O(5)	101.45(9)
Ge(2) – O(2)	1.779(2)	O(2) – Ge(2) – O(4)	97.44(8)
Ge(2) – O(5)	1.794(2)	O(5) – Ge(2) – O(4)	106.64(9)
Ge(2) – O(4)	1.819(2)	O(2) – Ge(2) – Ge(4)	120.26(6)
Ge(2) – Ge(4)	2.482(1)	O(5) – Ge(2) – Ge(4)	118.17(7)
Ge(3) – O(3)	1.777(2)	O(4) – Ge(2) – Ge(4)	110.29(6)
Ge(3) – O(6)	1.793(2)	O(3) – Ge(3) – O(6)	107.36(9)
Ge(3) – N(1)	1.998(2)	O(3) – Ge(3) – N(1)	96.1(1)
Ge(3) – Ge(4)	2.492(1)	O(6) – Ge(3) – N(1)	97.88(9)
O(3) – Ge(3) – Ge(4)	126.57(6)	O(6) – Ge(3) – Ge(4)	106.49(7)
N(1) – Ge(3) – Ge(4)	118.58(7)	Ge(2) – Ge(4) – Ge(3)	83.03(2)

The second product isolated in 21 % yield from the reaction of **7** and 2 equiv. of **8** was the octagermanium cluster $[Ge_8(\mu_3\text{-}O)_6(OC_6H_3\text{-}Bu^t\text{-}2\text{-}CH_3\text{-}4)_4]$ (**10**), via recrystallization from a hexane/toluene solvent mixture at -35 °C. An ORTEP diagram and the molecular structure of **10** are shown in **Figures 5** and **6** (respectively), while selected bond distances and angles are collected in **Table 3**. Complex **10** contains eight germanium atoms held together by six μ_3-oxo bridges, and four terminal aryloxide ligands are also present. All eight of the germanium atoms are in **10** are therefore in the +2 oxidation state. A Ge_4O_4 eight-membered ring containing Ge(2), Ge(3), Ge(6), Ge(7), O(5), O(7), O(8) and O(9) is present in **10**, and the four oxygen atoms are present in a distorted trigonal planar geometry, with average Ge – O – Ge bond angles of 117.6(1), 120.0(1), 120.0(1) and 118.2(1) °, (respectively). The four germanium atoms in the Ge_4O_8 ring adopt a highly distorted pyramidal geometry, with bond angles of 88.1(1), 89.8(1), 88.4(1) and 90.4(1) ° for Ge(2), Ge(3), Ge(6) and Ge(7) (respectively). A Ge_2O_2 rhombus, which has been reported for several other germanium(II) aryloxide species,[4,5,6,14] is also present in **10** (**Figure 5**). The bond angles within the rhombus average 99.6(1) ° and 80.5(1) ° for the Ge – O – Ge and O – Ge – O angles (respectively), which are similar to those found in related structures. The dimeric species $[Ge(OC_6H_3Pr^i_2\text{-}2,6)_2]_2$ has an average O_{br} – Ge – O_{br} angle of 72.38(6) ° and an average Ge – O_{br} – Ge bond angle of 107.0(6) °.[23] The compound {calix[4]}Ge_2 has an O_{br} – Ge – O_{br} angle of 72.11(6) ° and a Ge – O_{br} – Ge bond angle of 107.89(6) °.[6] The average O_{br} – Ge – O_{br} bond angle in {calix[8]}Ge_4 is 72.9(1) ° with an average Ge – O_{br} – Ge bond angle of 106.4(1) °.[6] The related compound {*p-tert*-butylcalix[8]}Ge_4 has an average O_{br} – Ge – O_{br} bond angle of 73.4(1) ° and an average Ge – O_{br} – Ge bond angle

of 106.7(1) °. The four O – Ge – O angles between the Ge_2O_2 rhombus and the Ge_4O_8 rings average 93.8(1) °, which is close to the expected value of 90 °.

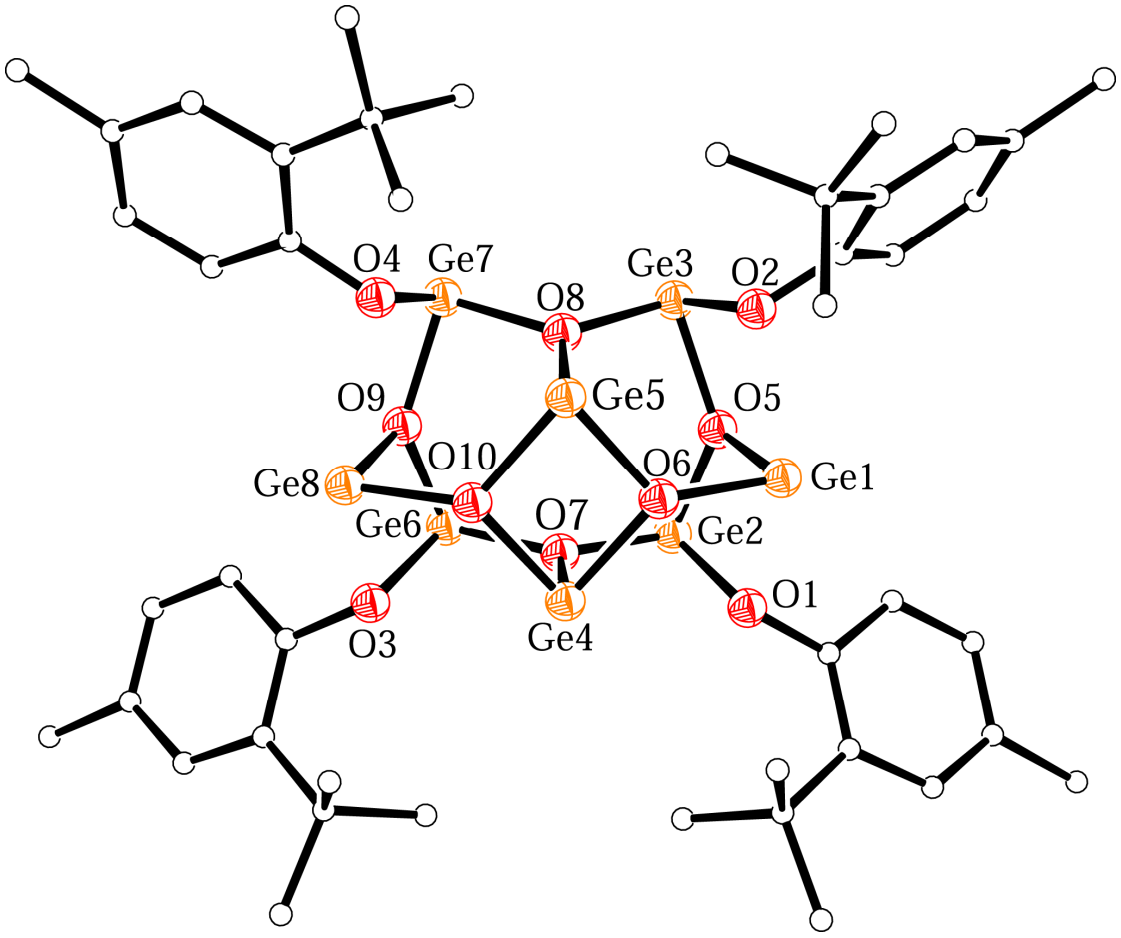

Figure 5. ORTEP diagram of **10**. Oxygen atoms are shown in red, germanium atoms in orange and carbon atoms are shown as white spheres.

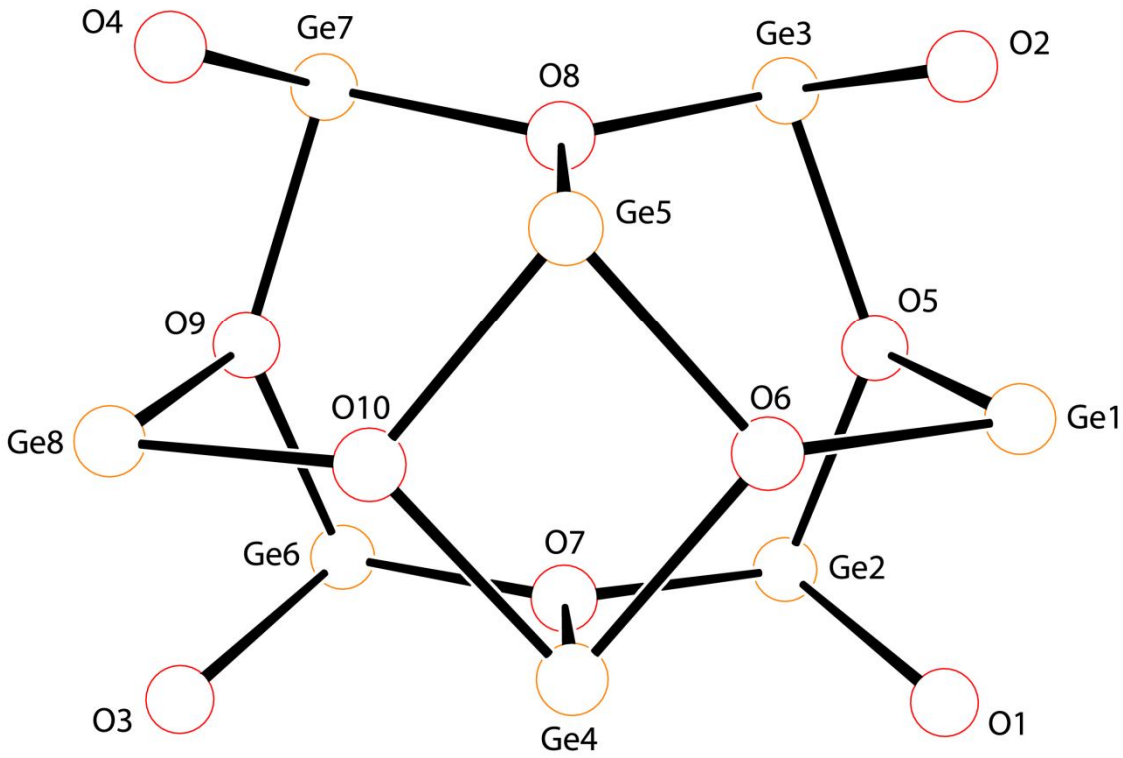

Figure 6. Molecular diagram of **10**. Oxygen atoms are shown as red spheres and germanium atoms as orange spheres.

Table 3. Selected bond lengths (Å) and angles (°) for 10

Ge(1) – O(5)	1.934(2)	O(6) – Ge(1) – O(5)	91.32(11)
Ge(1) – O(6)	1.885(2)	O(5) – Ge(2) – O(7)	93.82(10)
Ge(2) – O(1)	1.973(3)	O(5) – Ge(2) – O(1)	81.84(10)
Ge(2) – O(5)	1.907(2)	O(7) – Ge(2) – O(1)	88.74(10)
Ge(2) – O(7)	1.926(2)	O(8) – Ge(3) – O(5)	96.29(10)
Ge(3) – O(2)	1.945(3)	O(8) – Ge(3) – O(2)	90.24(11)
Ge(3) – O(5)	1.909(2)	O(5) – Ge(3) – O(2)	82.90(10)
Ge(3) – O(8)	1.905(2)	O(10) – Ge(4) – O(6)	80.77(10)
Ge(4) – O(6)	1.946(2)	O(10) – Ge(4) – O(7)	93.83(10)
Ge(4) – O(7)	1.956(2)	O(6) – Ge(4) – O(7)	93.20(10)
Ge(4) – O(10)	1.940(2)	O(6) – Ge(5) – O(8)	93.40(10)
Ge(5) – O(6)	1.951(2)	O(6) – Ge(5) – O(10)	80.13(10)
Ge(5) – O(8)	1.953(2)	O(8) – Ge(5) – O(10)	94.86(10)
Ge(5) – O(10)	1.961(2)	O(7) – Ge(6) – O(9)	95.84(10)
Ge(6) – O(3)	1.995(2)	O(7) – Ge(6) – O(3)	89.76(10)
Ge(6) – O(7)	1.902(3)	O(9) – Ge(6) – O(3)	79.66(9)
Ge(6) – O(9)	1.913(2)	O(9) – Ge(7) – O(4)	87.00(10)
Ge(7) – O(4)	1.893(2)	O(9) – Ge(7) – O(8)	93.51(10)

Ge(7) – O(8)	1.906(3)	O(4) – Ge(7) – O(8)	90.71(11)
Ge(7) – O(9)	1.878(2)	O(10) – Ge(8) – O(9)	90.10(10)
Ge(8) – O(9)	1.928(2)	C(1) – O(1) – Ge(2)	118.0(2)
Ge(8) – O(10)	1.877(3)	C(12) – O(2) – Ge(3)	113.8(2)
Ge(1) – O(1)	2.253(2)	C(23) – O(3) – Ge(6)	111.4(2)
Ge(1) – O(2)	2.337(2)	C(34) – O(4) – Ge(7)	116.1(2)
Ge(8) – O(3)	2.160(2)	Ge(2) – O(5) – Ge(3)	135.53(14)
O(1) – C(1)	1.379(4)	Ge(2) – O(5) – Ge(1)	108.21(11)
O(2) – C(12)	1.392(4)	Ge(3) – O(5) – Ge(1)	109.11(11)
O(3) – C(23)	1.408(4)	Ge(1) – O(6) – Ge(4)	124.90(12)
O(4) – C(34)	1.393(4)	Ge(1) – O(6) – Ge(5)	127.13(12)
Ge(4) – O(6) – Ge(5)	99.63(11)	Ge(6) – O(7) – Ge(2)	114.20(12)
Ge(6) – O(7) – Ge(4)	123.87(12)	Ge(2) – O(7) – Ge(4)	121.92(13)
Ge(3) – O(8) – Ge(7)	115.49(12)	Ge(3) – O(8) – Ge(5)	123.30(13)
Ge(7) – O(8) – Ge(5)	121.17(12)	Ge(7) – O(9) – Ge(6)	133.14(13)
Ge(7) – O(9) – Ge(8)	114.08(11)	Ge(6) – O(9) – Ge(8)	107.29(11)
Ge(8) – O(10) – Ge(4)	124.62(13)	Ge(8) – O(10) – Ge(5)	126.72(12)
Ge(4) – O(10) – Ge(5)	99.47(11)		

The Ge_2O_2 rhombus is also tethered to the Ge_4O_4 macrocycle by two bridging germanium atoms, having O – Ge – O bond angles of 90.1(1) and 91.3(1) °, and the bond angles about O(6) and O(10) average 125.8(1) °.

The bond distances in **10** from the germanium atoms to the oxygen atoms of the terminal aryloxide ligands are long compared to those in monomeric or dimeric germanium(II) aryloxides (1.802(8) – 1.828(3))[1,23] and vary from 1.893(2) – 1.995(2) Å with an average value of 1.952(3) Å. The Ge – O distances within the Ge_4O_4 macrocycle also span a wide range, from 1.878(2) – 1.926(2) Å with an average value of 1.906(2) Å. The Ge – O distances within the Ge_2O_2 rhombus average 1.950(2) Å, while those between the oxygen atoms in the Ge_2O_2 rhombus and Ge(1) or Ge(8) are short and average 1.886(3) Å. The remaining Ge – O distances, which connect the Ge_2O_2 rhombus to the Ge_4O_4 macrocycle either directly or via the bridging Ge(1) or Ge(8) atoms average 1.954(2) and 1.931(2) Å (respectively). The Ge – O distances between germanium and the oxo-atoms are therefore longer than those typically found between germanium and bridging oxygen atoms, and overall these distances span the wide range between 1.878(3) – 1.995(2) Å.

In the ^{1}HNMR spectrum that was obtained for $[Ge_4(\mu\text{-}O)_2(OC_6H_3Bu^t\text{-}2\text{-}CH_3\text{-}4)_4\cdot NH_3]_2$ (**11**), there is one peak present at δ 1.50 ppm that corresponds to the *tert*-butyl group of the aryloxide ligands. Despite the fact that the protons of the *tert*-butyl groups are present in a very similar magnetic environment they are not magnetically equivalent; therefore, the peaks that are observed overlap with each other and cannot be resolved, leading to only one peak being observed. Likewise, there is one peak present for the methyl group of the phenoxide ligand at δ 2.17 ppm. The *ortho*- and *meta*- aromatic

protons are not all magnetically equivalent and so germanium atoms that bear one aryloxide ligand (Ge(1) and Ge(3)) have chemical shifts for the aromatic protons that are further downfield while Ge(2) bears two aryloxide ligands and thus the chemical shifts of those aromatic protons are shifted upfield. The *meta*-proton on C(3) (see **Figure 7** below) has a chemical shift of δ 7.15 ppm for the aryloxide ligands that are bound to Ge(2) and δ 7.12 ppm for the aryloxide ligands that are bound to Ge(1) and Ge(3). These protons are observed as singlets. The *meta*-proton on C(5) is observed as a doublet and similar to the proton on C(3), there are two chemical shifts for the proton on C(5). For the aryloxide ligands on Ge(1) and Ge(3), the chemical shift is δ 6.89 ppm while the aryloxide groups on Ge(2) have a chemical shift of δ 6.84 ppm. The same trend is observed for the *ortho*-proton of C(6). There is a chemical shift of δ 6.76 ppm (seen as a doublet) for aryloxide ligands bound to Ge(1) and Ge(3) and a chemical shift of δ 6.73 ppm (seen as a doublet) for the ligands bound to Ge(2). In the ^{1}H NMR spectrum of the large Ge_8 cluster one peak is observed for the *tert*-butyl group at δ 1.47 ppm. One peak is observed for the methyl group at δ 2.20 ppm. With the loss of four aryloxide groups in the formation of $[Ge_8(\mu_3\text{-}O_6(OC_6H_3Bu^t\text{-}2\text{-}CH_3\text{-}4)_4]$ (**10**), all phenoxide ligands are magnetically equivalent and thus one peak is observed for each aromatic proton. The *meta*-proton on C(3) (see diagram below) is observed as a singlet at δ 7.17 ppm. For the *meta*-proton on C(5) the peak is seen at δ 6.85 ppm while the *ortho*-proton on C(6) is observed at δ6.72 ppm.

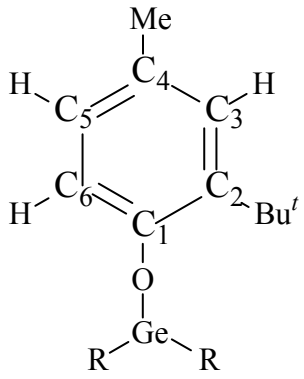

Figure 7. Schematic diagram of the aryloxide ligand of **10** and **11**. The R groups include the Ge(II) / oxo cluster.

In order to probe the pathway for the formation of the clusters **10** and **11**, the reaction mixture was analyzed by GC/MS and the reaction of **7** with **8** was monitored using ^{1}H NMR spectroscopy. The gas chromatogram of the reaction mixture indicated the presence of three volatile components, which were identified as $HN(SiMe_3)_2$, the silyl ether $Me_3SiOC_6H_3$-Bu^t-2-CH_3-4 (**12**), and the amine $HN(C_6H_3$-Bu^t-2-CH_3-4$)_2$ (**13**) by their mass spectra. The presence of **12** was further confirmed by analysis of an authentic sample of this material which was prepared using a literature method[24] (**Scheme 4**) that exhibited the same retention time and mass spectrum.

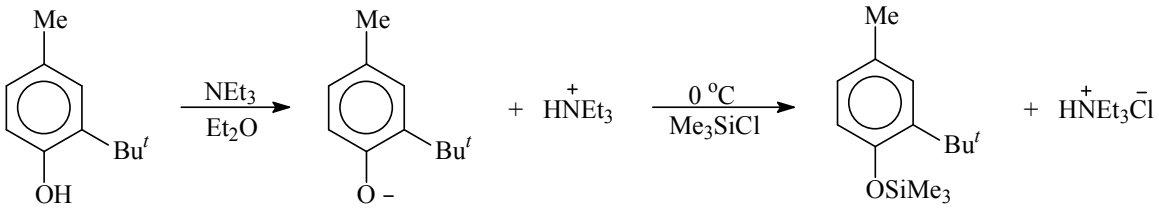

Scheme 4. Reaction of $HOC_6H_3Bu^t$-2-CH_3-4 with NEt_3 and Me_3SiCl to yield the silylated phenol $Me_3SiOC_6H_3Bu^t$-2-CH_3-4.

These findings indicate that some of the phenol **8** is silylated via reaction with $HN(SiMe_3)_2$, which was observed in reactions of 3,3'-disubstituted binaphthols with various metal(II) amides including $Ge[N(SiMe_3)_2]_2$ (**7**).[3,6] The presence of **13** suggests deoxygenation of **8** is also occurring in the reaction to generate the bridging oxo-atoms present in clusters **10** and **11**, and NH_3 that is generated in the silylation reaction could serve as the precursor for **13**.

It was determined by ^{1}H NMR spectroscopy that complete consumption of **8** and concomitant formation of $HN(SiMe_3)_2$ occurred immediately after mixing the two reagents, leading to the formation of a germanium aryloxide product which we speculate to be the dimeric species **11** (**Scheme 5**). Dimeric germanium(II) aryloxides undergo an exchange of the bridging and terminal ligands via an open intermediate **14**, as demonstrated for $[Ge(OC_6H_3Pr^i$-2,6$)_2]_2$.[4] The formation of compound **11** could potentially proceed via dimerization of the open intermediate **14** to generate **15**, which then loses aryloxide ligands via reaction with $HN(SiMe_3)_2$ to furnish **12** and also undergoes cleavage of the oxygen – carbon bonds of the bound aryloxide ligands to

provide the μ-oxo ligands and 1**4**. The presence of **10** was detected in the reaction mixture after a reaction time of 1.5 h, and after 18 h both **11** and **10**, along with the byproducts **12** and **13**, were present.

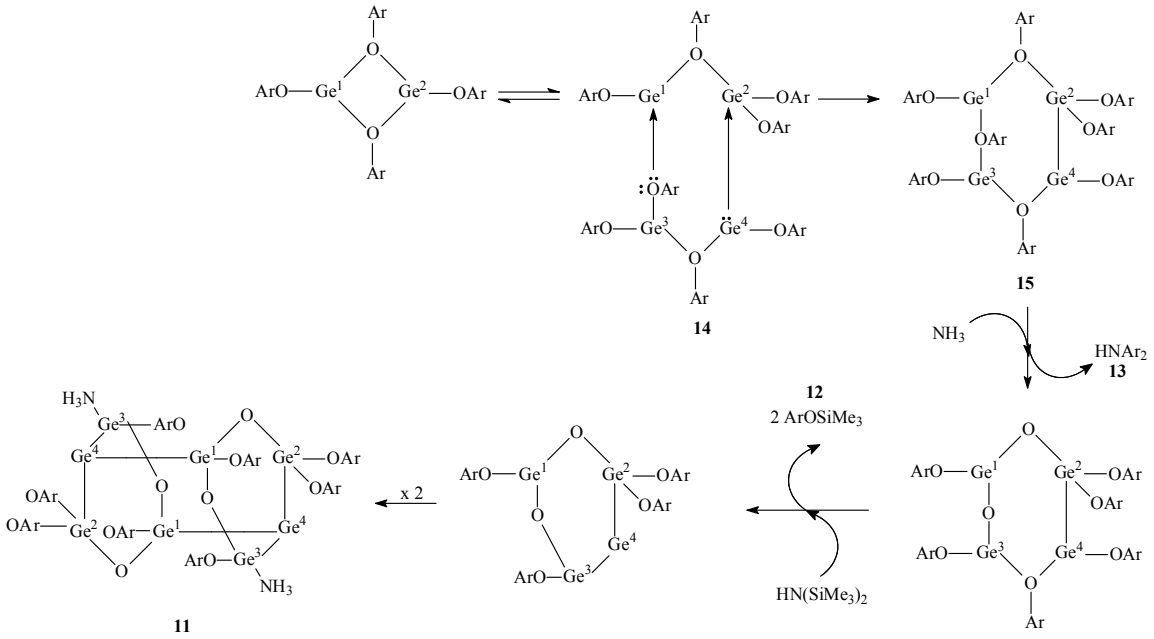

Scheme 5. Proposed pathway for the formation of clusters **10** and **11**.

Ar = -C_6H_3-Bu^t-2-Me-4.

No further change was observed in the ^{1}H NMR spectrum of the reaction after 18 h, but exposure of the NMR tube to dioxygen gas resulted in the complete conversion of **11** to **10** within 6 h, suggesting that **11** is an intermediate formed along the reaction pathway that generates the cluster **10**. The interconversion of **11** to **10** must involve migration of the aryloxide ligands and also insertion of oxygen into the Ge – Ge bonds of **11**, and the latter process has been reported for several germanium species which contain Ge – Ge bonds (**Scheme 6**).[25-28]

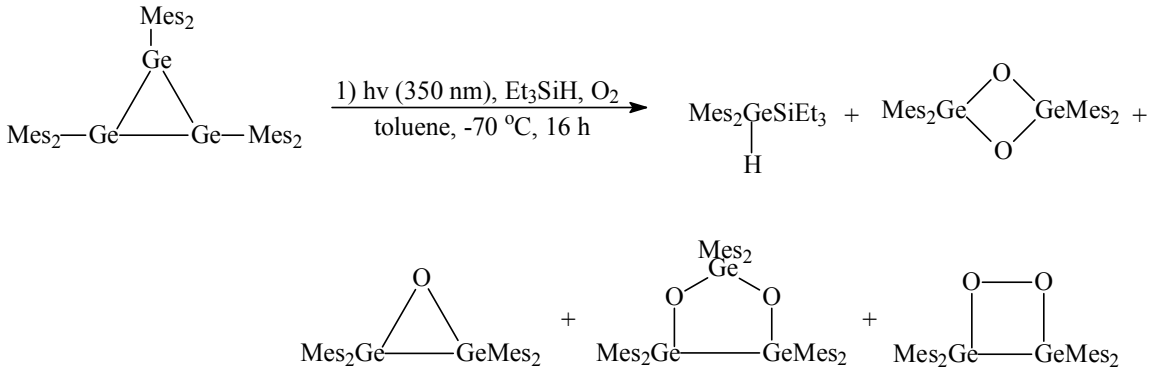

Scheme 6. Insertion of dioxygen into Ge – Ge single bonds.

Monitoring the reaction of a 4:5 stoichiometric ratio of **7** to **8** by ^{1}H NMR spectroscopy indicated that formation of cluster **10** was complete within 8 h, and the presence of **11** was also detected during the course of this reaction. However, no compound **11** remained after the reaction was concluded, and therefore cluster **10** was generated solely

by the deoxygenation of the phenol starting material **8**. This was confirmed by conducting the same reaction on a preparative scale, which resulted in the isolation of **10** in 74 % yield.

Treatment of $Ge[N(SiMe_3)_2]_2$ (**7**) with two equiv. of 4-*tert*-butyl phenol was also expected to yield a dimeric aryloxide due to the sterically unencumbering nature of the incoming ligand. However, the structure of the resulting product was again determined to be a cluster containing six rather than eight germanium atoms with the formula $Ge_6(\mu_3\text{-}O)_4(\mu_2\text{-}OC_6H_4Bu^t\text{-}4)_4$ (**16**). An ORTEP and molecular diagram of **16** is illustrated in **Figures 8** and **9** (respectively) while selected bond distances and angles are collected in **Table 4**. A scheme for the synthesis of **16** is shown in **Scheme 7**.

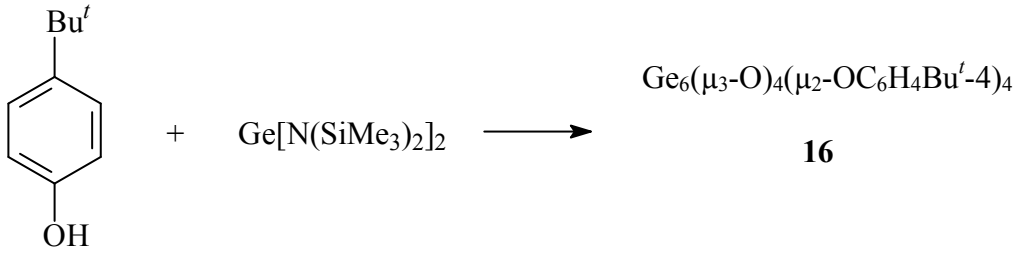

Scheme 7. Reaction of $HOC_6H_4Bu^t$-4 with $Ge[N(SiMe_3)_2]_2$ to yield the hexagermanium cluster $Ge_6(\mu_3\text{-}O)_4(\mu_2\text{-}OC_6H_4Bu^t\text{-}4)_4$.

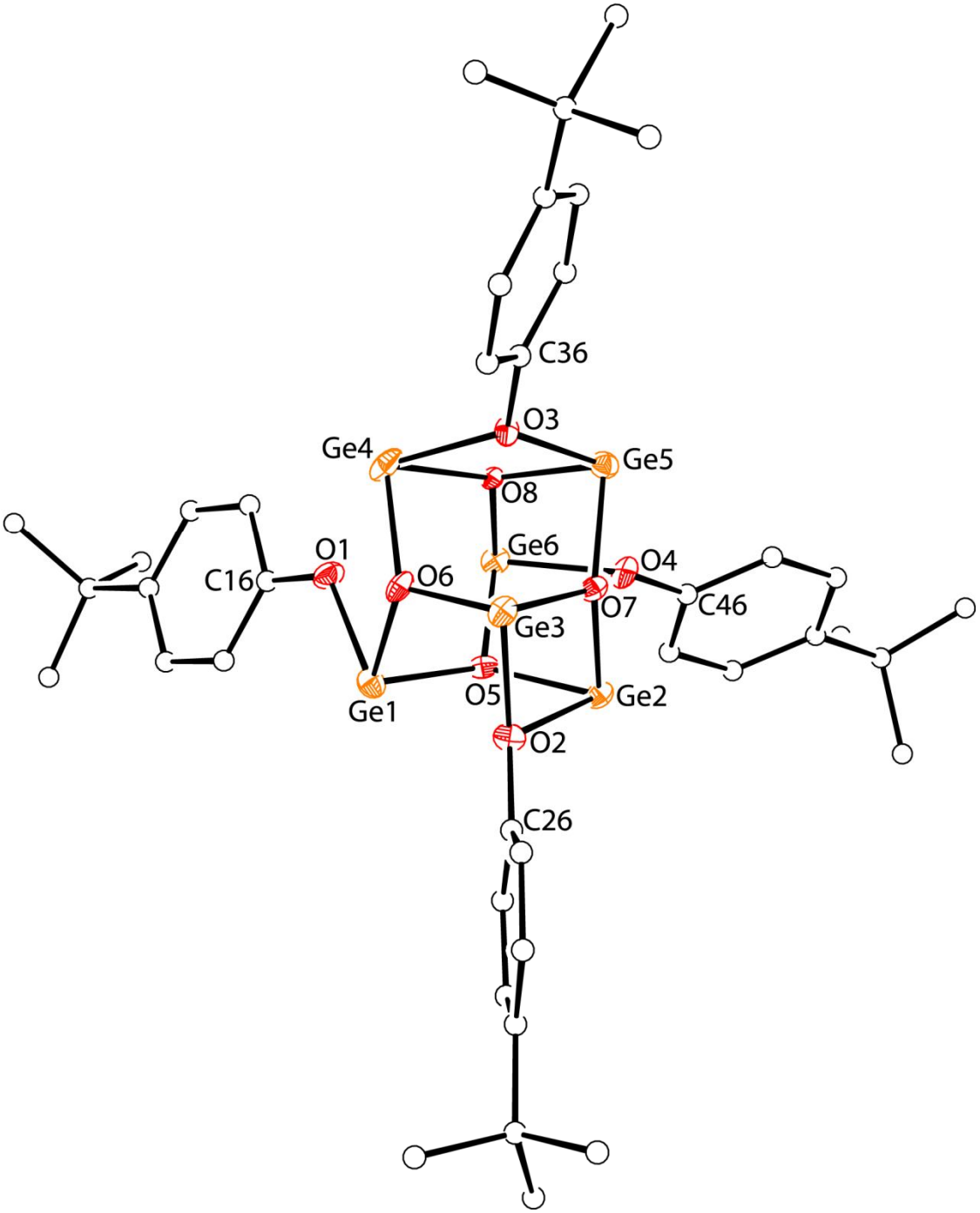

Figure 8. ORTEP diagram of **16**. Oxygen atoms are shown in red, germanium atoms are shown in orange and carbon atoms are shown as white spheres.

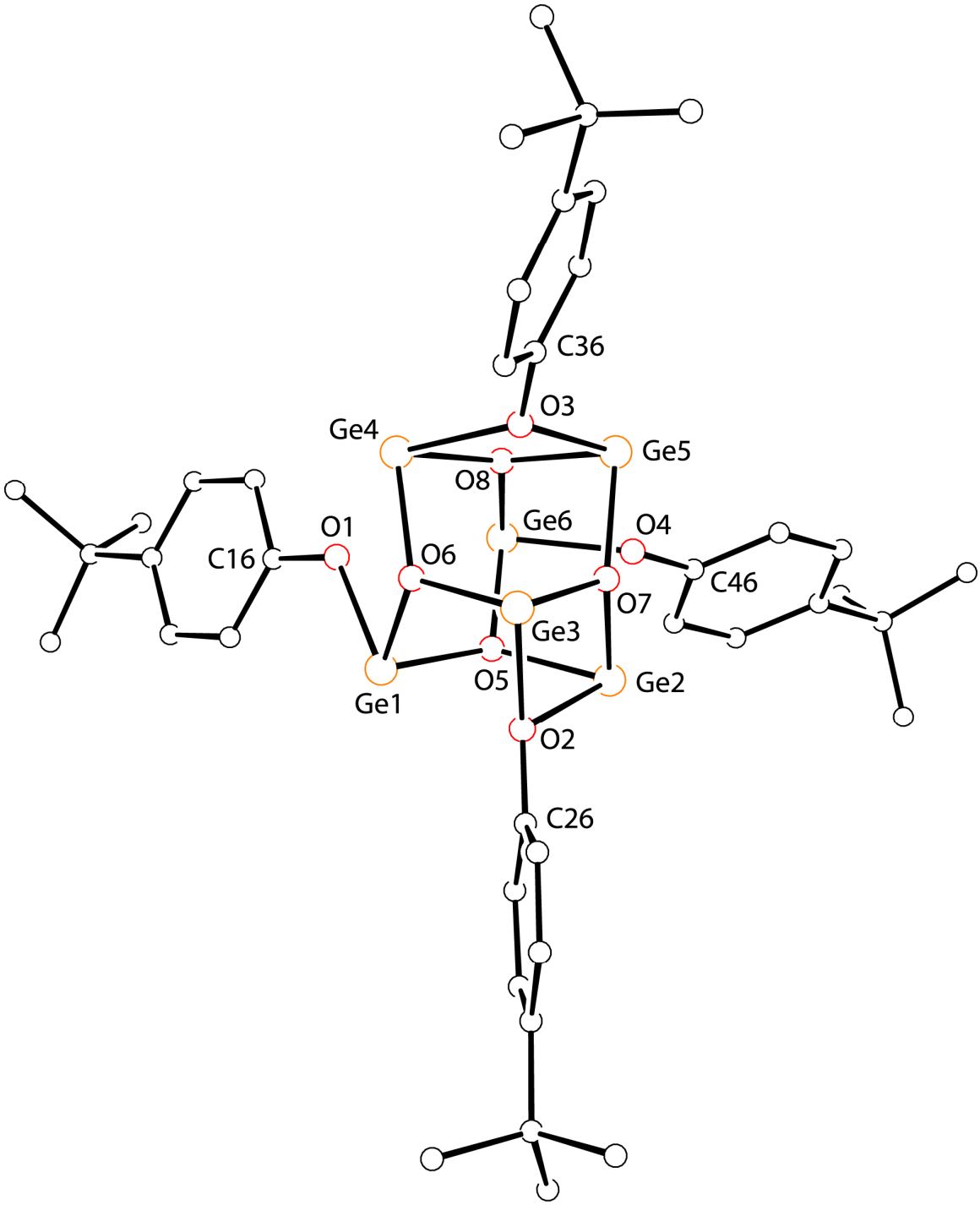

Figure 9. Molecular diagram of **16**. Carbon atoms are shown as black spheres, oxygen atoms as red spheres and germanium atoms as orange spheres.

Table 4. Selected bond distances (Å) and angles (°) for 16.

Ge(1) – O(5)	1.892(5)	O(5) – Ge(1) – O(6)	93.5(2)
Ge(1) – O(6)	1.924(5)	O(5) – Ge(1) – O(1)	85.9(2)
Ge(1) – O(1)	1.966(5)	O(6) – Ge(1) – O(1)	81.0(2)
Ge(2) – O(7)	1.931(5)	O(7) – Ge(2) – O(5)	94.1(2)
Ge(2) – O(5)	1.936(5)	O(7) – Ge(2) – O(2)	73.7(2)
Ge(2) – O(2)	2.146(5)	O(5) – Ge(2) – O(2)	82.5(2)
Ge(2) – O(4)	2.365(6)	O(7) – Ge(2) – O(4)	78.7(2)
Ge(3) – O(7)	1.905(5)	O(5) – Ge(2) – O(4)	73.1(2)
Ge(3) – O(6)	1.908(5)	O(2) – Ge(2) – O(4)	141.43(18)
Ge(3) – O(2)	2.001(5)	O(7) – Ge(3) – O(6)	92.7(2)
Ge(4) – O(8)	1.913(5)	O(7) – Ge(3) – O(2)	77.7(2)
Ge(4) – O(6)	1.913(5)	O(6) – Ge(3) – O(2)	84.9(2)
Ge(4) – O(3)	2.192(5)	O(8) – Ge(4) – O(6)	93.6(2)
Ge(4) – O(1)	2.379(6)	O(8) – Ge(4) – O(3)	75.2(2)
Ge(5) – O(7)	1.908(5)	O(6) – Ge(4) – O(3)	82.6(2)
Ge(5) – O(8)	1.919(5)	O(8) – Ge(4) – O(1)	81.0(2)
Ge(5) – O(3)	2.022(5)	O(6) – Ge(4) – O(1)	71.2(2)
Ge(6) – O(8)	1.893(5)	O(3) – Ge(4) – O(1)	143.16(18)

Ge(6) – O(5)	1.926(5)	O(7) – Ge(5) – O(8)	92.3(2)
Ge(6) – O(4)	1.977(5)	O(7) – Ge(5) – O(3)	84.4(2)
O(1) – C(16)	1.377(9)	O(8) – Ge(5) – O(3)	79.2(2)
O(2) – C(26)	1.380(8)	O(8) – Ge(6) – O(5)	93.6(2)
O(3) – C(36)	1.379(9)	O(8) – Ge(6) – O(4)	83.8(2)
O(4) – C(46)	1.365(9)	O(5) – Ge(6) – O(4)	82.9(2)
C(46) – O(4) – Ge(2)	112.2(4)	C(16) – O(1) – Ge(1)	123.6(5)
Ge(6) – O(4) – Ge(2)	93.2(2)	C(16) – O(1) – Ge(4)	139.6(5)
Ge(1) – O(5) – Ge(6)	117.9(2)	Ge(1) – O(1) – Ge(4)	94.1(2)
Ge(1) – O(5) – Ge(2)	118.8(3)	C(26) – O(2) – Ge(3)	130.6(5)
Ge(6) – O(5) – Ge(2)	110.2(3)	C(26) – O(2) – Ge(2)	120.8(4)
Ge(3) – O(6) – Ge(4)	119.2(3)	Ge(3) – O(2) – Ge(2)	98.2(2)
Ge(3) – O(6) – Ge(1)	116.7(2)	C(36) – O(3) – Ge(5)	122.2(5)
Ge(4) – O(6) – Ge(1)	112.6(3)	C(36) – O(3) – Ge(4)	129.5(5)
Ge(3) – O(7) – Ge(5)	117.5(2)	Ge(5) – O(3) – Ge(4)	95.7(2)
Ge(3) – O(7) – Ge(2)	109.7(3)	C(46) – O(4) – Ge(6)	122.3(5)
Ge(5) – O(7) – Ge(2)	121.5(3)	Ge(6) – O(8) – Ge(5)	116.9(2)
Ge(6) – O(8) – Ge(4)	122.7(3)	Ge(4) – O(8) – Ge(5)	109.3(2)

The Ge_6 framework of **16** is bound together by four μ_3-bridging oxo ligands and four μ_2-4-*tert*-butylaryloxide ligands. All six of the germanium atoms of **16** are again in the +2 oxidation state and there are no germanium – germanium bonds present in **16**. To our knowledge no other examples of a germanium(II) aryloxide compounds having a cluster-type structure similar to **16** have been described.

Four of the six germanium atoms in **16** are present in a highly distorted trigonal pyramidal geometry due to the geometric constraints enforced by the presence of bridging oxo- and aryloxo groups. The remaining two germanium atoms, Ge(2) and Ge(4), are four coordinate and are present in a highly distorted square planar geometry. The O – Ge – O bond angles in **16** span the wide range from 71.2(2) to 143.2(2) °, and the two most obtuse O – Ge – O angles that measure 141.4(2) and 143.2(2) ° occur between germanium and two of the aryloxo groups. The O – Ge – O bond angles ranging from 92.3(2) – 94.1(2) ° lie between germanium and two of the μ_3-bridging oxygen atoms, while the most acute O – Ge – O bond angles measuring less than 90 ° occur between germanium and one of the μ_3-oxo- and μ_2-aryloxo-oxygen atoms.

The structure of **16** can be regarded as being comprised of four interconnected Ge_2O_2 rhombi **16r$_1$** – **16r$_4$**, or alternatively as containing eight overlapping Ge_3O_3 six-membered rings **16c$_1$** – **16c$_4$**. The constituent germanium and oxygen atoms for these two types of cyclic frameworks are listed in **Table 4**, and ORTEP diagrams of the Ge_6O_8 cluster core illustrating the ring structures are shown in **Figure 10**.

Table 5. Cyclic framework for **16**.

Four Membered Rings	
Rhombus	Atoms
$16r_1$	Ge(1) – O(1) – Ge(4) – O(6)
$16r_2$	Ge(2) – O(2) – Ge(3) – O(7)
$16r_3$	Ge(2) – O(4) – Ge(6) – O(5)
$16r_4$	Ge(4) – O(3) – Ge(5) – O(8)
Six Membered Rings	
Chair Conformation	
$16c_1$	Ge(1) – O(6) – Ge(3) – O(7) – Ge(2) – O(5)
$16c_2$	Ge(1) – O(6) – Ge(4) – O(8) – Ge(6) – O(5)
$16c_3$	Ge(2) – O(5) – Ge(6) – O(8) – Ge(5) – O(7)
$16c_4$	Ge(3) – O(6) – Ge(4) – O(8) – Ge(5) – O(7)
Boat Conformation	
$16c_5$	Ge(1) – O(6) – Ge(3) – O(2) – Ge(2) – O(5)
$16c_6$	Ge(1) – O(1) – Ge(4) – O(8) – Ge(6) – O(5)
$16c_7$	Ge(2) – O(4) – Ge(6) – O(8) – Ge(5) – O(7)
$16c_8$	Ge(3) – O(6) – Ge(4) – O(3) – Ge(5) – O(7)

Comprised of Ge(1) – O(1) – Ge(4) – O(6) (rhombus **16A**), Ge(2) – O(2) – Ge(3) – O(7) (rhombus **16B**), Ge(2) – O(4) – Ge(6) – O(5) (rhombus **16C**), and Ge(4) – O(3) – Ge(5) – O(8) (rhombus **16D**).

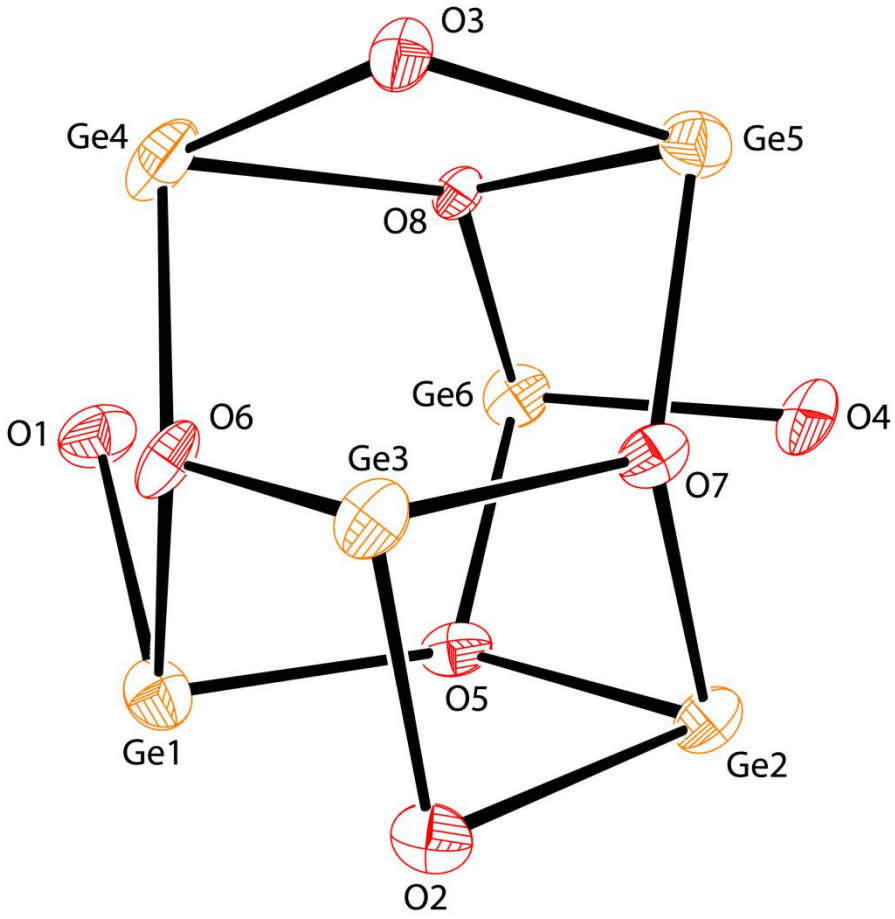

Figure 10. ORTEP diagram of Ge_6O_8 cluster core of **16**. Oxygen atoms are shown in red and germanium atoms are shown in orange.

Unlike previously reported structures having Ge_2O_2 rhombi that contain two μ_2-aryloxide ligands, one of the oxygen atoms in each of the rings of **16** is part of a μ_2-aryloxide ligand while the other is a μ_3-oxo ligand. Each of the individual Ge_2O_2 rhombi is puckered, by 8.5 ° (**16r$_1$**), 5.9 ° (**16r$_2$**), 7.4 ° (**16r$_3$**), and 5.7 ° (**16r$_4$**), and within the four Ge_2O_2 rhombi, one of the Ge – O – Ge bond angles is significantly more obtuse than the other by 18.5 ° (**16r$_1$**), 11.5 ° (**16r$_2$**), 17 ° (**16r$_3$**), and 13.6 ° (**16r$_4$**). Of the eight Ge_3O_3 rings, four of these adopt an approximate chair-type conformation similar to cyclohexane (**16c$_1$ – 16c$_8$**). All eight of the six-membered rings are distorted from these two idealized geometries due to the sharing of common bonds within the Ge_6O_8 cluster framework.

All of the Ge – O bonds in **16** are either μ_2- or μ_3-bridging in nature, and are therefore longer than typical terminal Ge – O distances. The two shortest bond lengths in **16** lie between Ge(1) – O(5) and Ge(6) – O(8), measuring 1.892(5) and 1.893(5) Å (respectively). The remaining bridging Ge – O bond distances fall within the expected range of 1.90 to 2.20 Å, with the exception of the Ge(2) – O(4) and Ge(4) – O(1) distances of 2.365(6) and 2.379(6) Å (respectively). Although these two bond distances are long relative to those of other germanium(II) compounds having bridging aryloxide ligands, they fall within the sum of the van der Waals radii for these elements.

The separation between Ge(1) and O(2) measures 2.61 Å and is well outside the sum of the van der Waals radii, as are the Ge(3) – O(3), Ge(5) – O(4), and Ge(6) – O(1) distances of 2.61, 2.56, and 2.68 Å (respectively). Bonding interactions involving these three sets of atoms would require the aryloxide ligands to be triply bonding in nature, and this bonding mode is unusual and is typically observed only in complexes having large metal centers bound to unsubstituted or sterically unencumbered aryloxide ligands.[15]

Examples of complexes having μ_3-aryloxide ligands include the large group 2 metal complexes $[Ca_3(\mu_3\text{-}OC_6H_5)_2(\mu_2\text{-}OC_6H_5)_3(HMPA)_6]^+$,[16] $[Sr_3(\mu_3\text{-}OC_6H_5)_2(\mu_2\text{-}OC_6H_5)_3(OPh)(HMPA)_5]$,[16] $[Ba_6(\mu_3\text{-}OC_6H_5)_2(\mu_2\text{-}OC_6H_5)_3(OPh)_7(TMEDA)_4]$[16]. This type of ligation has also been observed in the highly ionic lithium and sodium complexes $[Li_6(\mu_3\text{-}OC_6H_5)_6(THF)_6]$[17] and $[Na_4(\mu_3\text{-}OC_6H_4\text{-}Me\text{-}4)_4(DME)_4]$.[18] The triply bridging bonding mode has not, to our knowledge, been reported for any group 14 aryloxide complexes and therefore it is not surprising that μ_3-$OC_6H_4Bu^t$-4 ligands are not observed in **16**.

The reaction pathway for the formation of **16** was also investigated and it was noted through ^{1}H NMR spectroscopy that hexamethyldisilazane was produced as a by-product. It was also observed that the phenol was converted to a silyl ether due to the presence of peaks corresponding to the *tert*-butyl groups and three methyl groups of $Me_3SiOC_6H_4Bu^t$-4 that were observed at δ 1.22 and δ 0.19 ppm (respectively). These peaks were also observed in an authentic sample that was prepared from a literature method.[24] The presence of bis(4-*tert*-butylphenyl)amine was also noted in the ^{1}H NMR spectrum of **16** when compared to a ^{1}H NMR spectrum of an authentic sample of the amine with a peak for the two equivalent *tert*-butyl groups at δ 1.27 ppm. The GC/MS was obtained for the products of the protonolysis reaction between 4-*tert*-butylphenol and $Ge[N(SiMe_3)_2]_2$, and the presence of the two by-products was confirmed by analysis of the chromatogram and mass spectra. Bis(4-*tert*-butylphenyl)amine eluted at 9.48 minutes while the silylated phenol, $Me_3SiOC_6H_4Bu^t$-4 eluted at 11.15 minutes. The peak at *m/z* 281 for the parent molecule corresponds to bis(4-*tert*-butylphenyl)amine. Peaks present at *m/z* 222 and *m/z* 207 are attributed to the silylated phenol parent molecule and the loss

of a methyl group respectively. The silyl ether was prepared according to a literature procedure[24] while the amine was purchased from Aldrich and used as received. The GC/MS spectra of these authentic samples were also collected and confirmed the presence of these two products with retention times and the mass spectra matching those of the reaction products. It is also inferred that the ^{1}H NMR signals for the *tert*-butyl groups of **16** and the by-products overlap each other and cannot be resolved. The presence of bis(4-*tert*-butylphenyl)amine lends further credence that the oxo atoms in the cluster come from the deoxygenation of the starting phenol.

In conclusion, it has been demonstrated that phenol substrates that bear substituents in both the *ortho*- positions yield either monomeric or dimeric aryloxide compounds depending upon the steric bulkiness of the substituent. These products are formed by the protonolysis reaction between the phenol and $Ge[N(SiMe_3)_2]_2$ to yield hexamethyldisilazane as the by-product. It has also been determined that phenol substrates which lack substitution in both the 2- and 6- positions yield large germanium(II) aryloxide/oxo clusters that are held together by bridging aryloxide and/or oxo groups. These products are generated by protonolysis of the phenol with $Ge[N(SiMe_3)_2]_2$ as well as the deoxygenation of the phenol reactant, which has not been previously observed in reactions of germanium amides with phenols. The Ge_4 dimer was co-crystallized with the large Ge_8 cluster and is an intermediate in the reaction pathway for the formation of the large Ge_8 cluster. The large Ge_6 and Ge_8 clusters reported here are of interest from a structural standpoint in that a large aggregate containing only divalent germanium atoms has not been described before. In addition, the preparation of germanium(0) nanomaterials from both might also furnish species having unusual

morphologies, since both contain an ensemble of germanium atoms while precursors currently employed for these investigations contain only one or two Ge atoms. The reaction of $Ge[N(SiMe_3)_2]_2$ with one equivalent of the sterically unencumbering phenol $HOC_6H_4Bu^t$-4 yielded the first example of a cluster that contained only Ge(II) atoms that are connected together with bridging oxo atoms and bridging aryloxide groups. The synthesis of other Ge_n cluster complexes from **7** and other sterically unencumbering phenols, as well as investigations into the use of these compounds as molecular precursors for germanium nanomaterials, are currently underway.

Experimental

General Considerations

All manipulations were carried out under an atmosphere of nitrogen using standard Schlenk, glovebox, and syringe techniques.[1] The reagent $Ge[N(SiMe_3)_2]_2$ (**7**) was prepared according to literature methods.[2-4] The phenols $HOC_6H_3Bu^t$-2-Me-6 and $HOC_6H_3Bu^t$-2-Me-4 (**8**) were obtained from Aldrich and were sublimed under high vacuum (0.005 torr) prior to use. Solvents were dried using a Glass Contour Solvent Purification System. Benzene and benzene-d_6 were tested for the presence of moisture by treating 0.50 mL of solvent with 50 μL of a benzene solution of sodium benzophenone ketyl, and the intense blue color remained for a minimum of 8 h. NMR spectra (^1H and ^{13}C) were recorded on a Varian INOVA 400 NMR spectrometer operating at 400 or 100.58 MHz (respectively) and were referenced to the residual protio solvent in an

external sample of C_6D_6 by replacement. GC/MS data were acquired at 280 °C using a Hewlett-Packard G1800A GC/MS with a flow rate of 1.0 mL/min.

Preparation of $Ge_6(\mu_3\text{-}O)_4(\mu_2\text{-}OC_6H_4Bu^t\text{-}4)_4$ (16)

To a solution of $HOC_6H_4Bu^t$-4 (0.500 g, 3.33 mmol) in benzene (15 mL) was added a solution of $Ge[N(SiMe_3)_2]_2$ (**7**) (0.655 g, 1.66 mmol) in benzene (10 mL). The reaction mixture was stirred at room temperature for 4 h and the volatiles were removed *in vacuo* to yield a white solid. The crude material was recrystallized from hot benzene (10 mL) to yield 0.209 g (68 %) of **16** as clear and colorless crystals. ^{1}H NMR (C_6D_6, 25 °) δ 7.26 (d, J = 8.8 Hz, 8H, *meta*-H), 7.09 (d, J = 8.4 Hz, 8H, *ortho*-H), 1.24 (s, 36H, -C(CH_3)$_3$) ppm.

Preparation of $[Ge_4(\mu\text{-}O)_2(OC_6H_3\text{-}Bu^t\text{-}2\text{-}CH_3\text{-}4)_4\cdot NH_3]_2$ (11) and $[Ge_8(\mu_3\text{-}O)_6(OC_6H_3\text{-}Bu^t\text{-}2\text{-}CH_3\text{-}4)_4]$ (10)

To a solution of $HOC_6H_3Bu^t$-2-Me-4 (**8**) (0.756 g, 4.60 mmol) in benzene (15 mL) was added a solution of $Ge[N(SiMe_3)_2]_2$ (**7**) (0.906 g, 2.30 mmol) in benzene (10 mL). The reaction mixture was stirred at room temperature for 4 h and the volatiles were removed *in vacuo* to yield a pale yellow solid. The crude material was recrystallized from hot benzene (8 mL) to yield 0.246 g of **11** as colorless crystals (43 % based on Ge). The solvent was evaporated from the mother liquor *in vacuo* and the resulting solid was dissolved in 5 mL of a 1:1 mixture of hexane and toluene. The solution was stored at -35 °C to yield colorless crystals of **10** (0.082 g, 21 % based on Ge). **11**: ^{1}H NMR (C_6D_6, 25 °C) δ 7.15 (s, 4H, *meta*-H), 7.12 (s, 4H, *meta*-H), 6.89 (d, J = 6.2 Hz, 4H, *meta*-H), 6.84 (d, J = 6.7 Hz, 4H, *meta*-H), 6.76 (d, J = 6.2 Hz, 4H, *ortho*-H), 6.73 (d, J = 6.2 Hz,

4H, *ortho*-H), 2.17 (s, 24H, -CH_3), 1.50 (s, 36H, -C(CH_3)$_3$) ppm. ^{13}C NMR (C_6D_6, 25 °C) δ 139.4 (*para*-C), 129.8 (*ortho*-C_2), 128.3 (*ortho*-C_6), 127.7 (*meta*-C_5), 127.5 (*meta*-C_3), 35.2 (-*C*(CH$_3$)$_3$), 30.5 (-C(*C*H$_3$)$_3$), 21.2 (-*C*H$_3$) ppm. **10**: ^{1}H NMR (C_6D_6, 25 °C) δ 7.17 (s, 8H, *meta*-H_3), 6.85 (d, J = 8.1 Hz, 8H, *meta*-H_5), 6.72 (d, J = 8.1Hz, 8H, *ortho*-H), 2.20 (s, 24H, *p*-CH_3), 1.47 (s, 72H, *o*-C(CH_3)$_3$) ppm. ^{13}C NMR (C_6D_6, 25 °C) δ 152.5 (*ipso*-C), 139.4 (*para*-C), 129.8 (*ortho*-C_2), 128.3 (*ortho*-C_6), 127.4 (*meta*-C_5), 118.9 (*meta*-C_3), 34.8 (-*C*(CH$_3$)$_3$), 30.1 (-C(*C*H$_3$)$_3$), 21.1 (-*C*H$_3$) ppm.

Preparation of [Ge$_8$(μ$_3$-O)$_6$(OC$_6$H$_3$-Bu^t-2-CH$_3$-4)$_4$] (10)

To a solution of HOC$_6$H$_3$Bu^t-2-Me-4 (**8**) (0.827 g, 5.03 mmol) in benzene (110 mL) was added a solution of Ge[N(SiMe$_3$)$_2$]$_2$ (**7**) (1.584 g, 4.03 mmol) in benzene (10 mL). The reaction mixture was stirred at room temperature for 18 h and the volatiles were removed *in vacuo* to yield a colorless solid. Recrystallization of the crude reaction mixture from hot benzene (10 mL) yielded 0.496 g of **10** (74 %) as colorless crystals. ^{1}H NMR (C_6D_6, 25 °C) δ 7.17 (s, 8H, *meta*-H_3), 6.85 (d, J = 8.1 Hz, 8H, *meta*-H_5), 6.72 (d, J = 8.1Hz, 8H, *ortho*-H), 2.20 (s, 24H, *p*-CH_3), 1.47 (s, 72H, *o*-C(CH_3)$_3$) ppm. ^{13}C NMR (C_6D_6, 25 °C) δ 152.5 (*ipso*-C), 139.4 (*para*-C), 129.8 (*ortho*-C_2), 128.3 (*ortho*-C_6), 127.4 (*meta*-C_5), 118.9 (*meta*-C_3), 34.8 (-*C*(CH$_3$)$_3$), 30.1 (-C(*C*H$_3$)$_3$), 21.1 (-*C*H$_3$) ppm.

Preparation of Me$_3$SiOC$_6$H$_3$-Bu^t-2-CH$_3$-4 (12)[24]

To a solution of HOC$_6$H$_3$Bu^t-2-Me-4 (5.000 g, 30.4 mmol) in diethyl ether was added dropwise triethylamine (6.5 mL, 46.6 mmol). The mixture was cooled to 0 °C and chlorotrimethylsilane (5 mL, 39.4 mmol) was added dropwise using a syringe. The reaction mixture was stirred for 14 h, and then was filtered through a fritted glass filter.

The remaining triethylamine hydrochloride was washed with diethyl ether (2 x 25 mL). The filtrate and extracts were combined and the solvent was removed *in vacuo* to yield **6** (5.631 g, 78 %) as a colorless oil. ^{1}H NMR (C_6D_6, 25 °C) δ 7.19 (a, 1H, *meta*-H), 6.73 (d, J = 7.8 Hz, 1H, *meta*-H), 6.52 (d, J = 7.8 Hz, 1H, *ortho*-H), 2.20 (s, 3H, -CH_3), 1.48 (s, 9H, -C(CH_3)$_3$), 0.23 (s, 9H, -Si(CH_3)$_3$). GC/MS: t_r = 11.97 min, m/z = 236 (M^+), 221 (M^+ -CH_3).

NMR Scale Reaction of Ge[N(SiMe$_3$)$_2$]$_2$ with 2 Equiv. HOC$_6$H$_3$-Bu^t-2-CH$_3$-4

In a screw-cap NMR tube equipped with a septum, Ge[N(SiMe$_3$)$_2$]$_2$ (**7**) (0.500 g, 0.13 mmol) was dissolved in benzene-d_6 (0.30 mL). To this was added HOC$_6$H$_3$-Bu^t-2-CH$_3$-4 (0.0430 g, 0.26 mmol) in benzene-d_6 (0.20 mL) via microliter syringe. The reaction mixture was immediately placed in the NMR spectrometer and the ^{1}H NMR spectrum of the sample was recorded (**Spectrum A1**). The ^{1}H NMR spectrum was also recorded after a reaction time of 3.5 h (**SpectrumA2**), 18 h (**Spectrum A3**) and 36 h (**Spectrum A4**). The NMR tube was purged with a stream of O_2 and the spectrum was recorded after 30 min (**Spectrum A5**) and 6 h (**Spectrum A6**). ^{1}H NMR data (the boldface compound numbers in parentheses refer to the species shown in Scheme 2 (**10, 11, 12, 13**) and Scheme 7 (**16**):

Spectrum A1: δ 7.15 (s, **16**), 7.00 (d, J = 8.4 Hz, **16**), 6.71 (t, J = 8.1 Hz, **16**), 2.11 (s, **16**), 1.50 (s, **16**), 0.09 (s, HN(SiMe$_3$)$_2$) ppm.

Spectrum A2: δ 7.21 – 6.70 (m, **10-12,16**), 2.20 (s, **10**, **12**), 2.17 (s, **11**), 2.11 (s, **16**), 1.52 (s, **11**), 1.50 (s, **16**, **11**), 1.47 (s, **12**), 0.09 (s, HN(SiMe$_3$)$_2$) ppm.

Spectrum A3: δ 7.21 – 6.70 (m, **10** – **13**), 2.20 (s, **10**, **12**, **13**), 2.17 (s, **11**), 1.52 (s, **11**), 1.47 (s, **10**, **12**, **13**), 0.23 (s, **12**), 0.09 (s, HN(SiMe$_3$)$_2$) ppm.

Spectrum A4: δ 7.21 – 6.70 (m, **10** – **13**), 2.20 (s, **10**, **12**, **13**), 2.17 (s, **11**), 1.52 (s, **11**), 1.47 (s, **10**, **12**, **13**), 0.23 (s, **12**), 0.09 (s, $HN(SiMe_3)_2$) ppm.

Spectrum A5: δ 7.21 (s), 7.17 (s, **10** – **13**), 6.88 – 6.82 (m, **10** – **13**), 6.72 – 6.70 (m, **10** – **13**), 2.26 (s), 2.20 (**10**, **12**, **13**), 2.17 (s, **11**), 1.58 (s), 1.50 (s, **11**), 1.47 (s, **10**, **12**, **13**), 0.23 (s, **12**), 0.09 (s, $HN(SiMe_3)_2$) ppm.

Spectrum A6: δ 7.17 (s, **10** – **13**), 6.85 (d, **10** – **13**), 6.72 (d, **10** – **13**), 2.20 (s, **10** – **13**), 1.47 (**10** – **13**), 0.23 (s, **12**), 0.09 (s, $HN(SiMe_3)_2$) ppm.

NMR Scale Reaction of 4 Equiv. of $Ge[N(SiMe_3)_2]_2$ with 5 Equiv. HOC_6H_3-Bu^t-2-CH_3-4

In a screw-cap NMR tube equipped with a septum, $Ge[N(SiMe_3)_2]_2$ (**7**) (0.0300 g, 0.076 mmol) was dissolved in benzene-d_6 (0.20 mL). To this was added HOC_6H_3-Bu^t-2-CH_3-4 (0.0430 g, 0.0156 mmol) in benzene-d_6 (0.20 mL) via microliter syringe. The reaction mixture was immediately placed in the NMR spectrometer and the ^{1}H NMR spectrum of the sample was recorded (**Spectrum B1**). The ^{1}H NMR spectrum was also recorded after a reaction time of 3 h (**Spectrum B2**), 8 h, (**Spectrum B3**), and 18 h (**Spectrum B4**). ^{1}H NMR data (the boldface compound numbers in parentheses refer to the species shown in Scheme 2):

Spectrum B1: δ 7.15 (s, **16**), 7.00 (d, J = 8.4 Hz, **16**), 6.71 (t, J = 8.1 Hz, **16**), 2.11 (s, **16**), 1.50 (s, **16**), 0.09 (s, $HN(SiMe_3)_2$) ppm.

Spectrum B2: δ 7.20 – 6.69 (m, **10** – **13**), 2.20 (s, **10**, **12**, **13**), 2.17 (s, **11**), 1.52 (s, **11**), 1.47 (s, **10**, **12**, **13**), 0.23 (s, **12**), 0.09 (s, $HN(SiMe_3)_2$) ppm.

Spectrum B3: δ 7.17 (s, **10** – **13**), 6.85 (d, **10** – **13**), 6.72 (d, **10** – **13**), 2.20 (s, **10** – **13**), 1.47 (**10** – **13**), 0.23 (s, **12**), 0.09 (s, $HN(SiMe_3)_2$) ppm.

Spectrum B4: δ 7.17 (s, **10** – **13**), 6.85 (d, **10** – **13**), 6.72 (d, **10** – **13**), 2.20 (s, **10** – **13**), 1.47 (**10** – **13**), 0.23 (s, **12**), 0.09 (s, $HN(SiMe_3)_2$) ppm.

Crystallographic Data

Table 6. Crystal data and structure refinement for $Ge(OC_6H_3Bu^t\text{-}2\text{-}Me\text{-}6)_2$ (9), $Ge_6(\mu_3\text{-}O)_4(\mu_2\text{-}OC_6H_4Bu^t\text{-}4)_4$ (16), $[Ge_8(\mu_3\text{-}O)_6(OC_6H_3\text{-}Bu^t\text{-}2\text{-}CH_3\text{-}4)_4]$ (10) and $[Ge_4(\mu\text{-}O)_2(OC_6H_3\text{-}Bu^t\text{-}2\text{-}CH_3\text{-}4)_4\cdot NH_3]_2$ (11).

	9	**16**	**10**	**11**
Empirical formula	$C_{22}H_{30}GeO_2$	$C_{40}H_{52}Ge_6O_8$	$C_{44}H_{60}Ge_8O_{10}$	$C_{88}H_{126}Ge_8N_2O_{12}$
Formula weight	399.05	1096.36	1329.84	1984.858
Temperature	100(2) K	100(2) K	123(2) K	150(2) K
Wavelength	0.71073 Å	0.71073 Å	0.71073 Å	0.71073 Å
Crystal system	Orthorhombic	Monoclinic	Triclinic	Monoclinic
Space group	Pbca	P2(1)/n	P-1	P2(1)/c
Unit cell dimensions (Å / °)	a=20.418(1) α = 90	a=9.978(3) α = 90	a=12.5197(9) α=68.3760(10)	a=14.531(9) α = 90
	b=15.992(7) β=90	b=21.622(6) β=102.180(5)	b=15.384(1) β=77.7980(1)	b=15.160(1) β=101.046(8)
	c=25.061(12) γ = 90	c=20.237(5) γ = 90	c=17.2374(16) γ=88.3800(10)	c=27.040(2) γ=90
Volume	8183(7) $Å^3$	4268(2) $Å^3$	3012.1(4) $Å^3$	5846(6) $Å^3$
Z	16	4	2	2
Density (calculated)	1.296 g/cm^3	1.706 Mg/m^3	1.552 Mg/m^3	1.305 Mg/m^3
Absorption coefficient	1.509 mm^{-1}	4.220 mm^{-1}	3.983 mm^{-1}	2.082 mm^{-1}
F(000)	3360	2192	1404	2376
Crystal size	0.29 x 0.22 x 0.10 mm^3	0.40 x 0.06 x 0.04 mm^3	0.22 x 0.18 x 0.16 mm^3	0.32 x 0.28 x 0.22 mm^3

Crystal color, habit	Colorless plate	Colorless needles	Colorless plate	Colorless block
Theta range for data collection	1.63 to 25.48°	1.40 to 24.99°	1.43 to 25.45°	1.43 to 27.50°
Index ranges	-24<=h<=24, -19<=k<=18, -30<=l<=30	-11<=h<=11, -21<=k<=25, -23<=l<=23	-15<=h<=15, -18<=k<=18, -20<=l<=20	-18<=h<=18, -19<=k<=19, -34<=l<=34
Reflections collected	74817	24989	54583	145198
Independent reflections	7530 [R(int) = 0.0855]	7400 [R(int) = 0.1260]	11102 [R(int) = 0.0657]	13305 [R(int) = 0.0805]
Completeness to theta = 25.00°	99.9 %	98.5 %	99.8 %	100.0 %
Absorption correction	Multi-scan	None	Multi-scan	Multi-scan
Max. and min. transmission	0.8638 and 0.6687	0.8493 and 0.2831	0.5682 and 0.4745	0.6573 and 0.5555
Refinement method	Full-matrix least-squares on F^2	Full-matrix least-squares on F^2	Full-matrix least-squares on F^2	Full-matrix least-squares on F^2
Data / restraints / parameters	7530 / 0 / 467	7400 / 12 / 472	11102 / 0 / 554	13305 / 36 / 610
Goodness-of-fit on F^2	1.027	0.995	1.001	1.041
Final R indicies [I>2sigma(I)]	R1 = 0.0355, wR2 = 0.0801	R1 = 0.0593, wR2 = 0.0875	R1 = 0.0343, wR2 = 0.0653	R1 = 0.0339, wR2 = 0.0856
R indicies (all data)	R1 = 0.0617, wR2 = 0.0932	R1 = 0.1328, wR2 = 0.1071	R1 = 0.0583, wR2 = 0.0695	R1 = 0.0470, wR2 = 0.0930
Largest diff. peak and hole	0.812 and -0.426 e $Å^{-3}$	0.760 and -0.880 e.$Å^{-3}$	0.470 and -0.438 e.$Å^{-3}$	0.662 and -0.752 e.$Å^{-3}$

References

(1) Çetinkaya, B.; Gemrükçü, I.; Lappert, M. F.; Atwood, J. L.; Rogers, R. D.; Zaworotko, M. J. *J. Am. Chem. Soc.* **1980**, *102*, 2088.

(2) Gerung, H.; Boyle, T. J.; Tribby, L. J.; Bunge, S. D.; Brinker, C. J.; Han, S. M. *J. Am. Chem. Soc.* **2006,** *128*, 5244.

(3) Weinert, C. S.; Fanwick, P. E.; Rothwell, I. P. *J. Chem. Soc.*, *Dalton Trans.* **2002,** 2948.

(4) Weinert, C. S.; Fenwick, A. E.; Fanwick, P. E.; Rothwell, I. P. *J. Chem.Soc.*, *Dalton Trans.* **2003,** 1795.

(5) McBurnett, B. G.; Cowley, A. H.; *Chem. Commun.* **1999,** 17.

(6) Wetherby Jr., A. E.; Goeller, L. R.; DiPasquale, A. G.; Rheingold, A. L.; Weinert, C. S. *Inorg. Chem.* **2007,** *46*, 7579.

(7) Meller, A.; Gräbe, C. P.; *Chem. Ber.* **1985**, *118,* 2020.

(8) S. M. Sze, *Physics of Semiconductor Devices*, 2nd ed., John Wiley & Sons, Inc., New York, **1981**.

(9) Haller, E. E. *Mater. Sci. Semicond. Process.* **2006**, *9*, 408.

(10) Gacem, K.; El Hdiy, A.; Troyon, M.; Berbezier, I.; Szkutnik, P. D.; Karmous, A.; Ronda, A. *J. Appl. Phys*. **2007**, *102*, 093704/093701-093704/093704.

(11) Gerung, H.; Bunge, S. D.; Boyle, T. J.; Brinker, C. J.; Han, S. M. *Chem. Commun*. **2005**, 1914.

(12) Hascall, T.; Rheingold, A. L.; Guzei, I.; Parkin, G. *Chem. Commun*. **1998**, 101.

(13) Wetherby Jr., A. E.; Rheingold, A. L.; Feasley, C. L.; Weinert, C. S. *Polyhedron* **2008,** *27*, 1841.

(14) Green, R. A.; Rheingold, A. L.; Weinert, C. S. *Inorg. Chim. Acta* **2009**, *362*, 3159.

(15) Bradley, D. C.; Mehrotra, R. C.; Rothwell, I. P.; Singh, A. *Alkoxo and Aryloxo Derivatives of Metals*; Academic Press: London, 2001.

(16) Caulton, K. G.; Chisholm, M. H.; Drake, S. R.; Folting, K.; Huffman, J. C.; Streib, W. E. *Inorg. Chem.* **1993,** *32,* 1970.

(17) Jackman, L. M.; Cizmeciyan, D.; Willard, P. G.; Nichols, M. A. *J. Am.Chem. Soc.* **1993,** *115*, 6262.

(18) Evans, W. J.; Golden, R. E.; Ziller, J. W. *Inorg. Chem.* **1993,** *32*, 3041.

(19) Amadoruge, M. L.; Weinert, C. S. *Chem. Rev.* **2008**, *108*, 4253.

(20) Suh, S.; Hoffman, D. M. *Inorg. Chem.* **1996**, *35*, 6164.

(21) Jutzi, P.; Keitimeyer, S.; Neumann, B.; Stammler, H. *Organometallics* **1999**, *18*, 4778.

(22) Benet, S.; Cardin, C. J.; Cardin, D. J.; Constantine, S. P.; Heath, P.; Rashis, H.; Teixeira, S.; Thorpe, J. H.; Todd, A. K. *Organometallics* **1999**, *18*, 389.

(23) Weinert, C.S.; Fanwick, P.E.; Rothwell, I.P. *J. Chem. Soc. Dalton Trans.* **2002**, 2948.

(24) Nielson, A.J.; Harrison, J.A.; Shen, C.; Waters, J.M. *Polyhedron* **2006**, *25*, 1729.

(25) Mochida, K.; Ohto, J.; Masuda, M.; Nanjo, M.; Arii, H.; Nakadaira, Y. *Chem. Lett.* **2008**, *37*, 20.

(26) Ramaker, G.; Schäfer, A.; Saak, W.; Weidenbruch, M. *Organometallics* **2003**, *22*, 1302.

(27) Samuel, M. S.; Jennings, M. C.; Baines, K. M. *J. Organomet. Chem.* **2001**, *636*, 130.

(28) Kako, M.; Akasaka, T.; Ando, W. J. *J. Chem. Soc., Chem. Commun.* **1992**, 457.

VITA

Rebecca Anne Green

Candidate for the Degree of

Master of Science

Thesis: SYNTHESIS AND STRUCTURES OF GERMANIUM(II) CALIXARENES AND CLUSTERS

Major Field: Chemistry

Biographical:

Personal Data:

Born in Bridgeport, Connecticut in 1983.

Education:

Received Bachelor of Science degree in Chemistry from Towson University, Towson, Maryland in January 2006. Completed the requirements for the Master of Science in Chemistry at Oklahoma State University, Stillwater, Oklahoma in July 2009.

Experience:

Employed by Pharmaceutics International Incorporated as a chemist in the dissolution laboratory from January 2006 to July 2006.

Professional Memberships:

The National Society of Collegiate Scholars March 2002 – Present
The National Scholars Honors Society May 2007 – Present
Golden Key May 2007 – Present
American Chemical Society, Inorganic Division August 2008 – Present
Phi Lambda Upsilon December 2006 - Present

Name: Rebecca Green Date of Degree: July, 2009

Institution: Oklahoma State University Location: Stillwater, Oklahoma

Title of Study: SYNTHESIS AND STRUCTURES OF GERMANIUM(II)

CALIXARENES AND CLUSTERS

Pages in Study: 99 Candidate for the Degree of Master of Science

Major Field: Chemistry

Scope and Method of Study: The purpose of this work was to examine the structures of novel germanium containing compounds. This was accomplished by characterizing the products of the reaction between the germanium(II) amide, $Ge[N(SiMe_3)_2]_2$, and *para-tert*-butylcalix[8]arene with subsequent reaction with $Fe_2(CO)_9$. The phenols, $HOC_6H_3Bu^t$-2-Me-6, $HOC_6H_4Bu^t$-4 and $HOC_6H_3Bu^t$-2-Me-4, were selected due to their relative steric bulkiness and were also reacted with $Ge[N(SiMe_3)_2]_2$ and the products of the reactions were characterized. Products were characterized by NMR and IR spectroscopy, GC/MS spectrometry and X-ray crystallography.

Findings and Conclusions: The reaction between *para-tert*-butylcalix[8]arene and $Ge[N(SiMe_3)_2]_2$ yielded the germylene complex $\{p\text{-}Bu^t{}_8$calix[8]arene$\}Ge_4$ and contains two Ge_2O_2 rhombi located on opposite sides of the molecule. The two rhombi are planar where the Ge – O(terminal) bonds are shorter than the Ge – O(bridging) bonds. Each germanium is in the divalent oxidation state. In the subsequent reaction with $Fe_2(CO)_9$, the Fe – Fe bond was cleaved with addition of $Fe(CO)_4$ to two of the four germanium atoms with concomitant loss of $Fe(CO)_5$. The reaction of $Ge[N(SiMe_3)_2]_2$ yielded the monomeric complex $Ge(OC_6H_3Bu^t$-2-Me-6$)_2$. The reaction with $HOC_6H_4Bu^t$-4 yielded the hexagermanium cluster $Ge_6(\mu_3\text{-}O)_4(\mu_2\text{-}OC_6H_4Bu^t\text{-}4)_4$ that is held together by four μ_3-bridging oxo atoms and four μ_2-*p*-Bu^taryloxide ligands. The reaction with $HOC_6H_3Bu^t$-2-Me-4 resulted in the formation of two clusters that were structurally characterized. One is the octagermanium cluster $Ge_8(\mu_3\text{-}O)_6(OC_6H_3\text{-}Bu^t\text{-}2\text{-}CH_3\text{-}4)_4$ that is connected together by six μ_3-oxo atoms with four terminal aryloxide groups. The second structure that was determined was the dimer $[Ge_4(\mu\text{-}O)_2(OC_6H_3\text{-}Bu^t\text{-}2\text{-}CH_3\text{-}4)_4\cdot NH_3]_2$ that contains two Ge_4O_2 rings that are connected by two Ge – Ge single bonds. The dimer appears to be an intermediate in the formation of the larger octagermanium cluster. All of the germanium atoms are present in the divalent oxidation state.

ADVISER'S APPROVAL: Dr. Charles Scott Weinert